Emission of volatile organic compounds from a boreal coastal area—dynamics and environmental controls

Dissertation

Zur Erlangung des Doktorgrades der Naturwissenschaften im Department Geowissenschaften der Universität Hamburg
vorgelegt von

Arja Valtanen

aus

Kerava, Finnland

Hamburg
2010

Als Dissertation angenommen vom Department Geowissenschaften der Universität Hamburg

auf Grund der Gutachten von Prof. Dr. Walter Michaelis

und Prof. Dr. Kay-Christian Emeis

Hamburg, den 12.11. 2010.

Prof. Dr. Jürgen Oßenbrügge
Leiter des Department Geowissenschaften

Isälle / to my father

4.5.1947 – 1.9.2010

INDEX

ACKNOWLEDGEMENT

First of all I would like to thank two professors: Walter Michaelis and Helinä Hartikainen. Professor Michaelis I thank for his open-mind in taking a Ph.D. student from a far away northern country, introducing me to the fascinating world of halomethanes and last but not least for his guidance during my doctoral studies in Hamburg. Professor Hartikainen I warmly thank for her encouragement in going abroad and help and support in the important matter of financing the studies.

I warmly acknowledge the Maj and Tor Nessling foundation in Finland for granting me a 3,5-year scholarship, which made it possible to concentrate on the scientific work and write my Ph.D.-thesis.

Leif Lindgren and Jean-Erik Mattsson from Metsähallitus I would like to thank for their help in transport, accommodation and finding the halophytes on the island of Jungfruskär in the Finnish archipelago national park.

The members of the organic geochemistry group in the institute of biogeochemistry and marine chemistry I greatly thank for their support in practical issues and for the versatile scientific discussion. Judith Angelstorf and Sascha Herrlich I thank for the many hours they stood in the lab on my behalf. Sabine Beckmann I stand personally in dept for her willingness to sit with me in middle of the night in middle of nowhere catching few molecules. Frank Laturnus I warmly thank for his valuable comments during the writing process of the thesis.

My dear Ph.D. colleges Jan, Birte, Sebastian, Stefan and Stephan are thanked for the litres of coffee, beer and other liquids we shared together and the laughs and motivation.

My family and friends, thank you for love, support and believe in me. In the end there was only one person that kept me going and trusted my abilities to bring my writing to an end, Christian. Thank you for the motivation talks, patience and being there.

List of abbreviations

B.P.	before present
BVOCs	biogenic volatile organic compounds
CC	column chromatography
CFCs	chloro-fluoro-carbons
CIS	cold injection system
d.	diameter
EC	electric conductivity
e.g.	*exempli gratia*, for example
FAMEs	fatty acid methyl esters
FID	flame ionisation detector
FMI	Finnish meteorological institute
HVOCs	halogenated volatile organic compounds
i.e.	*id est,* that is
l.	length
LOI	loss on ignition
NMHCs	non-methane hydrocarbon compounds
OM	organic matter
OVOCs	oxygenated volatile organic compounds
PAR	photosynthetically active radiation
PFA	perfluoroalkoxy
PLOT	porous layer open tubular
ppt	parts per trillion
PUFAs	polyunsaturated fatty acids
Redox	reduction – oxidation
SAM	S-adenosylmethione
SPE	solid phase extraction
TD-GC-MS	thermal desorption – gas chromatography – mass spectrometry
TLE	total lipid extract
TOC	total organic carbon
TON	total organic nitrogen
UV	ultra violet
VOSCs	volatile organic sulphur compounds
VOCs	volatile organic compounds
XSD	halogen sensitive detector

Abstract

Chlorine radicals are well-known catalysts in ozone depletion reactions. This study was undertaken to monitor emissions of chloromethane (CH_3Cl), an important source of chlorine to the troposphere and stratosphere, from a boreal coastal meadow on the shoreline of brackish water sea. Fluxes of volatile organic compounds (VOCs) were measured above different types of vegetation. Two campaigns were conducted in 2007 and 2008, and measurements were made in July of each year. Five experimental sites were selected for investigation. Two sites were dominated by *Salicornia europaea*, and three sites were covered with mixed vegetation. A variety of substances of anthropogenic and natural origin were identified, but biogenic organic compounds predominated. The vegetation types did not differ markedly in their CH_3Cl flux rates in 2007 and 2008. The daily emission rate for the whole meadow vegetation was 10.36 (+/- 0.60) µg m^{-2} d^{-1} and 36.58 (+/- 2.54) ng g^{-1} d^{-1} when normalised to area and dry biomass, respectively. The recorded flux agrees well with those values reported for other coastal ecosystems. Emissions from boreal coastal areas might be a relevant CH_3Cl source on the local and global scales.

Marine and terrestrial organisms produce a wide variety of halogenated organic compounds, and over 3500 halogenated naturally produced compounds have been identified so far. In this study, three halophytic plant species were investigated to find halogenated lipophylic compounds. A series of long-chain1-chloro-n-alkanes were detected in the investigated species (*Sueda maritima* (Sea Blite), *Halimione portulacoides* (Sea Purslane) and *Salicornia europaea* (Glasswort)). The concentrations of these substances varied from 0.08 to 35 µg mg^{-1} HC (hydrocarbon) dry weight. No connection between the formation of long-chain chloroalkanes and CH_3Cl production by plants was found. The finding of chloroalkanes confirms the results from a prior study reporting the discovery of plant-derived Cl-alkanes.

1. Introduction

1.1 Biogenic volatile organic compounds (BVOCs) in the environment

Biogenic volatile organic compounds (BVOCs) are atmospheric trace gases released from biogenic sources (e.g., algae, bacteria and higher plants). BVOCs comprise compounds of varying chemical composition from simple saturated and unsaturated hydrocarbons to organic acids and esters. These compounds are often divided into subgroups, such as nonmethane hydrocarbons (NMHCs) and oxygenated volatile organic compounds (OVOCs), according to their chemical structure and reactivity. Isoprene and monoterpenes followed by alcohols and carbonyl group-containing compounds are the quantitatively predominant compounds or compound groups (Kesselmeier and Staudt 1999). BVOCs usually have atmospheric lifetimes of a few minutes to hours (Kesselmeier and Staudt 1999) and hence participate mainly in the tropospheric processes, influencing ozone concentration and the formation of secondary particles.

Since the end of the last decade, halogenated volatile organic compounds (HVOCs) and especially halomethanes (chloro-, bromo-, and iodomethane) have gained increasing attention (Butler 2000). They are interesting additions to the well-established group of BVOCs, as halogenated compounds were for a long time considered to be strictly anthropogenic compounds. Biogenic HVOCs are carriers of halogen contaminants to the stratosphere (Montreal Protocol 1987) and play a significant role in the destruction of stratospheric ozone as the concentrations of the anthropogenic source gases (CFCs and halons) decline (WMO 2006). Chloromethane (CH_3Cl) and other monohalomethanes were believed to be liberated mostly from marine sources (e.g., algae and sea spray reactions) until large terrestrial sources were discovered at the end of the 1990s and in 2000. The most interesting revelation of these studies was the discovery of higher plants as a substantial source of CH_3Cl. The emission rate of CH_3Cl from plants seems to be strongly related to the plant species, the amount of

photosynthetically active radiation, and the temperature of the surrounding air. Plant-derived emissions of chloromethane have been recorded in several independent studies and are approved as one of the major sources of atmospheric CH_3Cl. However, the data are still scarce, and the global budget estimations are based on measurements from rather narrow geographic areas.

1.2 Chloromethane in the atmosphere

1.2.1 Physical and chemical properties of chloromethane

The reactivity of a chemical compound depends on its physico-chemical characteristics, which govern its distribution and its overall fate in the environment. Chloromethane is chemically methane with one of the four hydrogen atoms substituted with a chlorine atom (Figure 1.1). It is a small molecule with a low molecular mass and boiling point (Table 1.1). Under normal temperature and pressure conditions (NTP: 20℃ and 1 atm), it is present in the gaseous form.

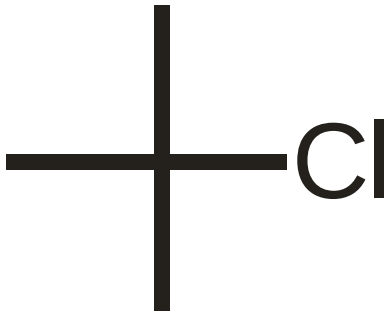

Figure 1.1 Structure of chloromethane as a skeletal formula.

Chloromethane is chemically very inert, and the halogen atoms form a very stable bond with carbon, which is demonstrated in the long lifetimes of halogenated compounds in the atmosphere (WMO 2006).

Partition modelling studies show that more than 99% of CH_3Cl released directly into the air also stays in this environmental compartment (OECD-SIDS 2005 and references therein). If CH_3Cl originates from a soil source, it is also expected to volatilise rapidly, first to soil air and then to the atmosphere. Due to its low octanol-water partition coefficient (Table 1.1), it has no tendency to bind with soil organic matter. However, chloromethane originating from marine sources stays in the water phase for the most part. In fact, only about 20% volatilises into the atmosphere (OECD-SIDS 2005). In addition, cold ocean waters can function as a sink for CH_3Cl (Moore 1996).

Table 1.1 Chemical and physical characteristics of chloromethane

Name	Chloromethane/ Methyl chloride
MW / g mol^{-1}	50.488
Physical Form (in NTP[a])	gas
mp [℃] [b]	-97
bp [℃] [c]	-24.09
ρ [g cm^{-3}]	0.911 (p >1 atm)
log P[d]	0.91
Vapour pressure [hPa] at 20℃	4800
Water solubility [mg l^{-1}] at 25℃	4800-5325
Henry's law constant [atm- m^3 mol^{-1}]	8.82*10^{-3}

a) = normal temperature and pressure: p = 1 atm, T = 20℃
b) = melting point
c) = boiling point
d) = log of the octanol – water partition coefficient (= log K_{ow})

1.2.2 Sources and abundance

The global CH_3Cl budget was imbalanced for a long time, with the known sinks outweighing the identified sources (WMO 2002, Rhew et al. 2002). However, the discovery of a possible tropical terrestrial CH_3Cl source (Yokouchi et al. 2000, Yokouchi et al. 2002) first helped to balance the sinks and sources (WMO 2006).

Most of the CH_3Cl present in the atmosphere originates from a natural source (Table 1.2), and the only significant anthropogenic sources are waste incineration, fossil fuel burning and industrial processes. Chloromethane is produced as a chemical mediator for the preparation of chlorinated solvents, but it has no use as such in industrial processes (OECD-SIDS 2005). Anthropogenic sources play only a minor role in the global CH_3Cl budget.

There are a wide variety of natural CH_3Cl sources. As one of the largest chlorine reservoirs in the world, the ocean was suspected to be the major source for biogenic chlorinated organic compounds at the time that these compounds were first discovered in the atmosphere (Lovelock 1975). However, in the following decades, oceans and especially cold ocean waters were found to be a relatively large sink for CH_3Cl (Moore et al. 1996). Warm oceans remain a relatively large source for this substance, representing about 5-20% of the total sources.

Table 1.2 Anthropogenic and natural sources of CH_3Cl for the atmosphere.

Source	**Estimate Gg a^{-1}**	**Modelled strength (Yoshida et al. 2004) Gg a-1**
Tropical and subtropical plants	820 - 8200	2900
Tropical senescent or dead plants	30 - 2500	
Biomass burning	325 - 1125	611
Oceans	380 - 500	508
Salt marshes	65 - 440	170
Fungi	43 - 470	-
Wetlands	48	48
Rice paddies	2.4 - 4.9	-
Fossil fuel burning	5 - 205	162
Waste incineration	15 - 75	
Industrial processes	10	
Total	**1743 - 13578**	**4399**

Table 1.2 was modified based on information from WMO 2006.

Tropical and subtropical plants and tropical senescent and dead plants are the biggest sources of CH_3Cl (Table 1.2). However, the estimations for their CH_3Cl contributions are characterised by a high degree of uncertainty (deviation up to

100%). Other terrestrial sources, which are partly located in other climatic zones, include salt marshes, fungi, wetlands and rice paddies. Nevertheless, mapping for terrestrial CH_3Cl sources is still in a relatively early stage and many of the estimated source strengths are based on measurements made in only one location and then extrapolated to a global scale. Therefore, the information presented in Table 1.2 should be used with some precaution.

Table 1.3 Major sinks for tropospheric CH_3Cl.

Sinks	**Estimated strength Gg a^{-1}**	**Modelled strength (Yoshida et al. 2004) Gg a^{-1}**
OH reaction	3800-4100	3994
Loss to stratosphere	100-300	-
Cl reaction	180-550	-
Soil	100-1600	256
Loss to cold waters (polar oceans)	93-145	149
Total	**4273-6695**	**4399**

Table 1.3 was modified based on information from WMO 2006.

Reactions with hydroxyl radicals are the largest CH_3Cl sink (Table 1.3). The other four destruction processes have partly overlapping estimates for their strengths, but they generally are all in the same range. From these minor sinks, soil has the most inaccurate estimate, ranging from 100 to 1600 Gg a^{-1}. Soils are extremely heterogenic in their mineral composition, chemical and physical properties, and biological activity; therefore, it is very challenging to estimate the global soil sink due to the large deviation in this estimate. The relationship between the sources and sinks governs the atmospheric concentration or mixing ratio of a given compound in the atmosphere.

The most recent estimations of the mean atmospheric mixing ratios for CH_3Cl in the atmosphere are 536 ppt and 541 ppt in the northern hemisphere and southern hemisphere, respectively (Simmonds et al. 2004). From these estimations, also called mean baseline mixing ratios, obvious peaks in the observed concentration data are removed. These peaks are the result of the air masses originating from the source areas for CH_3Cl and are excluded from the estimation of the atmospheric background concentration. The atmospheric CH_3Cl mixing ratio shows no clear trend in recent years; after a constant

decrease with a mean rate of 2.6% a^{-1} between the years 1998 and 2001 (Simmonds et al. 2004), a slightly increasing trend can be observed for the last four years in the northern hemisphere (green line in Figure 1.2, observations from Mace Head, Ireland). The overall CH_3Cl burden for the atmosphere is still close to that in pre-industrial times (Butler et al. 1999).

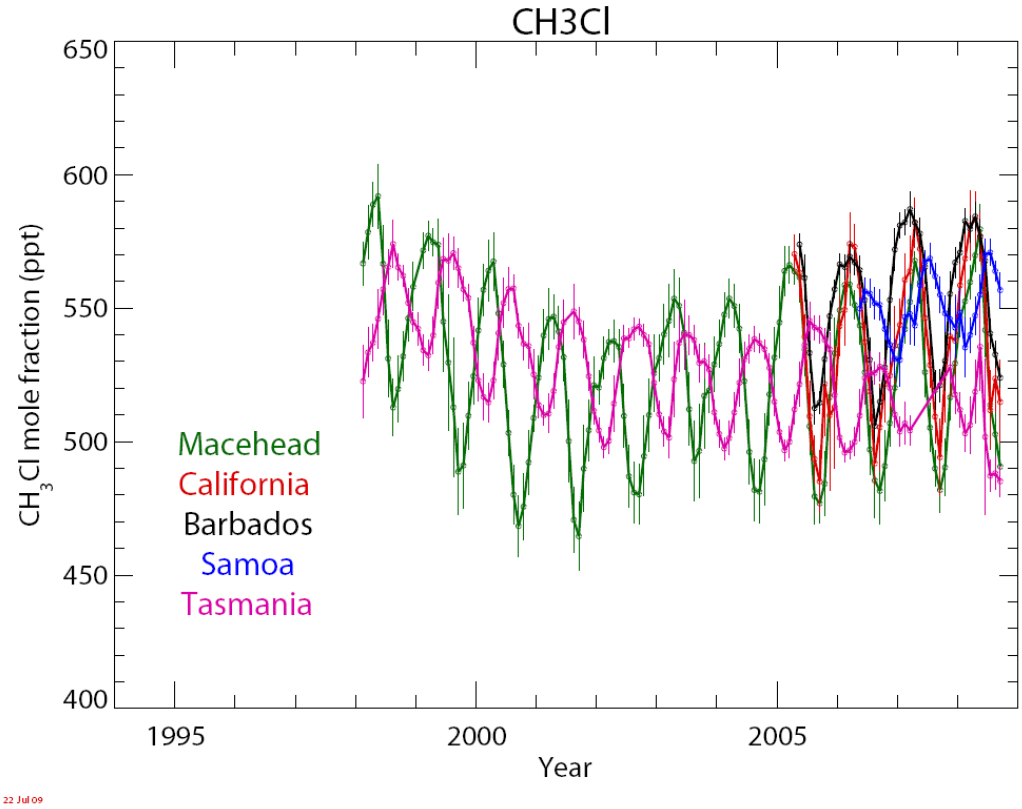

Figure 1.2 Global molar mixing ratios of CH_3Cl measured by the AGAGE network. (Source:http://agage.eas.gatech.edu/images/Data_figures/gc_ms_month/CH3Cl_gc_ms_comb_mon.pdf) Figure reproduced with the permission of AGAGE-network.

The atmospheric mixing ratio exhibits a clear seasonal behaviour, with a maximum in the early spring (April) and a minimum in late summer-autumn (August-September) (Figure 1.2 Mace Head, California and Barbados curves). The magnitude of the CH_3Cl seasonal cycle in Mace Head (representing the northern hemisphere) is about 79 ppt (15%) (Simmonds et al. 2004). The Californian observations seem to have a relatively similar amplitude as those observed for Mace Head, but the other northern hemisphere locations (Barbados and Samoa) exhibit a clearly lower seasonal trend, perhaps because of their vicinity to the equator, thus reducing the differences between various

seasons of the year. Seasonality is also observed in the southern hemisphere data, but with the opposite behaviour: a maximum occurring in the autumn and a minimum in the winter. These seasonal trends might be connected to the activity of the sinks. Increased biological activity in the soils might at least explain the minima in the late summer and autumn.

1.2.3 Atmospheric reactions

The reactivity of a volatile compound governs its fate and overall importance in atmospheric chemistry. Reactive chemical species like terpenes or organic acids tend to react quickly with other constituents in the atmosphere, therefore they mostly take part in secondary particle and ozone formation processes. Reactive species have short lifetimes in the atmosphere.

A different and equally complex problem derives from non-reactive gas species (such as CH_3Cl), which tend to accumulate in the atmosphere. These compounds have lifetimes from several months to several years and cause two major problems in atmospheric chemistry, namely the enhancement of the green house effect and the depletion of the stratospheric ozone layer. The atmospheric lifetime of volatile compounds depends on the following removal processes (Derwent 1995):

- ► photochemical oxidation by hydroxyl (OH) radicals in the troposphere
- ► photolysis in the troposphere and stratosphere
- ► deposition and uptake at the earth's surface
- ► reaction with other reactive species, such as chlorine atoms, nitrate radicals at night, and ozone

As mentioned in the previous chapter, the biggest CH_3Cl sink in the troposphere is photochemical oxidation by hydroxyl radicals. Reaction (1) can proceed after the initial step in various ways and with the participation of other atmospheric trace gases, such as nitrogen oxide radicals, but the final products of complete CH_3Cl oxidation are carbon dioxide (CO_2) and hydrogen chloride (HCl).

$CH_3Cl + \bullet OH \rightarrow \bullet CH_2Cl + H_2O \rightarrow\rightarrow CO_2 + HCl$ (1)

In the marine boundary layer, which has a strong oceanic source of chloride ions, CH_3Cl oxidation also might be initiated by chloride radicals. Other removal processes are of minor importance, such as dry and wet deposition, which have practically no effect on the CH_3Cl concentration in the troposphere, because CH_3Cl has a strong tendency to stay in the gaseous phase (due to the vapour pressure and Henry's Law constant, Table 1.1). The amount of radiation that penetrates into the troposphere does not posses enough energy to initiate photolytic CH_3Cl degradation. Therefore, CH_3Cl does not function as a precursor for reactive chlorine species in this part of the atmosphere and has only a minor influence on the ozone (O_3) concentration of the troposphere. Overall, CH_3Cl is relatively inactive in the troposphere, which can also be seen by its relatively long atmospheric lifetime of 1.0 a (WMO, 2006).

Its long atmospheric lifetime allows for CH_3Cl to be transported to the stratosphere. It is the only natural source for stratospheric chlorine, currently contributing about 16% of the total stratospheric chlorine (Figure 1.2).

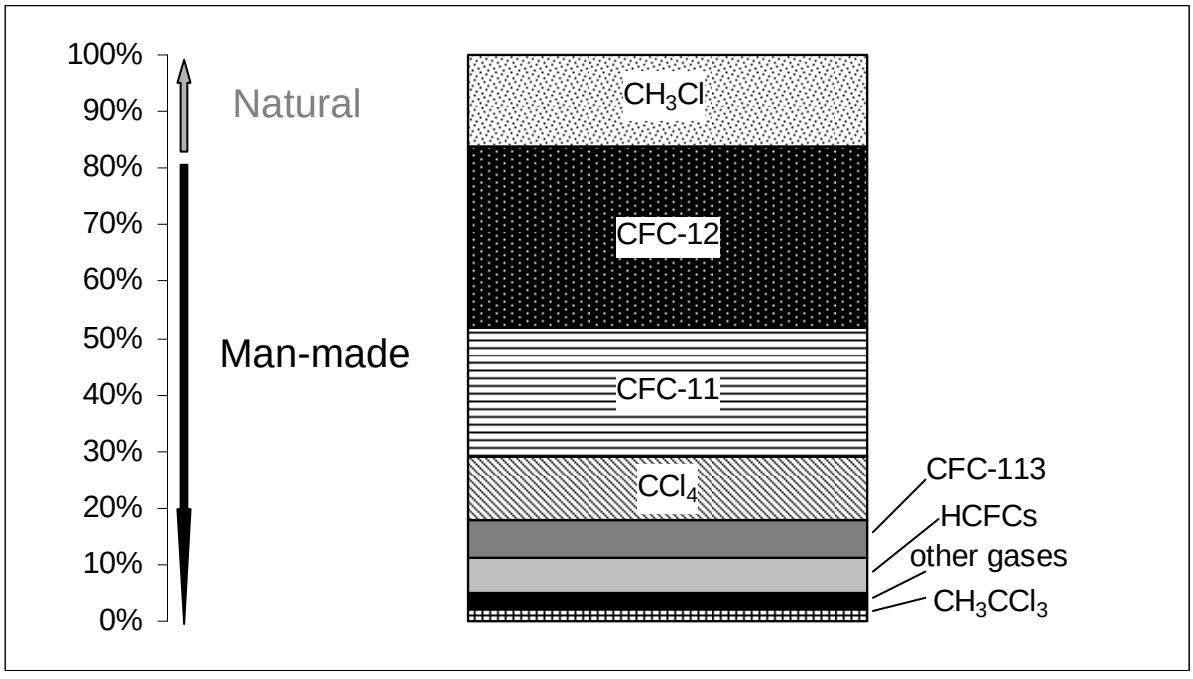

Figure 1.2 Primary chlorine source gases for the stratosphere. Figure modified from WMO 2006.

Although the majority of the stratospheric chlorine sources today are still anthropogenic, the amount of chlorine from man-made sources will likely decline in the future as a result of the enforcement of the Montreal Protocol and its amendments (reduced CFC concentrations in the troposphere have already been seen from the mid-1990s, WMO 2006). Chlorine originating from natural sources will play a key role in controlling the concentration of chlorine in the stratosphere in the future.

Chlorine is an important element in the chemistry of the stratosphere, as it interferes with the stratospheric ozone cycle. In the lower parts of the stratosphere (~ 20 km), there is a maximum in the ozone concentration, which is usually referred to as the ozone layer. This layer is of paramount importance for life on earth, as it protects the earth's surface from high-energy radiation, which is harmful for most biological organisms. Natural ozone synthesis and destruction can be described by the following equations (vanLoon and Duffy 2000):

Synthesis

$O_2 + hv\ (\lambda < 240\ nm) \rightarrow O + O$ (slow) (2.1)

$O + O_2 + M \rightarrow O_3 + M$ (fast) (2.2)

Decomposition

$O_3 + hv\ (\lambda \sim 230 - 320\ nm) \rightarrow O_2^* + O^*$ (fast) (3.1)

$O + O_3 \rightarrow O_2 + O_2$ (slow) (3.2)

*) oxygen species in the excited state (after photon absorption)

In reaction 2.2, M is a neutral third body, usually N_2 or O_2, which are the two predominant gas species in the atmosphere. Reactions 2.1 to 3.2 reveal that ozone is formed and decomposed in the stratosphere solely due to solar radiation. Reaction 3.1 protects the earth from harmful UV radiation. A balance is maintained, which leads to ozone accumulation in the lower stratosphere. If

other chemical species are involved, ozone destruction can be enhanced. However, the synthesis rate remains the same, eventually leading to destruction of the ozone layer.

When CH_3Cl reaches the stratosphere, it is photolysed due to high-energy UV radiation (equation 4) and releases reactive chlorine.

$$CH_3Cl + hv \rightarrow \bullet CH_3 + \bullet Cl \qquad (4)$$

Reactive chlorine species participate in the catalytic ozone destruction. Chlorine is responsible for about 10% of the total ozone destruction. The destruction mechanisms involving chlorine can be described as follows (equations 5.1-5.3):

$$\bullet Cl + O_3 \rightarrow ClO\bullet + O_2 \qquad (5.1)$$

$$\underline{ClO\bullet + O \rightarrow \bullet Cl + O_2} \qquad (5.2)$$

$$O + O_3 \rightarrow 2\ O_2 \quad \text{net reaction} \qquad (5.3)$$

There are also other catalytic cycles for ozone destruction, which can include bromide radicals, hydroxyl radicals or nitric oxides, but the net reaction is usually the same.

1.3 Chloromethane in the terrestrial environment

Land ecosystems, especially in tropical and subtropical regions, were recently identified as the main source of CH_3Cl (Rhew et al. 2000, Yokouchi et al. 2000, Saito and Yokouchi 2006, Yokouchi et al. 2007). The emissions are mostly connected to the vegetation but also to the soil to a minor extent. The main processes leading to CH_3Cl emissions or degradation in land-based ecosystems are described below.

1.3.1 Formation

1.3.1.1 Soil

Soils are highly complex, heterogenic environments consisting of varying amounts of mineral matter, organic matter, air, and water. They provide a living space for a vast majority of organisms from simple bacteria to fungi and higher animals, such as insects and worms. Therefore, it is not surprising that soils play a complex role in the cycling of CH_3Cl.

The role of soils as sinks or sources for CH_3Cl was previously introduced in terms of atmospheric cycling of CH_3Cl. The production of CH_3Cl is normally associated with soil organisms. For example, fungi belonging to *Basidiomycota* produce various chlorinated substances. Many of these substances have strong antibiotic activities. From the beginning of the 1970s, many investigators have recorded CH_3Cl emissions from different fungal cultures, especially from *Hymenochaetaceae* (Watling and Harper 1998). This family of fungi effectively converts Cl^- to CH_3Cl, especially in a cellulose-based growth media. The species *Phellinus* is particularly effective in making this conversion. This species tends to dominate over *Hymenochaetaceae* species in the tropics (Watling and Harper 1998). Almost all of the CH_3Cl-producing fungal families are white-rot fungi, which are specialised in the degradation of lignocellulose from plant debris. Although the biosynthetic route of CH_3Cl formation in fungi is still not completely resolved, many investigators believe that it is linked to S-adenosylmethione (SAM) activity (Watling and Harper 1998, Saxena et al. 1998). In addition, CH_3Cl seems to have an important metabolic role in the methylation of aromatic acids and in the biosynthesis of veratryl alcohol, which is central in the degradation of lignin. However, CH_3Cl is not the exclusive methylator in white-rot fungi, as they also produce at least two types of SAM-dependent O-methyltransferases (Coulter et al. 1993, Jeffers et al. 1997). Many questions considering fungal CH_3Cl metabolism remain, such as why certain fungal species release substantial amounts of CH_3Cl and others utilise the gas so efficiently that no emission can be detected.

Fungi emitting CH_3Cl are often associated with forested areas, because of their role as lignocellulose degraders. However, soil-derived emissions are also recorded in areas lacking trees. Manley et al. (2007) observed that about 8% of the total CH_3Cl emissions of a coastal salt marsh derived from unvegetated areas. They concluded the emissions to be of microbial origin, possibly from ectomycorrhizal fungi, which Redeker et al. (2004) previously reported to produce halomethanes. Soil having no vegetation coverage is still penetrated with roots and microbes.

Its possible abiotic formation is another interesting aspect of CH_3Cl formation in soils. Keppler et al. (2000) suggested a mechanism for a chemical reaction leading to CH_3Cl production in soils. They hypothesised that oxidation of soil organic matter catalysed by redox-active metals and in the presence of a substantial amount of halide ions would lead to halomethane formation. This hypothesis was simulated using purely chemical constituents in laboratory conditions (e.g., phenolic organic matter source, halide ions as potassium salts and ironhydrite as the mineral phase), which led to halomethane formation. Therefore, it is likely that chemical (i.e., abiotic) mechanisms for halomethane formation exist; it is only questionable how relevant the produced halomethane amounts are in comparison to those from biological production.

1.3.1.2 Plant material

Higher plants comprise the biggest single land-based CH_3Cl source (Table 1.2). Substantial CH_3Cl emissions have been recorded from many different species of living and dead plant material over the last decade (Hamilton et al. 2003). The production of halomethanes seems to be a common trait in many plant families, but their biosynthesis and roles within the plant remain uncharacterised. There are three main explanations for halomethane formation in plants: i) a metabolic accident resulting from a high amount of halogen ions in the plant tissue; ii) plants synthesise halomethanes through a specific pathway; or iii) halomethanes are formed abiotically in plants. There is evidence supporting all of these theories, so none can be completely ruled out. The observations supporting chemical formation of CH_3Cl are based on the isotopic

signature of carbon in the emitted CH_3Cl. The use of isotopes as a tool in finding out the origin of substances is widespread in geochemistry. Stable carbon isotope ratios (^{12}C /^{13}C) have been especially useful in biomarker studies. Atmospheric CH_3Cl emitted from coastal salt marshes was found to be relatively light or depleted in $\delta^{13}C$. The $\delta^{13}C$ was measured to be -65‰ (Bill et al. 2002), and the overall $\delta^{13}C$ of the biomass of C3 plants from this area was reported to be -27‰ (Rhew et al. 2002). The emitted CH_3Cl is clearly depleted in ^{13}C compared to the plant biomass, supporting i) biological production (enzymatic reactions favour ^{12}C over ^{13}C) and indicating that ii) the methyl source for CH_3Cl is depleted in ^{13}C. These results confirm the biological nature of these emissions, but they do not clarify the production mechanism of CH_3Cl in plants. Keppler et al. (2004) reported data from determining $\delta^{13}C$ signatures of different methyl pools in plants. Interestingly, they found that pectin, one of the major plant C1 pools, had a $\delta^{13}C$ signature of -78.3 ‰ (mean measured from C3 plants). Earlier work from Hamilton et al. (2003) reported that plant chloride was methylated by pectin at least in detached and senescent leaves and that this process was more efficient when the temperature was increased. Although these studies provide solid evidence for abiotic CH_3Cl formation, the effectiveness of this process in living plants and at ambient temperatures remains unknown.

1.3.1.3 Formation mechanisms

Living organisms contain a variety of enzymes capable of catalysing halogenation reactions (van Pee and Unversucht 2003). There are over 3500 naturally formed halogenated compounds identified so far (Gribble 1998, 2003 and 2004). Many fungi and macro algae produce polyhalogenated substances, which are the result of haloperoxidase activity. The production of monohalomethanes, such as CH_3Cl, is probably a result of methyltransferase activity (Manley 2002). Manley (2002) suggests that monohalomethanes evolve when ubiquitous halide ions are inserted into the active sites of numerous methyltransferases. In addition, genetic evidence supports methyltransferases as being key to halomethane formation. For example, when methyltranferases capable of catalysing the S-adenosyl-L-methionine (SAM)-dependent

methylation of halides is disrupted, halomethane production of the plants was largely eliminated (Rhew and Östergaard 2003). This study used *Arabidopsis thaliana* as a model plant, and it remains unclear if this genetic control mechanism works in the same way as in other plants capable of halomethane production. Nevertheless, methyltransferase activity has been identified in many saltmarsh plant species (Wuosmaa & Hager 1990, Saini et al. 1995) producing substantial amounts of halomethanes.

Halomethanes are so-called secondary metabolites in plants, meaning that they are not produced by the primary metabolism, which is associated with basic metabolism (photosynthesis, respiration, and production of common intermediates, such as proteins, lipids etc.). The role of halomethanes as secondary metabolites has yet to be unravelled. Because halomethane production was first recorded from salt-loving (halophytic) plant species (Rhew et al. 2000), it was suggested to be a mechanism for elimination of halide ions from the cell. Since these first observations, halomethane emissions have been detected from many different plant species, including several not halophytic, which makes it improbable that desalinisation of the cells causes production. Moreover, the amount of produced halomethanes is too low to make the reaction effective as a removal strategy of excess halides (Rhew et al. 2002). Many biologically produced halogenated (especially chlorinated) compounds have antibiotic activity (Gribble 1998), so it was also suggested that halomethane production gives an advantage to the plant individual by fighting against parasitic microbes. Chloro- and bromomethane are toxic to many organisms, and CH_3Br was used until recently as a pesticide in agriculture (Bill et al. 2002). However, monohalomethanes are extremely volatile and transported rapidly away from the area where they were produced, making it difficult for the plant to maintain concentrations in the natural environment high enough to induce antibiotic activity. The production of monohalomethanes either as desalinisation agents or for protection against microbial attack does not seem to be a totally satisfying explanation and needs further investigations.

In light of the current knowledge, there are two mechanisms mainly responsible for the plant material associated with monohalomethane production. In living

plant tissue, this process is most probably connected to the activity of SAM-utilising methyltransferase enzymes. By contrast, in senescent plant material, the halogenation of plant pectin methyl groups might have significant roles. However, both living and especially deteriorating plant material can be colonised by micro-organisms and it is nearly impossible to differentiate between emissions from the plant itself and those from possible epiphytic microorganisms. Leaf-cutter ant colonies were recently observed with elevated halomethane concentrations in their vicinity, implying that these widespread insects could be a novel source for several halogenated organic compounds, including CH_3Cl (Mead et al. 2008).

1.3.2 Degradation

In the following sections, biological (microbial) CH_3Cl degradation in soils is introduced. Abiotic degradation is omitted because there is no documented information about possible abiotic processes occurring in soils degrading relevant amounts of CH_3Cl or other halomethanes. Depending on the prevailing conditions in the soil environment, CH_3Cl degradation can proceed either as an aerobic (oxidation) or anaerobic (reduction) process.

1.3.2.1 Aerobic processes

In so-called “dryland” ecosystems where molecular oxygen is present, both CH_3Cl and generally halomethane degradation proceed as oxidation processes, leading to the formation of carbon dioxide (CO_2). Aerobic methylotrophic bacteria are the microorganisms in soil environments responsible for the majority of halomethane degradation (McAnnulla et al. 2000, Miller et al. 2001, Schäfer et al. 2007). Many of the isolated methylotrophic microbial strains are facultative methanotrophes, meaning they can grow using monohalomethanes and most commonly CH_3Cl as their carbon and energy source (Schäfer et al. 2007). Most of the isolated microbial strains capable of halomethane degradation belong to the *Hyphomicrobium* or *Methylobacterium* families, but there are also bacterial strains in *Aminobacter* and even in *Pseudomonas* that are capable of growing on CH_3Cl.

Studer (2001) extensively studied the genetic regulation of CH_3Cl oxidation by *Methylobacterium chloromethanicum* CM4-strain and identified the genes cmuA and cmuB to be essential for CH_3Cl oxidation. When these genes were disturbed, the bacteria lost their ability to grow on CH_3Cl. The utilisation of CH_3Cl is usually thought to be connected to methanemonooxygenase activity, but it is evident that other metabolic routes are also associated.

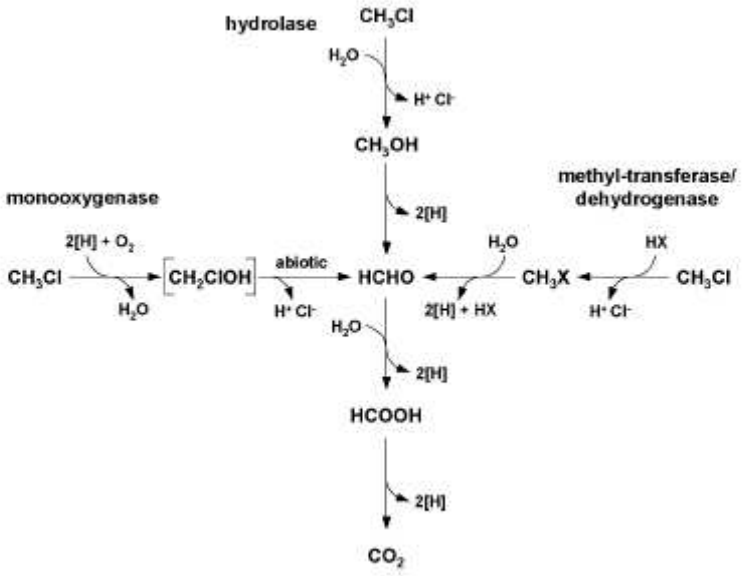

Figure 1.3 Possible CH_3Cl degradation pathways as suggested by Studer (2001).

Studer (2001) proposed three probable mechanisms for CH_3Cl metabolism in methylotrophs, all leading to the formation of formaldehyde (Figure 1.3). Monooxygenation of CH_3Cl would result in the formation of an unstable chlorohydrin compound, from which formaldehyde would be spontaneously formed. Substitutive hydrolytic dehalogenation would yield methanol and HCl without a requirement for molecular oxygen. This kind of mechanism was demonstrated for *Xanthobacter autotrophicus*, a bacterium growing solely on 1,2-dichloroethane (Janssen et al. 1994). The third possibility for methylotrophs might be a methyltransferase/dehydrogenase mechanism, in which formaldehyde would be produced without the formation of methanol as an intermediate. The third mechanism was found to be the most probable for CH_3Cl dehalogenation by the *Methylobacterium chloromethanicum* CM4-strain

(Studer 2001). It remains unknown how common this methyltransferase based mechanism is in methylotrophs, but many other methylotropic bacteria use the monooxygenase route, and some nitrifying bacteria follow the ammonia monooxygenase route (Schäfer et al. 2007).

Aerobic CH_3Cl-degrading microorganisms have been found in a wide range of environmental compartments, such as agricultural, woodland, and industrially contaminated soils, activated sludge, lake sediments, and estuarine and seawater samples (McAnnulla et al. 2001). In light of the current research, aerobic degradation seems to be the most common mechanism other than anaerobic degradation. Aerobic and anaerobic mechanisms sometimes can be difficult to separate fully from each other, because degradation can occur reductively under aerobic conditions or oxidatively under anaerobic conditions (van Pee and Unversucht 2003, Figure 1.3.). The division used in this chapter is based on the environmental conditions rather than on the chemical nature of the degradation pathway.

1.3.2.2 Anaerobic processes

Anaerobic reductive dehalogenation or halorespiration is coupled to energy metabolism. The halogenated substance, like tetrachloroethane or trichloroethane, functions as a terminal electron acceptor during the oxidation of an electron-rich compound, like hydrogen or organic matter (OM being the most probable electron source in soil) (Schumacher et al. 1997, Wohlfahrt and Diekert 1997). Reductive dehalogenase enzymes have been isolated from several bacteria, such as *Dehalococcus ethenogenes* or *Desulfitobacterium dehalogenans* (van Pee and Unversucht 2003). Many of the organisms reported to be capable of anaerobic dehalogenation have been isolated in contaminated soils, sewage sludge or aquifers and utilise polyhalogenated or halogenated aromatic compounds. It remains unknown if these bacteria can utilise monohalomethanes in the same way as polyhalogenated and halogenated aromatic compounds. At least one strictly anaerobic bacterial strain has been reported to grow solely on CH_3Cl. This *Hyphomicrobium* MC strain is a

homoacetogenic bacterium and was found in activated sludge (Traunecker et al. 1991).

Marine and coastal sediments or soils are usually very sulphur rich and emissions of various reduced sulphur gases have been recorded from these environments (Kelly and Smith 1990). Many bacteria capable of halomethane degradation are sulphate reducers. Monohalomethanes CH_3Cl and CH_3Br have been suggested to be transformed to methylated sulphur gases methanethiol (CH_3SH) and dimethyl sulphide ($(CH_3)_2S$) via anaerobic bacteria (Braus-Stromeyer et al. 1993 and Oremland et al. 1994). In a later study, it was concluded that the degradation process was initiated by nucleophilic substitution of the halogen ion with sulphide to form methanethiol, which can be metabolised by methanogenic and sulphate-reducing bacteria. Although the initiation reaction is abiotic, the activity of the anaerobic bacteria greatly enhanced the halomethane transformation.

The reported information concerning the degradation of CH_3Cl or other monohalomethanes in anaerobic soils under natural conditions is rather scarce, which is unfortunate because coastal terrestrial ecosystems (substantial sources of CH_3Cl) are often exposed to water logging. Because they are repeatedly inundated by the tidal movement, these soils experience periods of varying length under anaerobic conditions and with anoxic reactions governing the transformation of the chemical compounds present in the soils.

1.4 Introduction – summary

Chloromethane (CH_3Cl) is a chemically inert gaseous compound mostly found in the atmosphere. It accumulates in the troposphere and is transported to the stratosphere. After reaching the stratosphere, CH_3Cl breaks down to produce active chlorine forms, which enhance ozone destruction processes. Chloromethane is the largest single chlorine gaseous source for the stratosphere. The biggest sources for CH_3Cl are natural, especially living and dead plant material. The atmospheric CH_3Cl concentration is also governed by the strength of its sinks. One of the largest CH_3Cl sinks is soil, which is

associated with the biological activity of soil microorganisms. Soil microbes are ubiquitous and are able to degrade CH_3Cl with both aerobic and anaerobic reaction pathways.

2. Aims and Objectives

The aims of this study were to provide information on CH_3Cl emissions from a new climatic zone (the boreal zone), to determine the influence of soil parameters in the overall emissions and to discover metabolic traces of CH_3Cl formation in plant material. To achieve these goals, three sampling campaigns were made; the first two were to collect emission and soil data, and the third was to collect plant material for the analysis of the plant lipid content. The emission measurements and soil sampling had the following objectives:

i) identification of the main volatile organic substances emitted from the investigated sites;

ii) record the daily patterns and magnitudes of CH_3Cl emission fluxes from several vegetation types and soil moisture regions in the study site;

iii) characterisation of soil parameters under each vegetation type; and

iv) obtain information of CH_3Cl degradation processes in the soils.

Reduced sulphur gases, carbon disulphide (CS_2) and dimethyl sulphide (DMS) were quantified parallel to CH_3Cl emissions because they were emitted abundantly from the sampling site. They might elucidate the on-going processes in the studied soil-plant systems and provide an explanation for the changes in the CH_3Cl fluxes.

The formation pathway of chloromethane in plants has mostly not been elucidated. The pathway is probably connected to the activity of enzymes like haloperoxidase and methyltransferase, but the steps leading to halomethane formation still need to be characterised. In this study, we made an attempt to

find molecular markers that could be linked to the pathway of chloromethane formation. This task was simplified by screening for halogenated compounds in the plant lipid matrix. The discovery of halogenated higher molecular weight compound by introducing a halogenated intermediate of CH_3Cl formation process or by unravelling another plant-derived halogenated compound could help in understanding the chemistry associated to the formation of natural halogenated compounds in plants.

3. Material and methods

3.1 Sampling site

Samples were collected from a coastal meadow located on Jungfruskär Island (60°08`23.94``N; 21°04`39.80``E) in the Finnish Arc hipelago National Park in the Baltic Sea (brackish water, salinity of 6-7.5 ‰ in this part of the Baltic Sea) (Figure 3.1). The islands are rocky, and the covering soil layer is mostly less than one meter thick. These characteristics are a result of the retreating ice mass, which peeled off the loose soil material and exposed the bedrock at the end of the last ice age (10 000 y B.P.). The sampling location is biogeographically situated in the northernmost part of the temperate to boreal transition zone, also called the hemiboreal zone (Ahti et al. 1968). In this region, the duration of the growing season is approximately 180 days per year (Nordseth 1987). The meadow is located on the eastern side of the island. It surrounds a lagoon-like small bay and has an area of approximately 1 ha.

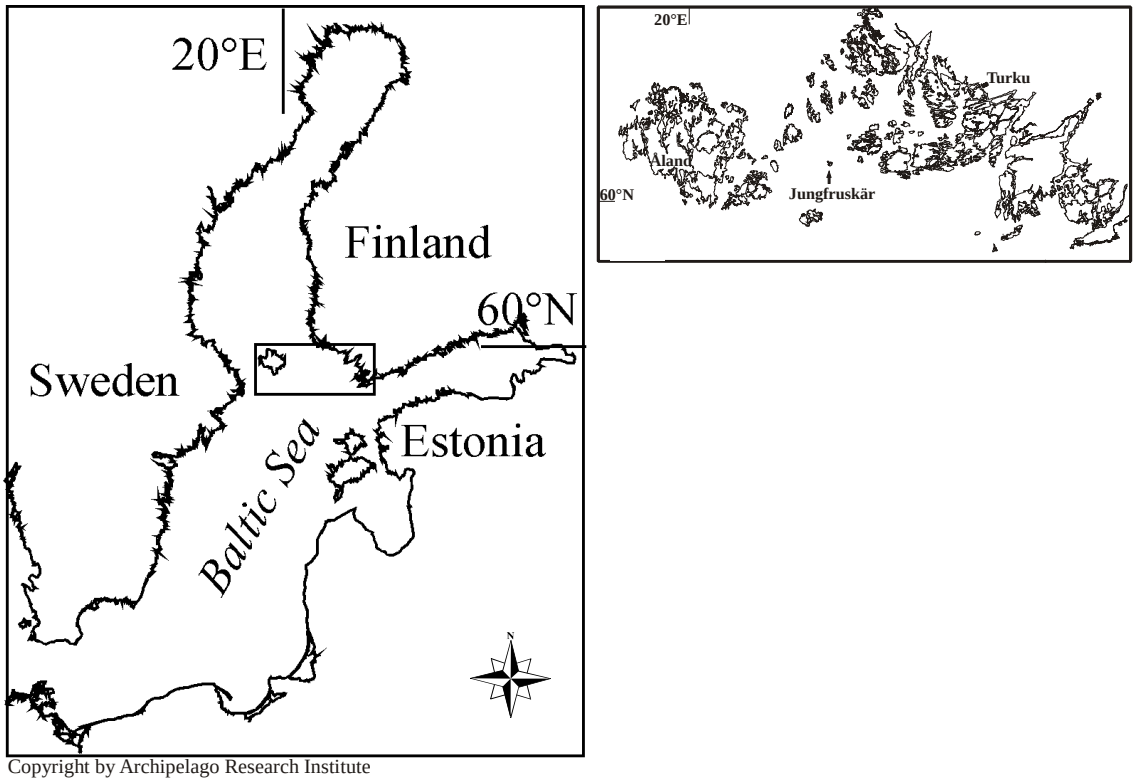

Figure 3.1 Map of the sampling site. The right hand panel shows the location of Jungfruskär in the Archipelago between the Finnish mainland and the Åland islands.

3.1.1 Site description - sampling campaign 2007

3.1.1.1 Vegetation

During the July 10 – 12, 2007 sampling campaign, the seawater level was unusually high and parts of the meadow vegetation were flooded. For the investigations, four sampling sites representing two different kinds of vegetation were chosen (Figure 3.2). In type 1 vegetation, *Salicornia europaea* was almost the only higher plant species present. Type 2 vegetation was a mixture of different plant species and consisted mostly of *Glaux maritime, Juncus gerardii*, *Agrostis stolonifera* and *Carex nigra*. Type 2 vegetation covered about 70-80% of the meadow area, while *S. europaea* grew mostly in a few smaller patches where the vegetation was burned off or in areas that were totally or partly flooded by brackish seawater. *Phragmites australis*, *Eleocharis palustris*, *Odontites littoralis* and *Carex panicea* were other species growing in the meadow.

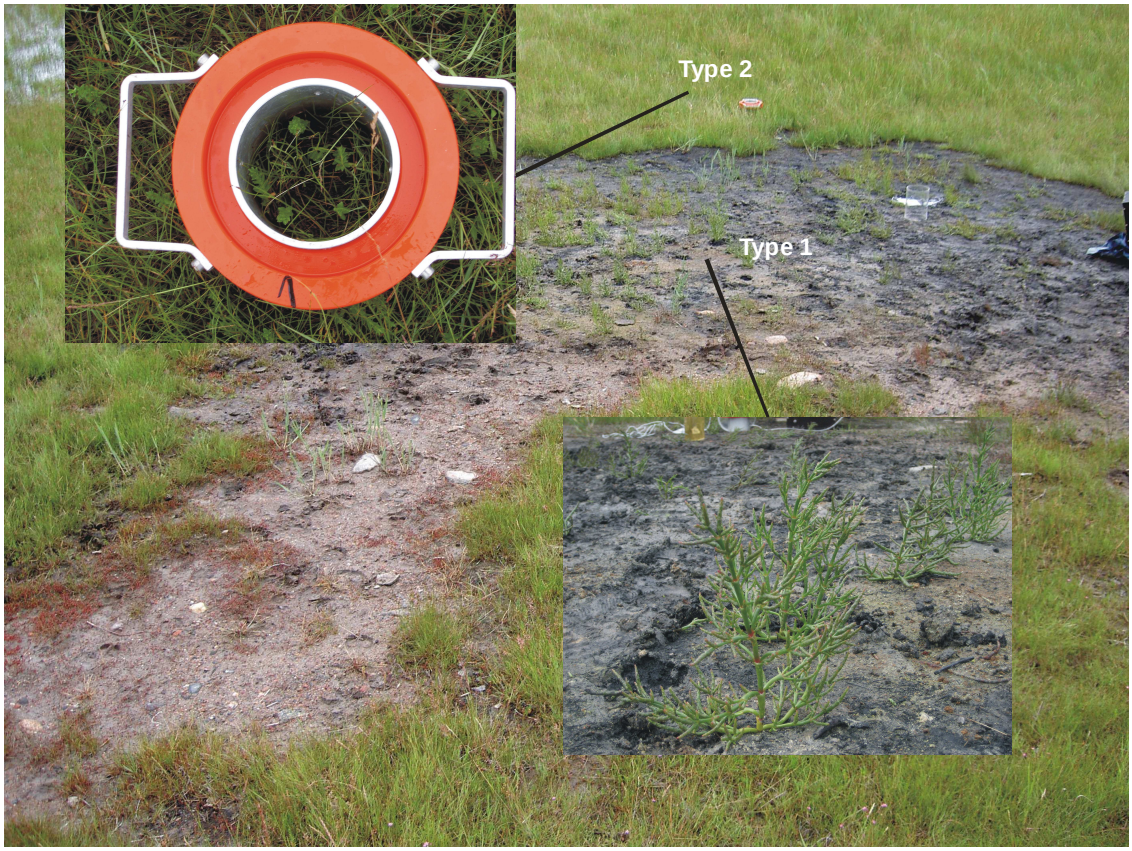

Figure 3.2 Sampled vegetation types.

3.1.1.2 Soil characteristics

Soil 1 (*S. europaea*) had an approximately 3.5 cm thick surface layer with the uppermost 1 cm enriched with organic material (OM) compared to the lower parts of the layer, where the amount of sand started to increase. This surface layer had a dark black-grey colour. The layer (3.5 - 7 cm) beneath the surface layer was pale yellow-brown and quite coarse in texture, and included several small stones. Right below the sandy layer, a grey clay layer began. Only the surface soil to about 20 cm depth was sampled and, therefore, the thickness of the clay layer could not be determined as it went deeper than the sampling depth. In the organic layer, the plant root growth was mostly shallow and near the soil surface. There were very few roots in the sandy horizon and no visible roots in the clay layer.

Soil 2 (mixed vegetation) had a thicker surface layer (about 7.5 cm) rich in OM and contained plenty of roots. The second visually distinct layer was a pale grey mixed sand/clay layer that also contained roots and appeared to have a higher water content and lower density than the clay layer in soil 1. This layer also extended beyond our sampling depth of 20 cm. The organic layer in soil 1 was thinner than in soil 2 because the recent burning of the surface vegetation had destroyed most of the decomposed organic material.

Both soils had a near neutral pH (Table 3.1) and could be classified as neutral chloride soils according to Siira (1984, 1985). The largest difference between the soil samples was in the TOC, which was three times higher in soil 2 than in soil 1. Furthermore, the concentrations of chloride and iron as well as the EC value were also somewhat higher in soil 2 than in soil 1, whereas the pH was lower.

Table 3.1 Soil parameters from the soil surface layers under the two vegetation types.

	pH	**$EC_{1:5}$** mS cm^{-1}	**TOC** %	**Mn/Fe** µg g^{-1}	**Cl^-** mg g^{-1}
Soil 1 *(S. europaea)*	6.7	1.9	3.2	1.2/11.4	2.4
Soil 2 (Mixed vegetation)	5.9	3.1	11.0	0.9/16.6	3.4

3.1.2 Site description sampling campaign 2008

3.1.2.1 Vegetation

The second sampling campaign was conducted on July 5 - 9, 2008. At this time, the whole meadow area was clearly drier than during the first sampling, and the shoreline had retrieved several meters compared to the year before. In addition, a part of the meadow vegetation was already harvested as a part of the management of this biotope. The harvested area was approximately 60 – 70% of the total meadow area. During this sampling campaign, two types of measurements were conducted: background and chamber-based emission measurements. In background measurements, the air above the meadow was sampled at two heights (0.5 m and 1.5 m). A location near the forest line in the southwest corner of the middle meadow was chosen for these measurements. Attention was paid to choose a location so that the air sweeping over most of the meadow by the generally north to northeast coming wind would be caught. Three different sites, representing different vegetation types and soil moistures, were selected for vegetation incubations. These sites are named sites 3, 4 and 5 to avoid confusion in later chapters of this work. Site 3 (Figure 3.3 A) was located nearest to the shoreline in immediate vicinity of the hydrolittoral *Phragmites australis*-dominated zone. The main species in this site were *Eleocharis palustris*, *Carex panicea* and *Phragmites australis*. Site 4 (Figure 3.3 B) was located approximately 10 m northwest from site 3 and had vegetation similar to the vegetation type 2 in 2007. Site 5 (Figure 3.3 C) was at a similar location as vegetation type 1 in 2007, and it contained a burned patch that was growing *S. europaea* solely and had a very coarse mineral soil practically devoid of any organic-rich layer. The sites were selected so that they would present a moisture gradient, with site 3 being the wettest and site 5 the driest. At each site, three parallel plots were sampled, resulting in a total of 9 sampled plots.

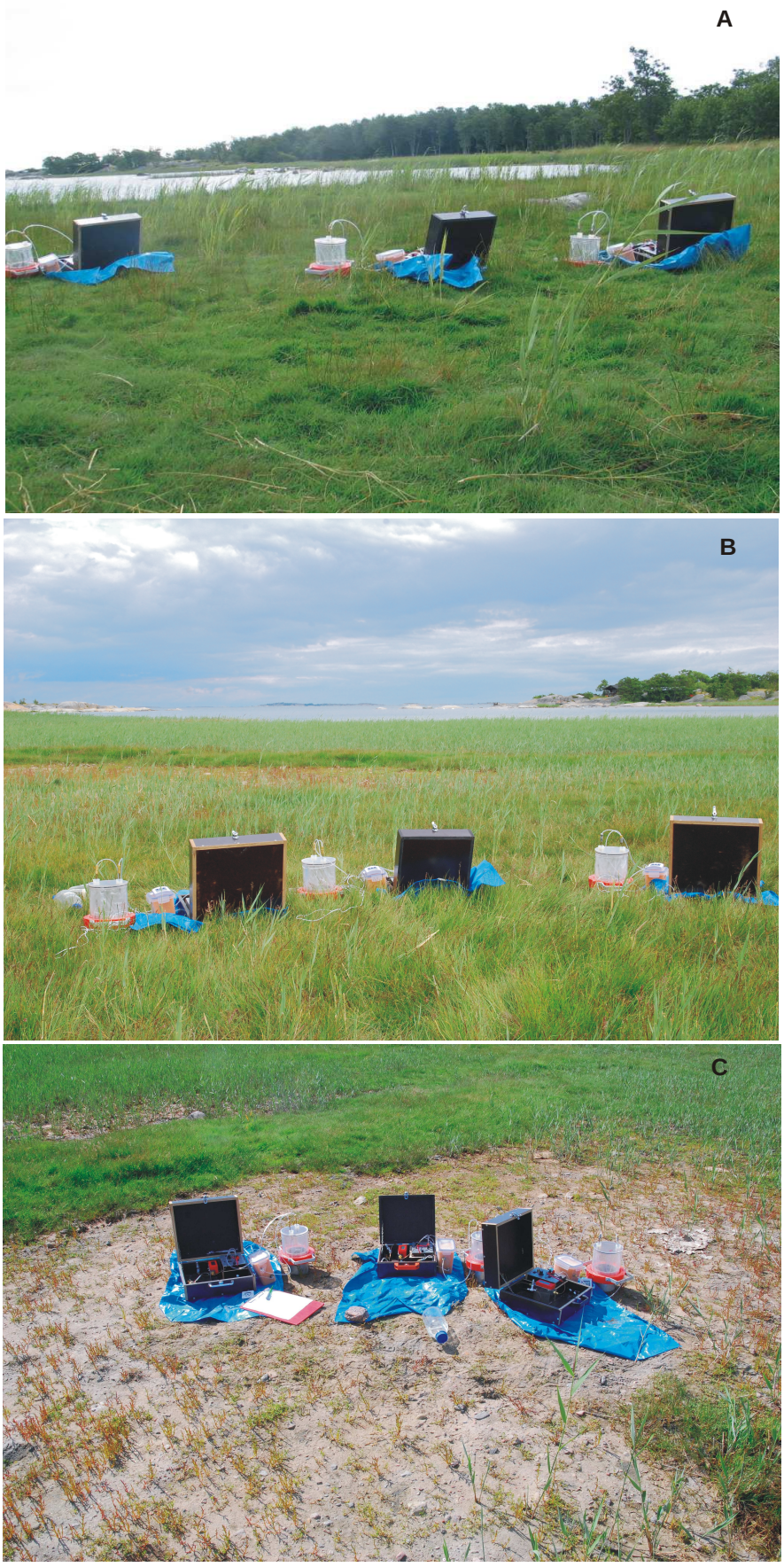

Figure 3.3 Sampled vegetation types A) site 1 B) site 2 C) site 3

3.1.2.2 Soil characteristics

Site 3 (*Eleocharis palustris*, *Carex panicea* and *Phragmites australis*) had a soil (soil 3) with a 8- to 9-cm thick organic matter-rich surface layer, which included several poorly degraded pieces of *Phragmites australis* stems. This layer had a very dark brown almost black colour and a high amount of roots. The surface layer was followed by a coarse sand/gravel layer and a clay layer corresponding to the soil samples from the 2007 sampling campaign. Soil 4 (site 4; *Glaux maritima*, *Juncus gerardii*, *Agrostis stolonifera* and *Carex nigra*) had similar layering as the soil 2 sample from the 2007 sampling campaign, but the organic-rich surface layer was approximately 4 cm thick. Soil 5 (site 5; *S. europaea*) might be described as a pure mineral soil, it had no visually distinct organic matter rich layer, but a 7- to 8-cm thick pale grey sandy surface layer followed by a dense clay layer. In fact, soil 5 had a total organic carbon (TOC) content of only 0.4 % (Table 3.2), corresponding to an organic matter content of 0.7 % (OM = 1.7 x TOC). Soils 3 and 4 had high organic matter contents of 39.4 and 30.3%, respectively. The loss on ignition (LOI) can also be used to describe the organic matter content of the soil. The measured LOI was higher for soil 4 than for soil 3 (Table 3.2), contradicting the results from the TOC measurements. The total organic nitrogen (TON) content of soils 3 and 4 were not markedly different from each other. As expected, soil 5 had a very low TON value.

Table 3.2 Loss on ignition (LOI), total organic nitrogen (TON), total organic carbon (TOC) and the carbon/ nitrogen ratio of the soil samples.

	LOI % *	**TON %***	**TOC %***	**C/N**
soil 3	10.8	1.4	23.2	16.9
soil 4	14.4	1.3	17.8	13.6
soil 5	1.2	0.1	0.4	6.1

*) LOI, TON and TOC are all mass percents according to the soil dry weight.

Visual observation showed that soil 3 was the wettest of the investigated soils; water percolated onto the surface of the soil if it was stepped on, and this soil had the highest water content (Table 3.3). Soil 3 had the lowest pH and was clearly an acidic soil; by contrast, soil 4 was only moderately acidic, and soil 5 had a neutral pH (Table 3.3). Soils 3 and 4 with high OM contents also had higher extractable iron and manganese concentrations (Table 3.3), indicating

organic matter playing a major role as a metal ion-binding site in these soils. The particle size distribution of the mineral matter in all soils gave a relative uniform picture (Table 3.4) with all having around 50% medium sand content. Soil 3 also had a large portion of fine sand, and soils 4 and 5 had almost equal amounts of coarse and fine sand. Therefore, all three soils are sand soils according to their mineral matter particle size distribution. Because of its coarseness (small surface area), mineral matter probably has only a minor role in soil reactions. All soil samples had less than 1% fine particles (i.e., particles less than 0.06 mm in diameter).

Table 3.3 Iron and manganese concentrations, pH, electrical conductivity (EC) and moisture of the soil samples.

	Fe (µg g^{-1})	**Mn (µg g^{-1})**	**pH**	**EC (mS cm^{-1})**	**H_2O (mass %)**
Soil 3	19.62	0.04	4.9	8.8	81.9
Soil 4	39.71	0.53	5.7	11.0	65.3
Soil 5	7.99	0.10	7.0	2.0	7.1

Table 3.4 Particle distribution of the mineral matter of the soil samples.

	Fine gravel [*] (mass %)	**Very coarse and coarse sand (mass %)**	**Medium sand (mass %)**	**Fine and very fine sand (mass %)**
Soil 1	-	8.3	51.3	40.5
Soil 2	-	30.0	50.2	19.8
Soil 3	1.1	26.6	46.5	25.8

[*)] Particle size categories according to USDA (United States Department of Agriculture) particle size limits: fine gravel 10 – 2 mm, very coarse and coarse sand 2 – 0.5 mm, medium sand 0.5 – 0.35 mm and fine and very fine sand 0.35 – 0.05 mm. The results reported in Table 5.3 were obtained using a European sieve series, resulting in categories > 2 mm, 2 – 0.63 mm, 0.63 – 0.2 mm and 0.2 -0.06 mm, which do not exactly correspond to the USDA divisions. However, the difference is very small and does not have a practical relevance considering the division for the particle size classes.

3.2 Gas sampling

3.2.1 Sampling system

Gas fluxes were recorded using a dynamic closed chamber method. Our chambers consisted of a transparent acryl glass cylinder (diameter of 14.4 cm, wall thickness of 0.3 cm, and height of 15.0, 20.0 or 30.0 cm) with a lid of the

same material mounted on an aluminium-plastic base. The base was constructed from an aluminium tube (diameter of 11.0 cm), which was surrounded by a plastic ring. The junction was made gas-tight with silicon gum. The plastic ring had a 2 - 3 cm-wide channel in which the acryl glass cylinder was placed. When the cylinder was in place, the channel was filled with saturated sodium chloride solution to assure a gas-tight seal and to prevent the dilution of gas in the sealing liquid. Acryl glass was chosen for the chamber material as it has almost the same inertness and density as mineral glass but is lighter and less fragile. It also shows a smaller absorbance of sunlight by letting through UV wavelengths that do not penetrate mineral glass. Hence, the light conditions during the enclosure were kept as natural as possible. In the 2008 campaign, the cylinders where lined with transparent Tedlar® foil to further reduce the possible adsorbance of the target compounds on the chamber inner walls.

Next to the chamber, the sampling system (Fig. 3.4) consisted of a moisture trap made of a plastic tube (229 mm x 38 mm) with aluminium ends filled with $Mg(ClO_4)_2$ granules, a stainless steel adsorbent tube (178 mm, OD 1/4´´, Gerstel), a regulation valve (Swagelok®), a thermal flow meter with totalisator (Profimess GmbH, Bremerhaven, Germany) and a membrane pump (KNF Neuberger GmbH, Freiburg, Germany). Different parts of the system were connected with Silcosteel®-coated stainless steel tubing (1/8´´) and gas-tight Swagelok® fittings or Tygon® tubing in places where more flexibility was needed. The tightness of the fittings was tested in the laboratory before sampling by placing the chamber on its collar in a basin filled with a saturated NaCl solution and letting the whole sampling system (collar, chamber and pump) to fill with helium. The tightness of the fittings was then detected by searching for leaking helium with a portable hand-held leak detector (Varian Inc. Scientific, Lake Forest, CA, USA). The adsorbent bed was made of a combination of three adsorbents: Tenax TA, Carboxen 569 and Carboxen 1018 (all from Supelco, Bellefonte, PA, USA). In the 2008 sampling campaign, the $Mg(ClO_4)_2$ granule-moisture trap was replaced with a Nafion® drier (DM™-series, Perma Pure LLC, Toms River, NJ, USA) placed in a desiccant (Silica gel) bed. Also, the Silcosteel®-coated stainless steel tubing was replaced with

(1/8´´) PFA tubing to make the system easier to handle. The PFA tubing is less rigid than steel tubing, which makes the whole system very flexible.

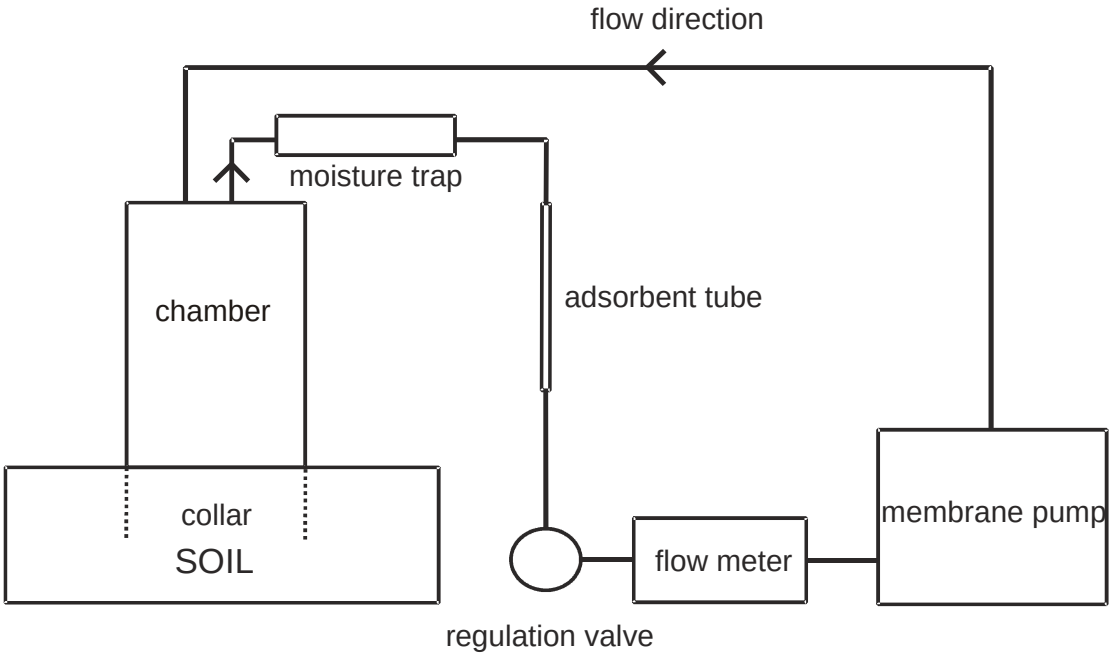

Figure 3.4 Schematic presentation of the closed chamber system.

3.2.2 Sample collection

In July 2007, the emission cycles (24 h) were measured for the two vegetation types. The emissions were recorded at five and six different time points for the *S. europaea* sites and mixed sites, respectively, as well as on five occasions during the day for control (no vegetation) enclosures. We tried to perform the vegetation and control incubations as evenly spaced as possible throughout the days and nights. At every sampling time point, parallel samples were taken (i.e., two plots of the same vegetation type were sampled simultaneously).

The aluminium base was inserted into the soil to a depth of 2-5 cm, and the cylinder was placed on the base channel and sealed as described above. The emission samples were collected on a mixed adsorbent bed (see below) by pumping the air from the chamber through the adsorbent tube continuously for two hours. The pump was turned on immediately after the placement of the chamber on its base. The sampling flow was kept at 50-60 ml min^{-1} during the

pumping. When the collection time was completed, the adsorbent tube was closed with 1/4´´ Swagelok® fittings with Teflon® ferrules and stored in a cool box until analysis in the laboratory. After the sampling time was completed, the chamber was removed from the base to allow the air surrounding the plant to mix with the ambient air. After the sampling period was completed for a given site, the plant material inside the enclosure was harvested for determination of the biomass.

During the 2008 sampling campaign, the background air concentration of CH_3Cl was recorded four times a day simultaneously at two different heights (0.5 m and 1.5 m) during two days. The sampling time points were 2:00-3:00, 10:00-11:00, 12:00-13:00 and 14:00-15:00 local time.

For chamber measurements in 2008, three parallel incubations were made with two simultaneous control incubations. In the control incubations, the chambers and bases were placed on a plastic dish, which was filled with a saturated NaCl solution. Chamber measurements were conducted three times a day (2:00-3:00, 10:00-11:00 and 12:00-13:00) on three successive days (one day for each site). During the 2008 campaign, the sample collection time was only one hour and the sampling flow was decreased to 30-40 ml min^{-1}. Distinct from the 2007 campaign, the samples were stored in solid CO_2 (-80℃) immediately after the sample collection was completed to assure the stability of the target compounds during storage and before analysis in the home laboratory. Otherwise, the samples were handled as in 2007.

3.3 Analytical methods

The samples were analysed by thermal desorption-gas chromatography-mass spectrometry (TD-GC-MS). Our analytical set-up consisted of a thermal desorption system (TDS 3) and a cold injection system (CIS) (both Gerstel GmbH & Co.KG, Müllheim an der Ruhr, Germany) combined with a gas chromatograph (GC) (Agilent series 6890N) and a mass selective detector (Agilent series 5975B). The adsorbent tube was placed in the thermal desorption (TD) oven (initial T: 20℃), which was then rapidly heated to 300℃

and flushed with helium to release the target compounds. During the entire heating step, the desorption flow was collected on a Tenax TA®-filled liner in the CIS, which was cooled down to -40℃ with liquid nitrogen. After completion of the desorption step of the TD system, the sample was injected to the GC by heating the CIS to 300℃. The GC was equipped with a high-resolution gas chromatographic column (GasPro PLOT, 30 m x 0.32 mm, J&W Scientific) and programmed with the following temperature programme: 40℃ (held 5 min), heated to 220℃ (rate of 6℃ min^{-1}) and held 10 min, and finally heated to 240℃ (rate of 25℃ min^{-1}) and held 10 min. The total run time was 55 min. The GC was operated in constant flow mode with a carrier gas flow of 2.7 ml min^{-1}. The thermal desorption system and cold injection systems were operated in solvent vent mode. The compounds were identified according to their retention times and mass spectra. The mass spectrometer (MS) was operated in scan mode with a range from 33-330 amu. Ionisation was done in electron impact (EI) mode with the energy at 70 eV. The MS interface had a temperature of 250 ℃ and a source of 200℃. The MS parameters stayed the same in both years. Due to further method development, the following changes were made to the TD, CIS and GC parameters for the analysis in 2008. The desorption temperature was decreased from 300℃ to 230℃, both in CIS and TD, to prolong the lifetime of the analytical column. In the higher desorption temperature fractures were often detected on the injector side of the analytical column. The column had a temperature maximum at 250℃, which meant that using 300℃ as the desorption temperature could lead to an accumulation of high boiling point substances on the column surface, potentially resulting in a declining chromatographic separation. The decreased desorption temperature had no influence on the recovery of the target substances from the adsorbent bed. Furthermore, to shorten the time needed to analyse one sample and thus increase the amount of samples able to be analysed during the same time period, we changed the GC temperatures. The programme used in 2008 was as follows: 40℃ to 166℃ (rate of 6℃ min^{-1}) and held for 4.2 min; heated to 240℃ (rate of 25℃ min^{-1}) and held for 10 min. The total run time was reduced to 38 min.

The GC-MS parameters and the choice of the analytical column were based on method development done in a former study at the Institute of Biogeochemistry and Marine Chemistry at the University of Hamburg (Christof, O., 2002). However this study was conducted using different hardware to our study. In the current study, a new GC-MS apparatus was used with the improvement of an automated thermal desorption and cool injection systems, which were controlled together with GC-MS by one software programme (Maestro®, Gerstel GmbH & Co.KG, Müllheim an der Ruhr, Germany). The old software programme required a separate start of the TD and GC-MS, which sometimes led to shifts in the retention times.

To achieve complete adsorption of the highly volatile hydrocarbons in ambient temperatures, strong adsorbent types had to be used. In this study (see section 3.2.1), Tenax TA was the weakest adsorbent and was set to trap mainly higher boiling point substances, which adsorb irreversibly on stronger adsorbent types, therefore blocking their adsorbance sites from the more volatile substances (Brown and Shirey, Supelco Technical Report). Irreversible adsorption can lead to reproducibility problems and ultimately destroy the adsorption capacity of the adsorbent. When taking atmospheric samples, strong adsorbents are always used in combination with weaker ones.

The detected compounds were identified by comparing their recorded mass spectra with those in the spectral library (NIST). Isobutane, butane, and butene and its structural isomer 2-methyl-propene (isobutene) were identified by comparing their retention times with the retention times of gas standards containing butane, butene and their isoforms (C_1 - C_4 alkane and C_2 - C_4 alkene standards, Linde Gas, Germany).

For quantification of chloromethane, carbon disulphide and dimethyl sulphide, one-point calibration with single or multiple compound calibration standards were used (Table 4.1). The calibration standards were measured at least three times daily. A 1000 ppm standard and a 100 ppm standard were used in 2007 and 2008, respectively, for quantification of chloromethane. CS_2 and DMS were quantified only in the 2008 samples. The standards were injected via a 20-µl or

50-µl stainless steel sampling loop (VICI, Valco Instruments Co. Inc., Houston, Texas, USA) for TD-GC-MS. Further details of the analytical method can be found in S. Solloch (in prep.).

3.4 Stability of the target compounds

A storage test was conducted under laboratory conditions to investigate the stability of the target compounds on the adsorbent bed. Altogether, 24 adsorbent tubes were spiked with 50 µl of 100 ppm CH_3Cl, CH_3Br and CH_3I standards and placed in a freezer at -20℃. Three adsorbent tubes were analysed once a week for a three-week time period.

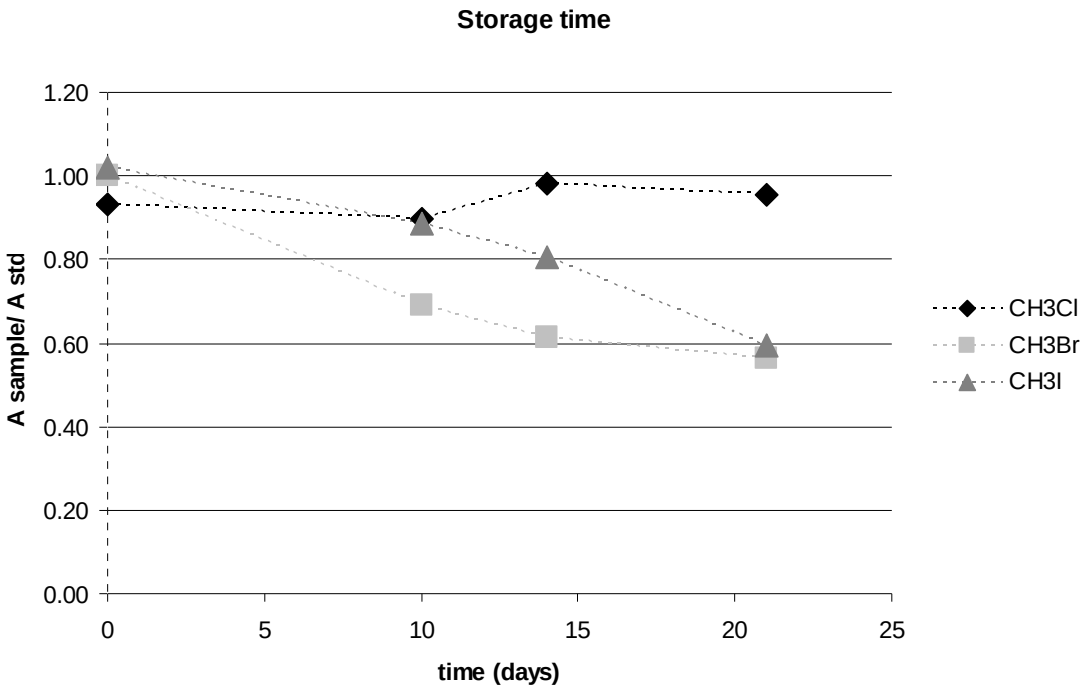

Figure 3.2. Peak area of the target compounds from stability test samples relative to the peak area of the standards analysed on the same day. Three samples were analysed each day.

Only chloromethane remained stable during the three weeks of storage. Bromomethane (CH_3Br) and iodomethane (CH_3I) experienced a relatively rapid concentration loss after three weeks and only 60% of the spiked amount of the compounds could be recovered. The stability of the sulphur-containing gases on

the adsorbent material was not tested. Therefore, the CS_2- and DMS-fluxes might have been underestimated in the calculations.

3.5 Calculation of gas fluxes

The fluxes were calculated with the following equation:

$$\text{Flux} = \{[M_T - M_T^0/(VT\,(1- e^{-JT/V})\,V^2/J)]\,V/A\}\,60\ \text{min},$$

where:

M_T = mass of the emitted target compound in ng collected from the plant during the sampling time t

M_T^0 = mass of the emitted target compound in ng collected from the soil without vegetation during the sampling time t

V = volume of the chamber in dm^3

T = sampling time in min

J = sampling flow in $dm^3\ min^{-1}$

A = area of the chamber base in m^2

When the emissions were normalised to biomass, the term V/A was replaced with V/m, where m represents the dry biomass of the plants harvested at the sampling area.

This equation is valid if the following conditions apply inside the chamber:

1) the target compound flux stays constant during the incubation time,

2) the emitted substance is immediately distributed equally into the whole chamber volume after its liberation and

3) there is a constant laminar air flow sweeping through the chamber.

In 2007, the sampling areas without vegetation were located as close as possible to the corresponding vegetated sampling site. In all cases, the distance between the different sampling spots was less than three meters. A total of five incubations without vegetation at different times of day were conducted over the course of the three days. For calculation of the fluxes, we used the average of these five values. The equation used and its induction are presented in detail in the appendix.

In 2008, the chambers used for the control samples stood on a shallow plastic basin, which was coated with a sheet of Tedlar® foil. The chamber was placed with its base on the foil, and a small amount of saturated salt solution was poured into the basin to seal the chamber base from the surrounding air. The chambers were also placed in close vicinity to the sampling spots with vegetation. For three spots with vegetation, we always had two controls having no plant material or soil inside the chamber. The mean amount of the target compound collected from all control sampling spots was used as M_T^0 in calculating the emission flux rates.

3.6 Soil analyses

In 2007, two soil samples (0-20 cm) were collected under each vegetation type and the soil properties were determined to obtain information on abiotic parameters most likely to affect the chloromethane production and hydromorphological features of the soil. A steel corer (length of 50 cm, diameter of 8 cm) was used for collection. All the analyses except for TOC were conducted on fresh surface layers of the soils, which we considered to be the most relevant for possible chloromethane production (Laturnus et al. 1995). The total organic carbon was analysed from air-dried surface layers. The visual

characteristics of the soil cores (laminas and their colour) were recorded. The determination of soil texture was based on sensory analysis in the field, and no textural analysis was conducted in the laboratory. For the laboratory analyses, the organic soil horizon was separated from the mineral soil, and the plant roots and small stones were then removed. The organic soil material was then homogenised by sieving through 2-mm mesh sieve. The soil under vegetation type 1 (*S. europaea*) is referred to as soil 1 and soil under vegetation type 2 (mixed hay and grass species) is referred to as soil 2.

During the second sampling campaign in 2008, an iron shovel was used to collect a surface soil sample under each vegetation type. After the sampling, the soils were air dried at room temperature (expect for the part used for determining the soil moisture) and homogenised by sieving through a 2-mm diameter sieve prior to analysis. The following parameters were determined: **pH**, **electrical conductivity (EC)**, total organic carbon and nitrogen (**TOC/TON)**, loss on ignition (L.O.I) , water content, mineral matter particle size distribution, and iron (**Fe)** and manganese **(Mn)** concentrations. All the determinations printed in bold were conducted as in the year before, with the exception that the air-dried samples were used.

pH and electrical conductivity

For pH measurements, 1 g of fresh soil was suspended in 2.5 ml of 0.01 M $CaCl_2$, shaken by hand for several minutes and allowed to stabilise for approximately 15 min before dipping the glass electrode into the solution. For electrical conductivity (EC), a soil suspension of 1:5 (w/v) (fresh soil) in milliQ-purified water was shaken by hand and allowed to stabilise for 15 minutes prior to measurement with a conductivity meter (CDM210, MeterLab Radiometer, Copenhagen, Denmark). Both pH and electrical conductivity were determined in triplicate.

Chloride (Cl^-) concentration

The chloride concentration in the suspension used for the EC measurement was measured by pipetting 0.5 ml of the suspension into the analyser vial, and

the analysis was conducted with an MK II Chloride Analyser 926 (Sherwood Scientific Ltd, Cambridge, UK).

Iron (Fe) and manganese (Mn) concentrations

Manganese and iron were extracted according to Niskanen (1989). Soil samples of 2.5 g were shaken in 50 ml of ammonium oxalate (0.029 M $(NH_4)_2C_2O_2$ + 0.021M $H_2C_2O_4$, pH 3.3) for 2 h (150 rpm) in a vertical table shaker, centrifuged, and the supernatants were filtered through filter paper (S & S, Blauband) prior to analysis. The iron and manganese concentrations in the extracts were measured with an ICP-MS (Elan 6000, Perkin-Elmer, USA).

Total organic carbon and nitrogen (TOC and TON)

The total organic carbon (TOC) in the air-dried samples was determined with an automatic TOC analyser (TOC-Vcph + TNM-1, Shimadzu). For soils 1, 2, 3 and 4 300-400 mg of air-dried sieved soil was weighed for the determination. Approximately 1 g of soil 5, which had low organic matter content, was weighed.

For the total organic carbon, iron, manganese and chloride analyses, five determinations were conducted in parallel.

Soil water content

About 5 g of fresh soil was weighed and dried overnight at 105℃. The samples were weighed again and the soil moisture content was calculated by subtracting the dry mass from the fresh mass and dividing by the mass of the fresh soil. The result was then multiplied by 100%. These determinations were carried out in triplicate.

Loss on ignition (L.O.I.)

After drying at 105℃, the soil samples were moved to a muffle oven and heated to 400℃ overnight to burn the organic matter. The loss on ignition was then calculated by subtracting the mass of the burned soil from the mass of the dried soil, dividing by the mass of the dried soil, and then multiplying by 100%. The L.O.I. measurements were conducted in triplicate.

Particle size distribution

A small amount of water (10 ml) was added to the soil samples (10 g) and placed in a 1000-ml decanter vessel and the gained slurry was heated to 70-80℃. Concentrated hydrogen peroxide (H_2O_2) (30%) was added in 10-ml portions to remove the organic matter, which was binding the primary particles in the mineral soil. Hydrogen peroxide (H_2O_2) was continuously added until no organic matter was left in the samples (i.e., foam was not forming inside the glass). After removal of the organic matter, 90 ml of distilled water and 10 ml of 2 M hydrochloride acid (HCl) were added. The acid was added to remove Al-oxides, Fe-oxides and carbonates, which would bind the primary particles to form larger aggregates. The suspension was stirred for a few minutes. The vessels then were filled with distilled water and left aside overnight. The following day, the excess water was removed and 50 ml of 0.05 M sodium pyrophosphate ($Na_4P_2O_7$) was added to enhance the dispersion of the soil particles. The soil slurry was moved to a 400-ml glass cylinder, which was filled with water and stirred throughout. Subsamples were pipetted corresponding to the sedimentation times calculated by Stoke's formula (Scheffer and Schachtschabel 2002). The subsamples were thereafter dried in an oven and weighed to calculate the relative abundances of the particle size fractions.

Stoke's formula presumes that the sedimentation of the particles in the fluid is laminar. This assumption does not apply for particles having diameters bigger than 0.06 mm as these particles sink too fast. Therefore, coarser particle classes were separated using sieves. After the pipetting was completed, the soil slurry was transferred to a 0.06-mm diameter sieve. The suspension was washed under running water. The soil material staying on the sieve was transferred into a decanter glass and dried overnight at 105℃. The following day, the sample including the coarser particles was sieved using a sieve series of 2mm – 0.6mm – 0.2mm – 0.06mm for five minutes and each particle size fraction was weighed.

3.7 Material and methods – summary

Two sampling campaigns were conducted on a boreal coastal meadow in the beginning of July in 2007 and 2008. Gas emissions samples from different vegetations types were collected and analysed. Sample collection was made with chambers in which the vegetation was enclosed and the target compounds were trapped on an adsorbent tube. The samples were analysed in the laboratory with TD-GC-MS. In addition to the gas samples, soil samples were also collected and analysed from five sites located on the meadow. Several parameters including pH, EC, TOC and Fe and Mn concentrations were determined from each of the soil samples.

4. Results

4.1 Chloromethane fluxes

4.1.1. Area-normalised fluxes

The flux measurements in 2007 had a relatively large gap in the site 1 plots between 08:00 and 14:00 local time (Table 4.1), due to our limited amount of sampling equipment at hand, which led to low sampling intensity. The highest flux value for site 1 (841 ng CH_3Cl m^{-2} h^{-1}) was observed between 14:00 and 16:00. From site 2 vegetation, the highest flux value (562 ng CH_3Cl m^{-2} h^{-1}) was recorded in late afternoon between 16:00 and 18:00. The lowest chloromethane fluxes occurred between evening and early morning in sites 1 and 2 (Table 4.1, Figure 4.1 a - c). Site 3 had CH_3Cl emission rates from 3 to 645 ng m^{-2} h^{-1}; the lowest rate was recorded during the night-time measurement (2:00 – 3:00), and the highest rate was recorded at midday. Site 4 had the highest area-normalised net emission of CH_3Cl among all sites; the lowest flux of
26 ng m^{-2} h^{-1} at this site was measured between 2:00 - 3:00 and the highest flux of 1817 ng m^{-2} h^{-1} at 10:00 - 11:00. Site 5 was the only site where an overall negative CH_3Cl flux (-168 ng m^{-2} h^{-1}) was measured during the night-time, but had similar flux rates as sites 3 and 2 (Table 4.1). The emissions between sites 1 and 5 are somewhat difficult to compare (at least during the daytime) due to the lack of data. However, the measured fluxes from site 5 are inside the range of the flux rates measured from site 1.

Table 4.1 Net area-normalised chloromethane fluxes in ng m^{-2} h^{-1} from plant incubations at sites 1 and 2 (2007) and sites 3, 4 and 5 (2008).

Date	**Time**	**Site 1 A**	**Site 1 B**		**Site 1 average**
11/07/07	3-5	337	502	-	419
11/07/07	7-9	63	596	-	329
10/07/07	14-16	865	817	-	841
10/07/07	18-20	138	644	-	391
10/07/07	22-24	117	480	-	299
Date	**Time**	**Site 2 A**	**Site 2 B**		**Site 2 average**
12/07/07	0-2	-	593	-	
12/07/07	4-6	0*	292	-	144
12/07/07	8-10	220	606	-	413
11/07/07	12-14	252	705	-	478
11/07/07	16-18	365	759	-	562
11/07/07	20-22	166	718	-	442
Date	**Time**	**Site 3 A**	**Site 3 B**	**Site 3 C**	**Site 3 average**
7/7/08	2-3	-8	-410	426	3
7/7/08	10-11	659	161	615	478
7/7/08	11-12	109	1482	343	645
Date	**Time**	**Site 4 A**	**Site 4 B**	**Site 4 C**	**Site 4 average**
8/7/08	2-3	-	26	-	-
8/7/08	10-11	290	-	3343	1817
8/7/08	11-12	731	162	3029	1307
Date	**Time**	**Site 5 A**	**Site 5 B**	**Site 5 C**	**Site 5 average**
9/7/08	2-3	-275	-212	-17	-168
9/7/08	10-11	324	449	1123	632
9/7/08	11-12	126	-322	809	204

*) Calculated flux was slightly negative. Because only positive fluxes were considered possible (no mechanism is known for the degradation of chloromethane in plants), the positive flux is given as 0 for this measurement. However, negative fluxes were possible (due to degradation by soil) in 2008 measurements because of differences in sampling methods (see Chapter 3). Note that the 2007 emission fluxes derive from vegetation only and 2008 fluxes are vegetation + soil flux.

The net fluxes showed relatively large differences in magnitude and diurnal distribution between the different sites of the same vegetation type (Tables 4.1 and 4.3, Fig. 4.1 a - b). In site 1, the net emission fluxes varied from 63 to 865 ng CH_3Cl m^{-2} h^{-1} for plot A and from 480 to 817 ng CH_3Cl m^{-2} h^{-1} for plot B. In site 2, the net emissions were between 0 - 365 and 292 - 759 ng CH_3Cl m^{-2} h^{-1} for sites A and B, respectively. In sites 3, 4 and 5, the discrepancies between the parallel plots were the same magnitude as for sites 1 and 2 (Table 4.1). The discrepancies between the parallel plots became smaller when normalised to the dry biomass for site 1 (Figure 4.1 a), but they remained relatively wide for sites 2 (Figure 4.1 b) 3, 4 and 5 (Table 4.3).

4.1.2 Biomass-normalised fluxes

S. europaea (at site 1) had higher tissue water content (Table 4.2 a) than the other sampling sites (Table 4.2 a and b), leading to reduced emission values when the fluxes were related to the fresh biomass. On the other hand, site 1 plots exhibited a higher above-ground biomass than at site 2 (Table 4.2 a), which explains why they had higher area-normalised fluxes than at site 2. The mean flux values normalised to dry biomass showed almost no differences between the two vegetation types (Figure 4.1 c).

Table 4.2 a) Biomass water content and mean above-ground biomass at sites 1 and 2.

	Fresh biomass (g)	**Dry biomass (g)**	**Water content (%)**	**Mean biomass (above-ground)**	
				(kg f.w. m^{-2})*	**(kg d.w. m^{-2})***
Site 1 A *(S. europaea)*	27.2	2.6	90.4		
Site 1 B *(S. europaea)*	40.4	4.0	90.2		
Mean	33.8	3.3	90.3	3.6	0.4
Site 2 A (Mixed)	5.8	1.9	67.0		
Site 2 B (Mixed)	10.0	2.4	76.7		
Mean	7.9	2.1	72.8	0.8	0.2

*) f.w.= fresh weight, d.w.= dry weight

Table 4.2 b) Mean above-ground biomass at sites 3, 4 and 5.

	Mean biomass (above-ground)	
	(kg f.w. m^{-2})*	**(kg d.w. m^{-2})***
Site 3 (Eleocharis palustris cp, Carex panicea sp-cp and Phragmites australis cpp)	1.19 (0.19)	0.32 (0.05)
Site 4 (*Glaux maritima* stcp, *Juncus gerardii* cp, *Agrostis stolonifera* cpp and *Carex nigra*.)	0.83 (0.14)	0.31 (0.01)
Site 5 *(Salicornia europaea)*	0.95 (0.07)	0.12 (0.01)

*) f.w. = fresh weight, d.w.= dry weight
The numbers in parentheses indicate the standard deviation of three replicates for each vegetation type.

There were no significant differences in the amount of biomass enclosed either between the different sites or between plots at the same site for sites 2, 3, 4 and 5 (Table 4.2.b). Site 4 had a biomass density corresponding to that of the mixed site 2, which was expected as the sites had a very similar vegetation species

distribution. However, the *S. europaea* sites of 2007 (site 1) and 2008 (site 5) differed markedly; the 2008 site had only one third of the biomass density compared to the year prior.

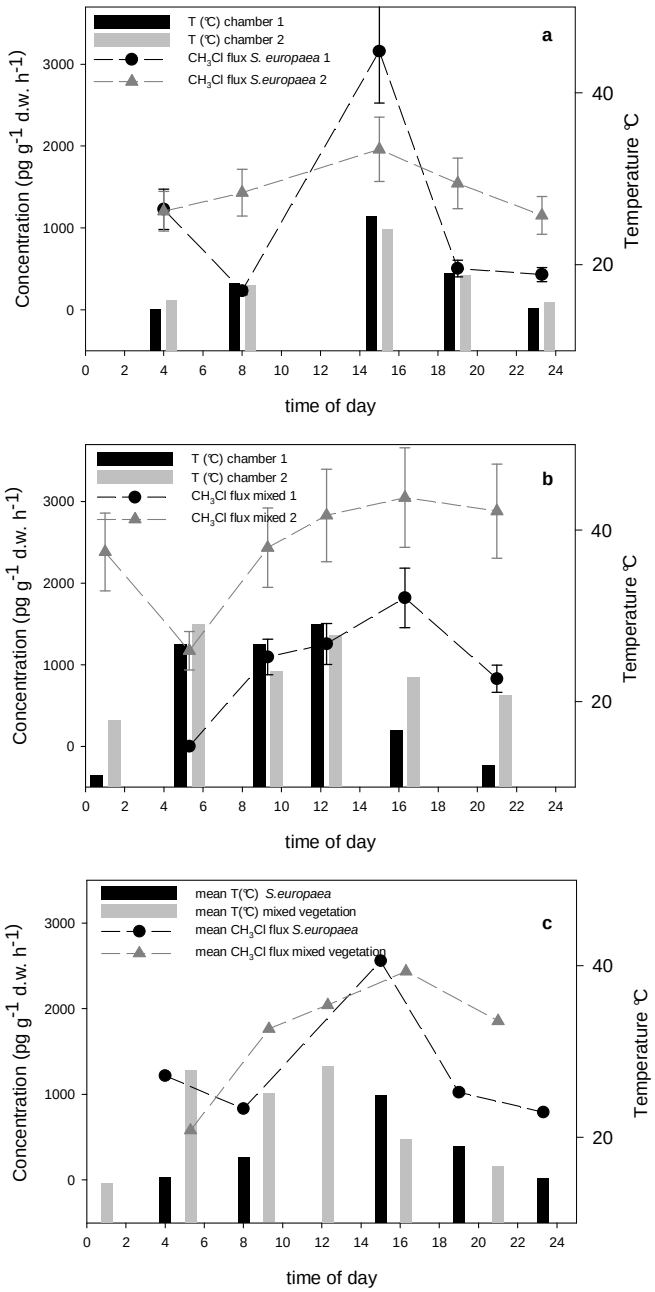

Figure 4.1 Dry biomass-normalised chloromethane fluxes and the corresponding average temperatures in the chambers during the incubations. a) Site 1 plots A and B (*S. europaea*), b) Site 2 plots A and B (mixed vegetation), c) mean emission from site 1 and 2. In plots A and B, the error bars indicate analytical uncertainty of +/- 20% for the GC-MS-system used for sample analysis.

Large inner-site variations of the CH_3Cl fluxes are clearly visible in the biomass-normalised net flux rates of the 2008 campaign (Table 4.3). The flux size varied by one order of magnitude and from positive to negative values between the three plots of the same site. Therefore, the calculated mean has a large deviation, which should be considered when comparing the differences between the sites. The temperature, photosythetically active radiation (PAR) and relative humidity stayed relatively constant during the time when the measurements were conducted (Table 4.3). On July 8, the PAR and temperature were a bit higher than during the previous two days. The PAR and temperature could have had some effect on the flux values recorded on July 8, but the difference from the previous days is not significant. Overall, the biomass-normalised net CH_3Cl emissions were lowest from site 3 in 2008 (Table 4.3).

Table 4.3 Biomass-normalised CH_3Cl emission rates in pg CH_3Cl g^{-1} h^{-1}, temperature, relative humidity (RH) inside the chamber and the photosynthetically active radiation during the incubations in 2008.

site	time	date	Fresh weight	Fresh weight average	Dry weight	Dry weight average	T (°C *)	PAR (µmol s^{-1} m^{-2})	RH (%) *
3	2-3	7.7.08	-6	-	-24	-	-	-	-
3	2-3	7.7.08	-284	35	-1071	126	11	-	87
3	2-3	7.7.08	396	-	1472	-	-	-	-
3	10-11	7.7.08	498	-	1887	-	-	-	-
3	10-11	7.7.08	106	428	398	1605	19	645	48
3	10-11	7.7.08	681	-	2529	-	-	-	-
3	12-13	7.7.08	84	-	319	-	-	-	-
3	12-13	7.7.08	1028	477	3870	1792	23	956	39
3	12-13	7.7.08	319	-	1185	-	-	-	-
4	2-3	8.7.08	33	33	89	89	14	-	82
4	10-11	8.7.08	290	-	930	-	-	-	-
4	10-11	8.7.08	4735	2512	10213	5572	20	627	60
4	12-13	8.7.08	730	-	2345	-	-	-	-
4	12-13	8.7.08	177	1812	475	4195	26	1147	43
4	12-13	8.7.08	4528	-	9765	-	-	-	-
5	2-3	9.7.08	-259	-	-2073	-	-	-	-
5	2-3	9.7.08	-208	-162	-1609	-1279	15	-	83
5	2-3	9.7.08	-19	-	-154	-	-	-	-
5	10-11	9.7.08	322	-	2577	-	-	-	-
5	10-11	9.7.08	444	696	3435	5629	24	1189	60
5	10-11	9.7.08	1323	-	10875	-	-	-	-
5	12-13	9.7.08	132	-	1021	-	-	-	-
5	12-13	9.7.08	-303	242	-2419	1989	28	1437	38
5	12-13	9.7.08	896	-	7364	-	-	-	-

*) average of three values

4.1.3 Daily fluxes

There were no apparent differences in the emission rates between the various vegetation types at sites 1 and 2; therefore, the flux data from both sites was combined to one group (all species 2007) to calculate the daily flux from the study area for 2007. The 2008 data was handled as its own group because of the differences in sampling methods. The flux data from sites 1 and 2 describe the emissions from only vegetation. The fluxes from sites 3, 4 and 5 also included the possible contribution from soil. The observations from sites 1 and 2 (n = 21) were divided into two groups: 1) background emission fluxes recorded during 0:00 - 14:00 and 18:00 - 24:00 (n = 17) local time and 2) maximum emission fluxes recorded during 14:00 - 18:00 (n = 4). The mean fluxes (+/- standard deviation) were 378 (+/- 241) ng m^{-2} h^{-1} and 1330 (+/- 863) pg g^{-1}(d.w.) h^{-1} normalised to area and dry biomass, respectively, for background group and 701 (+/- 228) ng m^{-2} h^{-1} and 2496 (+/- 704) pg g^{-1}(d.w.) h^{-1} normalised to area and dry biomass, respectively, for maximum group. The background mean flux was assumed to represent the mean flux for 20 hours of the day, whereas the maximum flux represented the mean flux for 4 hours of the day. The daily flux was calculated as the sum of the background and maximum fluxes times their duration in hours; the weighted mean was found by dividing this number by 24 hours. The weighted means for all species were 432 (+/- 25) ng m^{-2} $h^{-1}$and 1524 (+/- 105) pg g^{-1}(d.w.) h^{-1}, resulting in daily fluxes of 10.36 (+/- 0.60) µg m^{-2} $d^{-1}$and 36.58 (+/- 2.54) ng g^{-1}(d.w.) d^{-1}. The numbers in brackets indicate the standard errors.

As in 2007, no substantial differences were found between the CH_3Cl fluxes of the three vegetation types in 2008, although site 3 had overall somewhat lower emission fluxes, especially when considering the dry biomass-normalised values. The measurements were combined into two groups to make the statistical analysis more valid for estimation of night-time and daytime fluxes for 2008. The groups were formed as follows: night-time group consisting of all the night-time measurements (n = 7) and daytime measurements (n = 17) from the morning (10-11) and midday (12-13). The mean CH_3Cl night-time flux in 2008 was -67 (+/- 271) ng m^{-2} h^{-1} or -481 (+/- 1198) pg g^{-1}(d.w.) h^{-1} for the area- and

dry biomass-normalised values, respectively. The daytime average was 790 (+/- 997) ng m^{-2} h^{-1} and 3339 (+/- 3882) pg g^{-1}(d.w.) h^{-1} for the area- and dry biomass-normalised values, respectively. The values in the brackets indicate the standard deviation of the measurements. No mean daily flux was calculated for 2008 because the dataset was temporally rather limited, covering only three different time points during 24 hours.

4.2 Dimethyl sulphide (DMS) and carbon disulphide (CS_2) fluxes

Positive carbon disulphide (CS_2) and dimethyl sulphide (DMS) emissions were recorded in every measurement point at site 3. The recorded fluxes ranged from 61 to 263 ng m^{-2} h^{-1} and from 1083 to 1599 ng m^{-2} h^{-1} for CS_2 and DMS, respectively. DMS did not seem to have any diurnal emission pattern; the recorded flux rates were rather similar during the night-time, morning and noon measurements. The DMS emissions were also the quantitatively largest of the three gas species recorded (CH_3Cl included), and no negative fluxes were recorded in any of the plots of this site during the whole measurement period. Site 3 was the only site where DMS fluxes were detected.

The daytime CS_2 fluxes were negative at site 4, ranging from -16 to -201 ng m^{-2} h^{-1}. The only positive CS_2 flux of 61 ng m^{-2} h^{-1} was measured during the night. At site 5, a relatively large positive CS_2 flux (163 ng m^{-2} h^{-1}) was measured in the night. In the morning, however, this was reversed; this site had a rather large negative CS_2 flux. Surprisingly, this gas was liberated with a positive flux rate of 233 ng m^{-2} h^{-1} at the noon measurement.

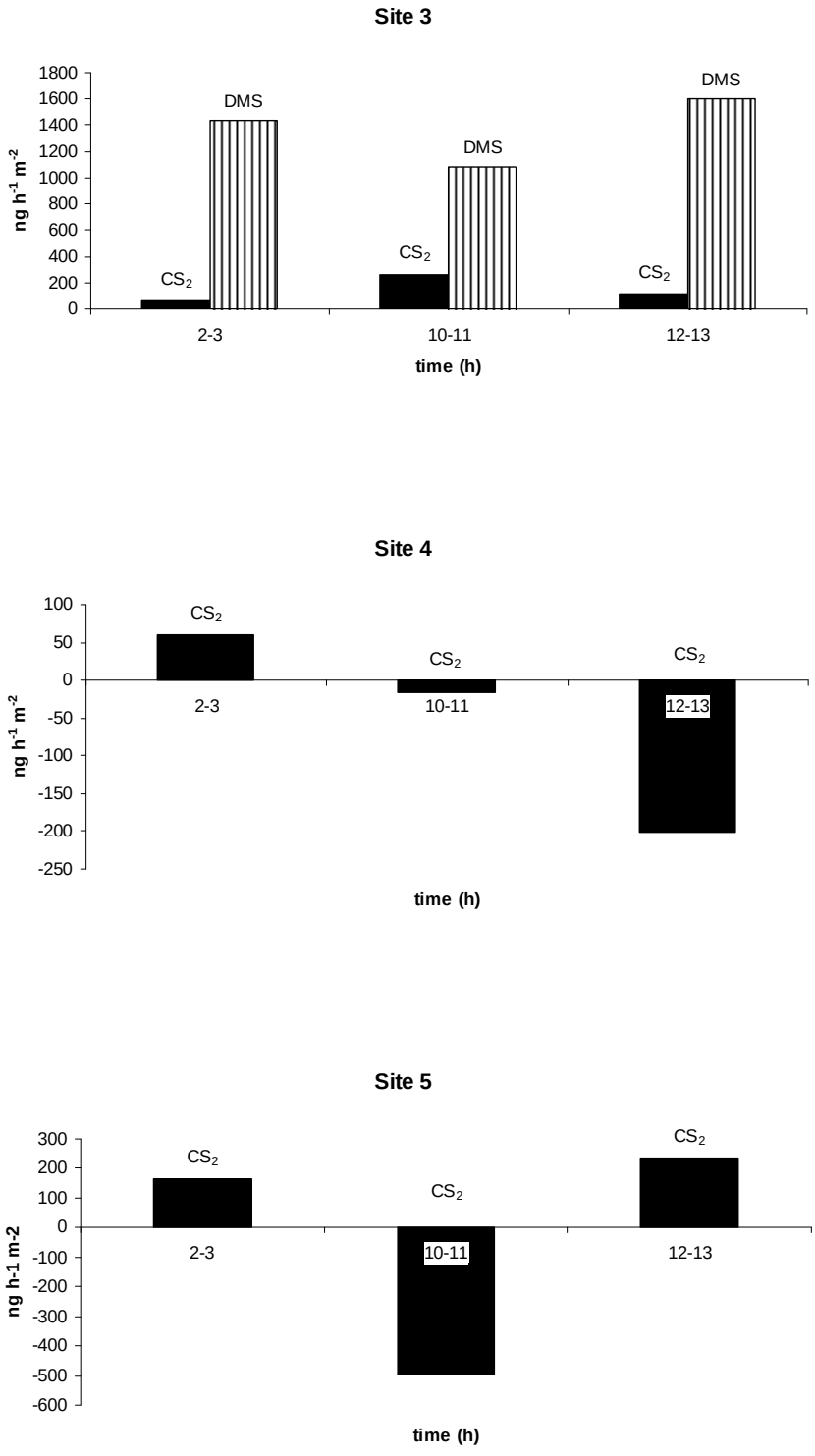

Figure 4.2 Area-normalised sulphur gas fluxes from sites 3-5. One vertical bar represents the average of the three parallel measurements; in some cases only one measurement point was quantifiable.

4.3 Background CH_3Cl

The mixing ratio of CH_3Cl varied from 306 pmol mol^{-1} on July 5 (12:00-13:00, height 0.5 m) to 744 pmol mol^{-1} on July 6 (2:00-3:00, height 1.5 m). There was no systematic difference in the concentrations of CH_3Cl between the two heights on either of the two sampling days (Figure 4.3). The atmospheric CH_3Cl concentration did not follow any distinct daily pattern. The mixing ratios were generally lower on July 5 than on July 6, and the daily average mixing ratios (both heights) were 443 and 551 pmol mol^{-1}, respectively.

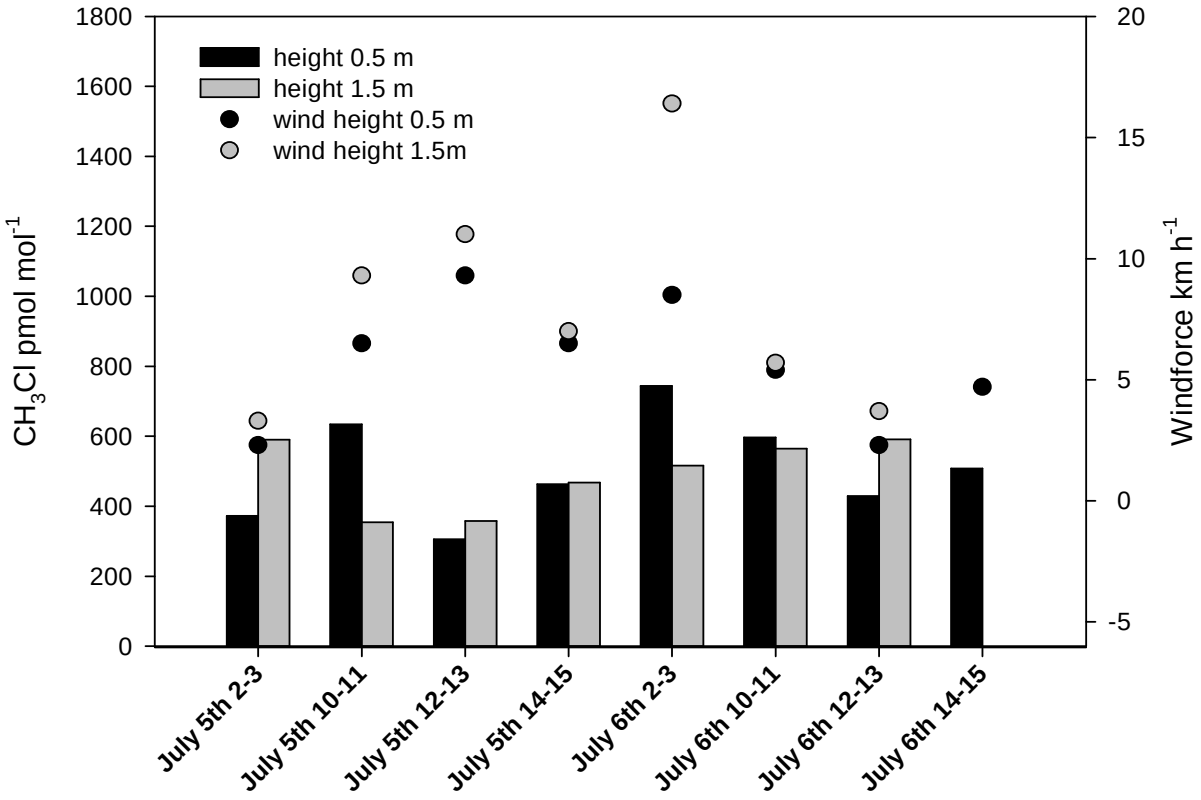

Figure 4.3 Atmospheric chloromethane mixing ratios (the columns) in the air sampled above the meadow area and average wind force (the round dots) at both sampling heights.

The recorded wind forces were higher at 1.5 m than at 0.5 m (Figure 4.3, Table 4.4). The largest difference between the heights was measured on the night of July 6, where the difference of the wind forces at the heights of 0.5 and 1.5 m was 7.9 km h^{-1}; in all other measurements, the difference was between approximately 0.3 and 3.5 km h^{-1}. Considering the measured one-hour mean

wind forces, July 5 was windier than July 6, with the exception of the high average wind force of 16.4 km h^{-1} in the night-time measurement on this day.

Temperatures varied from 12 to 15℃ in the night-ti me measurements and 15 to 26℃ in the day-time measurements (Table 4.4). Over all July 5 was warmer than July 6. The PAR values showed a very similar picture on both days, with the highest radiation occurring in the afternoon (14:00-15:00) and with an increasing trend from morning towards afternoon. The only exception was the measurement on July 6 from 12:00 to 13:00, which showed lower radiation values than the morning measurement, probably due to slight cloudiness during the measurement.

Table 4.4 Wind force, photosynthetically active radiation (PAR) and temperature recorded on July 5-6, 2008.

Date	Time	Height (m)	Wind force (km h^{-1})	Wind force 1 h-mean (km h^{-1})*	PAR (µmol s^{-1} m^{-2})	T ℃
5.7.08	2-3	0.5	2.3	-	-	15
5.7.08	2-3	1.5	3.3	-	-	15
5.7.08	10-11	0.5	6.5	-	-	25
5.7.08	10-11	1.5	9.3	10.7 (max 26)	1107	24
5.7.08	12-13	0.5	9.3	-	-	24
5.7.08	12-13	1.5	11.0	11.7 (max 30)	1551	26
5.7.08	14-15	0.5	6.5	-	-	21
5.7.08	14-15	1.5	7.0	13.7 (max 32)	1610	23
6.7.08	2-3	0.5	8.5	-	-	12
6.7.08	2-3	1.5	16.4	16.4 (max 31)	0	12
6.7.08	10-11	0.5	5.4	-	-	17
6.7.08	10-11	1.5	5.7	5.3 (max 12.9)	1209	15
6.7.08	12-13	0.5	2.3	-	-	18
6.7.08	12-13	1.5	3.7	5.0 (max 11.7)	935	15
6.7.08	14-15	0.5	4.7	-	-	19
6.7.08	14-15	1.5	5.0	5.4 (max 12.7)	1633	16

* measured at the height of 1.7 m.

4.4 Identified VOCs

The mean temperature within the chambers on the sampling days (July 10. – 12., 2007) was 20.6℃, and the mean relative humidity was 72%. No temperature rise or humidity accumulation was observed in the majority of the incubations. The major components in the emission samples were acetone and hexanal, followed by methyl acetate, pentanal, ethyl acetate, benzene and toluene (Figure 4.4).

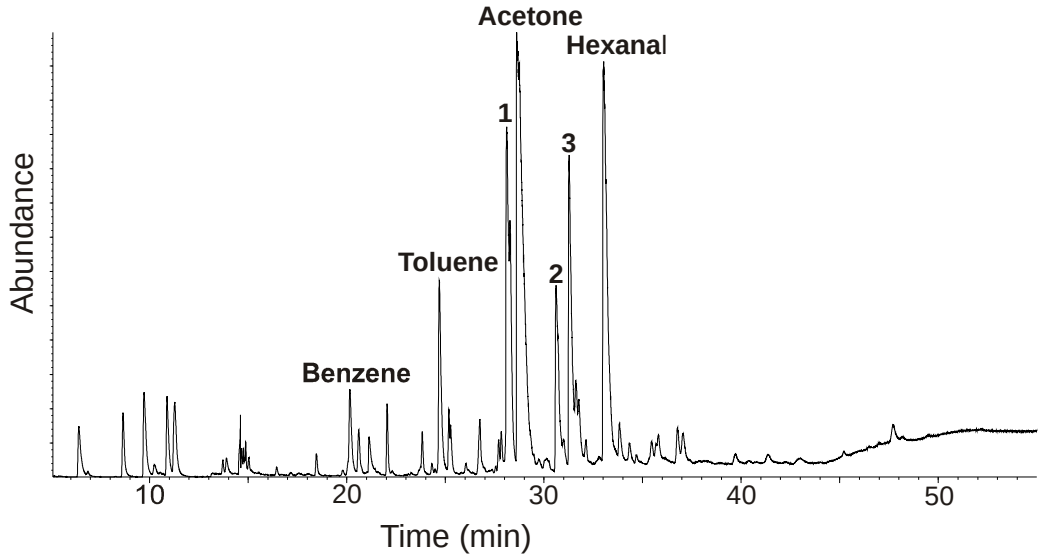

1) Methyl acetate 2) Pentanal 3) Ethyl acetate

Figure 4.4 Typical chromatogram of a plant (*S. europaea*) emission sample (5-55min).

The most abundant VOCs in our samples were isobutane, 2-methyl-propene, butene and pentane (Figure 4.5). Isobutane normally eluted immediately before chloromethane. However, in a few samples where isobutane was present in a high concentration relative to chloromethane, partial co-elution was observed (Figure 4.5 a). On such occasions, quantisation was conducted with the help of the extracted ion chromatograms (Figure 4.5 b). Some sulphur-containing compounds were observed in the emission samples. Carbon disulphide (CS_2) and sulphur dioxide (SO_2) were present in large amounts, but dimethyl sulphide and methanethiol were also often detected. Carbon disulphide and dimethyl sulphide are biogenic compounds and were therefore studied in more detail during the 2008 sampling campaign (results presented previously). Sulphur dioxide (SO_2) is an artefact generated by the adsorbent materials during the

desorption step. Sulphur dioxide was also detected in the blank runs, where only the conditioned adsorbent tubes were analysed. Several halogenated C_1 and C_2 compounds could be detected in the collected gas samples, with $CHCl_3$, CH_2Cl_2, CCl_3F (CFC-11) and CH_3Cl being the most abundant.

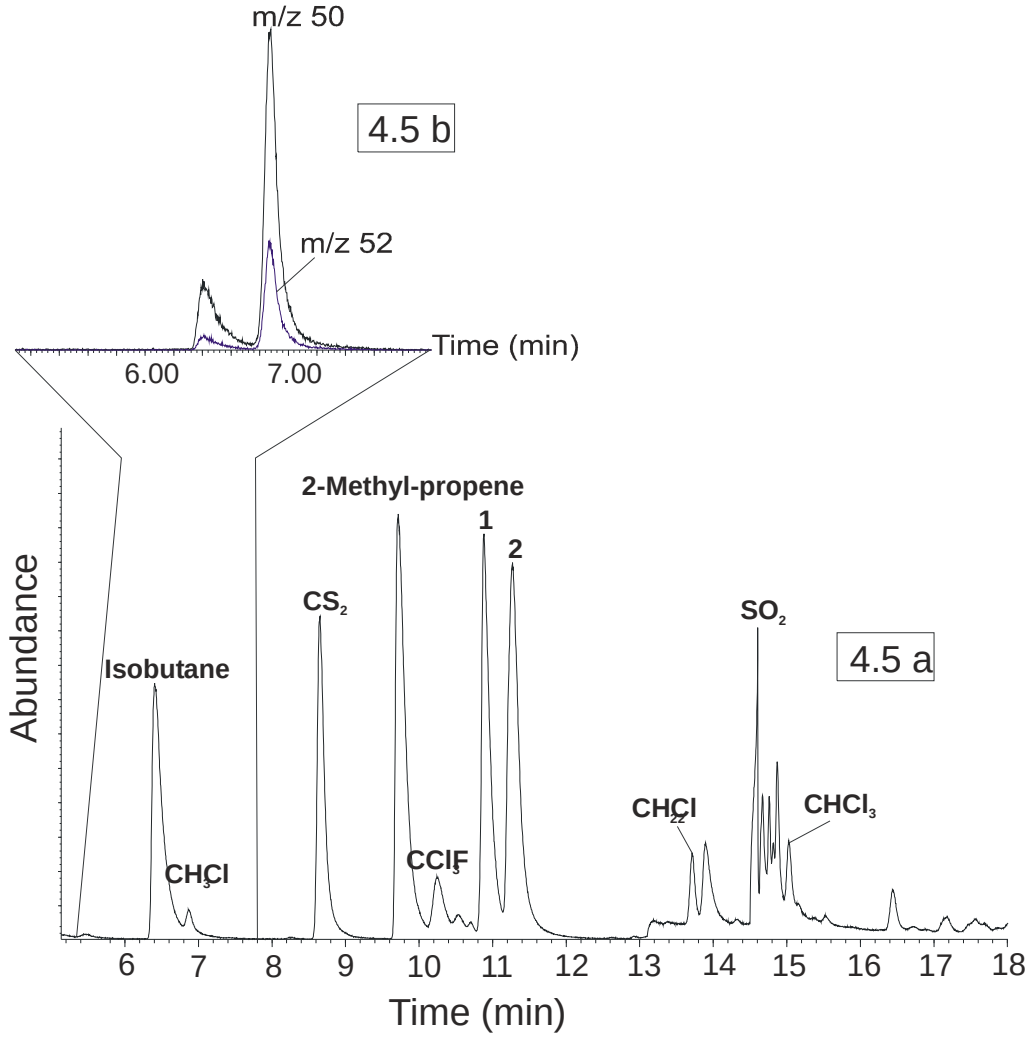

1) Butene 2) Pentane

Figure 4.5 a) Magnification of the retention times from 5 to 18 min (same chromatogram as in Figure 4.4), b) extracted ion chromatogram displaying the main ion fragments (m/z 50 and 52) of chloromethane.

4.5 Results – summary

The CH_3Cl fluxes varied from uptake (negative flux) to emission rates of 1817 ng m^{-2} h^{-1} and 5572 pg g^{-1}(d.w.) h^{-1}. Large discrepancies were detected inside the same site (vegetation type) and did not diminish when emission rates were normalised with fresh or dried biomass. The soil analyses revealed differences in the soil parameters between the study sites. Sulphur-containing gases were emitted from all measured sites, although only site three also emitted DMS. The DMS flux was positive during all of the measurement times, but the CS_2 flux varied between uptake and emission. The background CH_3Cl concentration in the air above the meadow varied between 306 and 744 ppt and did not show a diurnal trend.

5. Discussion

5.1 Chloromethane

5.1.1 Emission by plants

In this study, relatively large discrepancies remained between the chloromethane emission levels among the different sites of the mixed species after normalising to dry biomass. For *S. europaea* (site 1), the differences between the two sites became much smaller when normalised to biomass. The differences in the fluxes from the mixed vegetation sites could be partly due to variation in the relative coverage of different plant species at the sites. Halomethane flux rates have been found to strongly depend on the species (Manley et al. 2007, Yokouchi et al. 2007). There might also be differences between the emissions rates from plant individuals of the same species. In fact, high intra-species variations have been detected in tropical plants (Yokouchi et al. 2007) and salt marsh vegetation (Rhew et al. 2002). The amount of biomass for a given species is not solely responsible for variations in the extent of the emissions; the developmental stage and overall health of the individual plant might also contribute to differences in emissions. The correlation between the flowering of plants and halomethane (not necessarily chloromethane) emissions found by Manley et al. (2007) suggests that the plant age and developmental status are key factors in the regulation of the amount of liberated gas.

Overall, the differences in CH_3Cl emission rates between the various vegetation types in this study were not substantial, especially in comparison to over 100-fold differences between Californian salt marsh species (Table 5.1) found by Manley et al. (2007). The mean area-based net flux (= daily mean divided by 24) recorded in 2007 was 432 ng m^{-2} h^{-1}, which is in the same range as the fluxes obtained by Cox et al. (2004), Dimmer et al. (2001), and Rhew et al. (2001) for a *Larrea tridentata*-dominated site and Varner et al. (1999) for a rich fen. The fluxes reported for *Atriplex canescens* (Teh et al. 2008), *Spartina* and *Salicornia* (Manley et al. 2007) as well as for a poor fen (Varner et al. 1999)

were approximately 2-fold higher than our daily maximum value. The daily average values obtained by Manley et al. (2007) were all recorded between 09:00 and 14:00, which partly overlaps within the window of time wherein the maximum emissions were found in this study. Hence, the comparison of the maximum values seems to be appropriate.

Only three studies listed in Table 5.1 report emission values in which the influence of the soil emissions is deducted, whereas all of the other studies give total emission values that include soil emission. Only a few studies (Dimmer et al. 2001 and Rhew et al. 2001 and 2000) took daily variations into account. These facts complicate comparisons between the emission values from different studies.

The subtropical biomass based-emissions rates (Table 5.1) are three orders of magnitude larger than our mean biomass-normalised rate of 1.52 (+/-0.11) ng g^{-1} (d.w.) h^{-1} for all species. This discrepancy derives from the differences in the vegetation composition and environmental parameters (e.g., temperature, salinity and insolation) (see 5.1.1.2). Chloromethane formation is a characteristic feature probably regulated at the genus level in plants (Yokouchi et al. 2007). The magnitude of emission is likely also controlled at the genus level. The two *Salicornia* (*europaea* and *virginica*) species have emission rates of the same magnitude, despite having differences in their geographic settings. There is a three-fold difference in the dry biomass-normalised fluxes of *Salicornia* between our study and that of Manley et al. (2007). In addition, different *Frankenia* species have shown about two-fold differences in their dry biomass-normalised emission rates: *F. salina*: 1367 - 1494 ng g^{-1} h^{-1} (Rhew & Abel 2007) and *F. grandifolia:* 582 ng g^{-1} h^{-1} (Manley et al. 2007). These results may have been partly caused by methodological differences in the calculation of the daily mean fluxes and partly by differences between the sites. As already mentioned, it is difficult to compare the emission rates of *S. bigelovii* (Rhew et al. 2000) with other data, because this study neither differentiated between soil- and vegetation-derived emissions nor presented biomass-normalised rates. Compared to data presented in this study, the most similar biomass-normalised emission rates were reported for the short grass steppe species *A. canescens*

(Teh et al. 2008) and coastal salt marsh species *S. virginica* (Manley et al. 2007).

Fewer chamber measurements were made in one day during the 2008 campaign because ambient air was also sampled; therefore, the sampling capacity left for the chamber measurements was limited. Two measurements were conducted in the daytime and one was made during the night. The aim of this study was to record the extent of the daily variation (i.e., the difference between the minimum and maximum emission fluxes). Interestingly, we measured a negative flux during the night-time at site 3 (*S. europaea*). A negative (uptake) flux resulted when a smaller flux was recorded from the vegetation enclosure than from the empty enclosure (see chapter 4). At site 3, a negative flux was observed in all three parallel incubations during the 2-3 h measurement from -17 to -275 ng CH_3Cl m^{-2} h^{-1} resulting in an average flux of -168 ng CH_3Cl m^{-2} h^{-1}. A negative (uptake) flux of CH_3Cl in a terrestrial ecosystem is not completely unexpected. Soils are considered to be one of the major sinks for this gas species (WMO 2006). Several other investigators have measured negative CH_3Cl fluxes in various wet and dry land ecosystems (for example, Rhew et al. 2007 and Rhew and Abel 2007). In these investigations, the change between CH_3Cl production and consumption was associated with the difference in the season (growing season/non-growing season) but not with changes in the light-dark-period. In two of the parallel plots at site 3, negative fluxes (-8 and - 410 ng CH_3Cl m^{-2} h^{-1}) were detected, but due to the relatively high positive flux of the third parallel plot, the average flux from site 3 was slightly on the positive side. At site 4, only one of the parallel measurements was interpreted because the two other samples were lost due to analytical and storage difficulties. This measurement yielded a small positive night-time flux for site 4. In the light of these results, it seems that CH_3Cl fluxes decline dramatically in the night-time and can even transform to uptake fluxes in some locations.

In comparison to the 2007 background and maximum emission groups, the daytime average was slightly higher in 2008 and the night-time emission flux was somewhat lower. The average fluxes of 2008 fit nicely inside the variation

of the background and maximum groups of 2007, thus confirming the estimation made for the daily emission of this ecosystem based on the 2007 data.

5.1.1.1 Atmospheric concentration

In 2008, campaign CH_3Cl was measured next to the chamber enclosures from the ambient air. The CH_3Cl concentration of the background air seemed to be mostly controlled by the wind force (Figure 5.1), however, with variable kinds of behaviour at different heights.

At the lower height (upper picture), the wind force was correlated positively with the mixing ratio (i.e., higher wind forces occur with higher mixing ratios). By contrast, at a height of 1.5 m, a decreasing wind force was correlated with increasing mixing ratios. At both heights, reasonable correlations were achieved when the highest wind speeds were excluded from the observations. At a height of 0.5 m, a wind speed of 9.3 km h^{-1} led to the reverse situation compared to other wind speeds (from 2.3 to 8.5 km h^{-1}). At the higher height, the same phenomenon was observed at a wind speed of 16.4 km h^{-1} (all of the other observations were from 3.3 to 11 km h^{-1}). The exclusion of these “abnormal” wind speeds was justified because they caused either too much turbulence or were so high that a different source area could be affecting the CH_3Cl mixing ratio.

The measurements were made in the southwest corner of the meadow and most of the time the wind was blowing from the northeast sweeping over the meadow. Unfortunately, based on a visual estimation, about 70% of the meadow vegetation was harvested prior to our measurements, leading to several patches of vegetation rather than uniform intact vegetation growing on the meadow, thus complicating the interpretation of the data.

The wind speed correlations with the mixing ratio might be interpreted as follows: at a height of 0.5 m, the distance to the CH_3Cl source (i.e., intact vegetation) was so great that only a small amount of the produced CH_3Cl was transported to the measurement point and observed with low wind speeds. With

increasing wind speed, the transport of emitted CH_3Cl became more effective and the amount of collected/observed CH_3Cl increased relative to the wind speed. The general rule between the measurement height and distance of the source area could be simplified as follows: as the measurement height increased, the distance of the source area and the measurement point increased. With uniform wind speeds at the measurement heights, the source area for a lower height was nearer to the measurement point than at a higher height. If the CH_3Cl observed at heights of 0.5 m and 1.5 m originates from the same source area, the logical explanation for the dependence between the CH_3Cl mixing ratio and wind speed would be that the transport of the air is too efficient at high wind speeds. Therefore, CH_3Cl is transported past the measurement point at lower heights and is not detected at a height of 1.5 m. As the wind speed ceases, the vertical transport slows down and an increasing amount of the emitted CH_3Cl reaches the 1.5 m height and can now be detected.

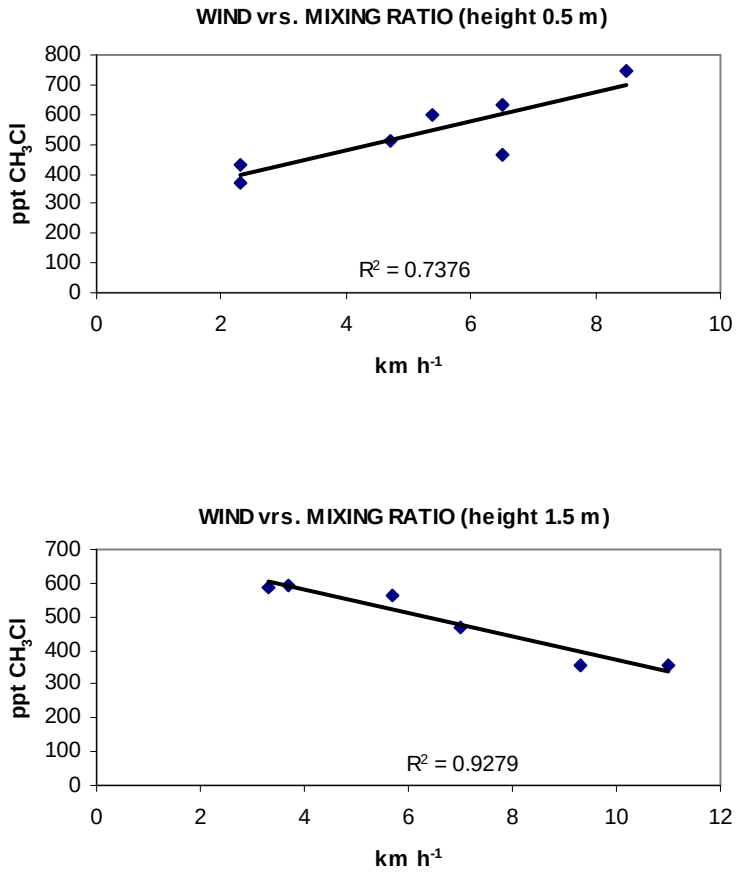

Figure 5.1 Dependency between wind force and ambient mixing ratio of CH_3Cl at two heights (up: 0.5 m, down: 1.5 m)

No correlation or other systematic behaviour between the ambient CH_3Cl concentration and the time of the day or PAR was detected. A reasonable negative correlation ($r^2 = 0.78$) between the CH_3Cl mixing ratio and the ambient temperature at the height of 1.5 m was detected. At the height of 0.5 m, no correlation between the temperature and mixing ratio was detected.

The mean molar fraction (mixing ratio, concentration) of CH_3Cl in the atmosphere is around 550 ppt (see Chapter 1). The ambient air samples of this study had large discrepancies, with this value ranging from 300 to 700 ppt; however, the mean concentration of all measurements (n= 26) was 499 +/- 124 ppt (+/ - st. dev.), which lies in the range of the global average mixing ratio. The mean difference between the parallel measurements was 105 ppt (max-min of the parallel measurements divided by the number of the pairs), which is rather large discrepancy. The CH_3Cl concentration of the ambient air above the

meadow varied widely, but this discrepancy was not large enough to totally mask a diurnal cycle. It seems probable that the area around the sampling point functioned as a sink and source for CH_3Cl, which can be seen in the correlation between wind speeds and concentrations. The meadow vegetation acted as a source for CH_3Cl and the emissions had a diurnal cycle, and similar results were seen from the chamber measurements. Therefore, it is probable that the varying wind speeds mixed the air masses so that this signal was missing from the ambient air measurements. In more stable wind conditions and with intact vegetation cover, it may have been possible to see the diurnal variation of the CH_3Cl concentration in the ambient air at this site.

5.1.1.2 Effects of environmental factors

In addition to plant species and physiological characteristics, environmental factors also may regulate emission rates. Halomethane emissions have been correlated with air temperature and the amount of photosynthetically active radiation (Dimmer et al. 2001, Rhew et al. 2002, Saito & Yokouchi 2007). Manley et al. (2007) pointed out the difficulty in field studies to differentiate between effects caused by changes in the light intensity and those caused by temperature, as these two factors are normally strongly correlated. During the sample and control incubations, the temperature and relative humidity in the chambers were monitored because they are major factors affecting enzyme activity in plant cells (Heldt, 2004). In most cases, temperature in the chamber correlated well with the amount of emitted chloromethane (r^2 coefficient of determination, linear regression = 0.63 - 0.98 (n = 5 or 6)); only the mixed vegetation site 2 B had a poor correlation (r^2 = 0.45, n = 6) between these two parameters.

Salinity has also been proposed to be an important factor in halomethane production (WMO 2006), but it is not directly correlated with emission rates (Yokouchi et al. 2002, Manley et al. 2007). Nevertheless, soil salinity is an important environmental parameter with a strong influence on the type of vegetation that grows in a given ecosystem. Investigations made in different kinds of shrubland (Rhew et al. 2001) and grassland (Rhew & Abel 2007, Teh et

al. 2008) ecosystems reveal a close relationship between the net chloromethane production and the halophytic plant species present. The highest chloromethane net emission rates measured from dry grassland have been obtained from a hypersaline site (Rhew & Abel 2007). There might also be a certain temperature and salinity “threshold” in the northern ecosystems for chloromethane production. For example, Dimmer et al. (2001) could detect relatively high halomethane emission rates from Irish peatlands and forest floors, but Hellén et al. (2006a) could not detect any emissions from Finnish inland peatland or the coniferous forest floor. These results suggest that the salinity at inland sites in Finland was probably not high enough to initiate halomethane formation. In this study, which was performed on a coastal area of the Baltic Sea, chloromethane emissions could be detected. Thus, the halogenated hydrocarbons measured by Hellén et al. (2006 b) in the air of urban and residential areas in southern Finland may have originated from areas affected by brackish water. Hellén et al. (2006 b) modelled the measured halogenated hydrocarbons as having their origin from a distant source, but the type of source could not be identified. A temperature threshold might have contributed to why Rhew et al. (2007) could record almost no halomethane emission from a tundra coastal site in Alaska, where the salinity is most probably at least the same or higher than on the Baltic Sea coast in Finland.

Interestingly, in dryland ecosystems, the water content in the soil seems to be an important factor controlling the chloromethane net emission and uptake. In the studies of Rhew et al. (2001), Rhew & Abel (2007) and Teh et al. (2008), chloromethane net emissions occurred only during dry seasons (soil water content ≤ 10%). Water content is of crucial importance in controlling the biological activity in the soil. Soil bacteria can degrade chloromethane either under oxic or anoxic conditions; however, in general, aerobic degradation processes are considered to be more efficient and faster than anaerobic processes. Further studies are needed to determine if there is a moisture regime optimal for microbial oxidation.

5.1.1.3 Effect of geographic location

When considering the CH_3Cl emissions from vegetation, the (bio)geographic location of the sampling site is of paramount importance. This factor mainly determines the vegetation type dictating the length of the growing season, temperature and diurnal light conditions. When reviewing the existing estimates for the terrestrial CH_3Cl input, most of the data comes from the northern hemisphere temperate climate zone between latitudes of ~30° - 50°. No studies of direct land-based emission measurements from the tropics (23,5°N to 23,5°S) have been published yet, although indirect estimates of the source strength from this region does exist (Saito and Yokouchi 2006). However, Yokouchi et al. (2007) reported emission data just from the northernmost boundary of this zone.

The CH_3Cl flux rates do not seem to be governed by the geographic location alone. There are equally high rates reported for the tropical plants as for the vegetation in temperate regions (Table 5.1). However, the total annual flux is strongly affected by seasonal variations, especially by changes between the growing and non-growing seasons (Rhew and Abel 2007). In the higher latitudes, the length of the growing season shortens, resulting in decreasing annual fluxes. The boreal region has a relatively short growing season. For example, the growing season lasted 5 months (starting at the end of April and lasting approximately to mid-October (FMI, weather statistics)) at the sampling site of this study. This short season is a limiting factor for the annual emission from this site. Measurements in this study were done during the mid-growing season. Therefore, it remains unclear how the CH_3Cl dynamics in this ecosystem behaves during other times of the year and what the strength of this source is for the whole year.

Table 5.1. Reported terrestrial net CH_3Cl- emission rates

Reference	Location	Predominant vegetation	CH3Cl flux area ($ng^{-1}m^{-2}\ h^{-1}$)	CH3Cl flux dry biomass ($ng\ g^{-1}\ h^{-1}$)
Teh et al. (2008)	NE Colorado U.S. 40°N, 104°W short grass steppe	*Atriplex canescens*	924 +/- 122	0.74 +/- 0.05
Rhew & Abel (2007)	California U.S 38°N, 121°W grassland	*Frankenia salina, Cressa truxillensis*	72-88 x 10^3	1367--1494
		Lepidium latifolium	5 x 10^3	23
Yokouchi et al. (2007)[a]	Iriomote Island, Japan 24°N, 123°E subtropical forest	33 different subtropical and tropical species	24 x 10^3	140
Manley et al. (2007)[a]	California U.S. 33°N, 117°W coastal salt marsh	*Spartina foliosa*	1370	7.99
		Salicornia virginica	1370	1.83
		Frankenia grandifolia	297 x 10^3	582
		Batis maritima	160 x 10^3	297
Saito & Yokouchi (2006)[a]	Glasshouse	*Cyatheaceae podophylla*	-	2400 +/- 600
		Cyatheaceae lepifera	-	490 +/- 170
Cox et al. (2004)	Tasmania 41°S, 145°E coastal wetland	*Pachycornia arbuscula*	300	-
Dimmer et al. (2001)	Ireland 53°N, 9°W coastal marsh	*Ranunculus flammula, Apium inundatum*	380	-
	conifer forest floor (median)	*Pinus sylve, Picea sitchensis, Abies alba*	3850	-
	peatland (median)	grasses, mosses	605	-
Rhew et al. (2001)[b]	California U.S. 32-33 °N 116-117°W three shrubland biomes	*Brassica juncea*	2314	-
		Carbobrotus edulis	1178	
		Artemisia californica	3702	-
		Larrea tridentata	168	-
Rhew et al. (2000)	California U.S. 32°N, 117°W coastal salt marsh	*Batis maritima/ Salicornia*	158 x 10^3	-
		Salicornia bigelovii	274 x 10^3	-
		Batis maritima	1010 x 10^3	-
Varner et al. (1999)	New Hampshire U.S 43°N, 71°W wetland	*Sphagnum* spp., *Carex* spp., shrubs (poor fen)	1103	-
		Sphagnum spp.(rich fen)	386	-

Fluxes were calculated per hour by dividing the data from the original source given as daily or yearly average fluxes by 24 or 24 x 365 if they were not already given in the units used. The fluxes given in molar units were also transformed into mass unit fluxes. [a)] emissions only from vegetation, soil emissions deducted [b)]daily maximum value

5.1.2 Abiotic production in soil

In soil samples 1 and 2, the clay layer starting at a depth of 7-8 cm had a uniform pale grey colour and showed no visual signs of oxic conditions (e.g., any red-brown colour from oxidised iron). Therefore, it is probable that the subsoils stay anoxic because of the high water level due to the proximity of the shoreline and poor penetration of oxygen-containing water through the compact clay layer.

According to Keppler et al. (2000), the main factors influencing abiotic chloromethane production are i) soil chloride concentration, ii) organic carbon content, and iii) reducible iron (Fe III) concentration. The ambient environmental conditions, such as temperature, soil moisture and pH, and the chemical composition of the soil OM play major roles. In the present study, the investigated soils differed in pH, EC and Cl concentrations. The pH was lower in soil 2 (mixed vegetation 2007) due to its high content of OM known to contain humic and fulvic acids. It is likely that the higher EC in soil 2 was attributable primarily to the higher Cl^- concentration caused by flooding of brackish water, although the dissolved organic acids may also have had some effect.

The major factor determining the vegetation type in the experimental location was the burning-over that cleared the patches (soil 1) of other vegetation and gave an advantage to the pioneer species *S. europaea*, rather than any chemical or physical differences between the soils.

Soils possess a variety of biological component that either produce or degrade chloromethane. Chloromethane production has been reported for ectomycorrhizal fungi (Redeker et al. 2004) and wood-rotting fungi (Watling & Harper 1998). On the other hand, several bacterial strains have been found to be capable of using chloromethane as a sole carbon source (reviewed in McDonald et al. 2002 and Schäfer et al. 2007). Thus, soil can function as a sink (WMO 2006) or a source for chloromethane and hence form a highly complex biological system, which renders it challenging to assess the possible abiotic generation of volatile compounds.

In light of the measured soil parameters, abiotic halomethane formation would be more likely in soils 2 and 4 because of the high content of OM, chloride and redox-sensitive elements (iron). Therefore, abiotic chloromethane production might be a factor affecting the flux data for mixed vegetation sites (in 2007), especially as all the soil controls were measured on soil 1 (*S. europaea,* 2007), because no unvegetated patch was available at sampling site 2. Thus, the chloromethane fluxes for the mixed vegetation sites in 2007 might be overestimated due to underestimation of the contribution from soil.

The soil sampled at site 3 had very high organic matter and water contents, implying anaerobic and reduced conditions in this soil. In addition, the relatively high emissions of sulphur-containing gases suggest that anaerobic microbial processes might play a key role in the on-going reactions in this soil. Soil 3 had only about half of the amount of extractable iron as soil 4, which is probably due to the lower pH, which enhances the mobilisation of metals from the soil (Scheffer and Schachtschabel 2002). In the organic-rich surface layers, iron and manganese are mostly present in organic forms. The sandy mineral matter of these soils is not likely to contain substantial amounts of iron or manganese, which can also be seen in the low iron content of soil 5.

Soil 4 had the highest electrical conductivity from the 2008 investigated soils, probably because of the accumulation of soluble salts. This soil was markedly drier than soil 5, but it was close enough to the shoreline to be effected by sea spray or occasional flooding. As the meadow has a dense, poorly permeable clay horizon (noticed in all 5 soil samples), which hinders the transport of water to lower parts of the soil profile to some extent, it is probable that the salts from seawater accumulate in the soil in “arid” (evaporation is higher than precipitation) weather conditions. This pattern was seen in soil 4, with a relatively high pH and EC. The so-called alkali cations (Na^+, Ca^{2+}, Mg^{2+}) raise the pH of the soil. In soil 3, this pattern was not seen, as this soil is almost constantly connected to the seawater (nearness to shoreline). Soil 5 had the lowest EC in 2008, which could also partly originate from the method used for the determination of the EC (chapter 3). Dry soil containing a lot of organic matter has a much higher water holding capacity than coarse mineral soil,

therefore more water was added to soils 3 and 4 to get the volumetrically same dilution as for the soil 5; however, it is questionable if a comparable dilution was reached between the organic and mineral surface soil samples. One other explanation for the low EC of soil 5 could be the lateral washing out of the cations as the patch of soil 5 did not contain a lot of vegetation to prevent the lateral movement of water in case of heavy rain. Perhaps the most probable explanation for the low EC is the coarse texture of the soil and the lack of organic matter, which causes soil 5 to poorly adsorb cations. In coarse-textured soils, the surface area available for cation adsorption is very low, leading to washing out of cations from the soil.

5.1.3 Biotic production in soil

Next to the factors influencing the abiotic chloromethane production in soils, which was discussed in the previous passage, soil moisture is also considered to be very important in regulating the net CH_3Cl emission from terrestrial systems (Teh et al. 2008). Soil is one of the biggest sinks for CH_3Cl (WMO 2006) and CH_3Cl degradation by bacteria is mostly responsible for this function. Aerobic methylotrophic bacterial strains using halomethanes as their sole carbon source have been isolated from different environments agricultural soil, woodland leaf litter and coastal seawater (Miller et al. 2001). Teh et al. (2008) discovered that soil moisture was more important than temperature in different dryland ecosystems in terms of chloromethane emissions. The dryland ecosystems generally functioned as a sink for chloro- and bromomethane. A large-scale survey of soil biological processes was beyond the scope of this study, but an effort was made to measure chemical and physical parameters of the soils that could provide some clues about the microbiological activities in them.

The three sampling sites from the 2008 campaign captured a representative range of hydrological regimes and had substantial differences in the chemical and physical properties of their soils. It is possible that soil 4 had the biggest potential to support abiotic CH_3Cl formation, but also provide suitable conditions for CH_3Cl-oxidising bacteria. Soil 3 had a lower amount of redox-active metals

and soluble salts, which might lower its ability to produce CH_3Cl by abiotic mechanisms. On the other hand, soil 3 had acidic pH values, which would be favourable for fungus growth. Soil 5 did not have enough organic material for abiotic CH_3Cl production to occur in relevant amounts, but it also possessed unfavourable qualities to support microbial growth. When considering the potential of these soils to produce chloromethane, it is hard to distinguish between soils 3 and 4, but soil 5 can be seen as an improbable source for CH_3Cl. In soil 3, the production of CH_3Cl is probably lower than in soil 4; because of the likely anaerobic nature of this soil, CH_3Cl degradation would also occur by slower anoxic processes. Soil 4 would have the most favourable characteristics for CH_3Cl production, but also for its oxidation. It is apparent that soil processes have an effect on the net CH_3Cl emission within soils 3 and 4, but it is difficult to estimate in what way.

It is somewhat difficult to compare the soil parameters between samples 1 and 2 (sampled 2007) and samples 3, 4 and 5 (sampled 2008), because of the differences in the methods used in the determinations. The methodological differences arise from the fact that 2007 samples were analysed immediately after the collection, which made it possible to use soil samples with their natural water content. Unfortunately, the 2008 samples were analysed a few months after their collection (except for the moisture content, which was done a few days after obtaining the samples), which led to differences in some of the methods and to additional dilution by soil water of the 2007 samples. The largest variation due to different methods can be seen in the EC values. Therefore, these values are only compared with other samples collected in the same year. In 2008, the Cl^--concentration was not determined, but a number of other determinations (soil water content, L.O.I., and texture) were conducted. This study was started in 2006; the 2007 sampling campaign was the first to be conducted and therefore had a preliminary nature. There was no certainty if the selected sampling site would be interesting considering the scope of this study. Therefore, a somewhat limited set of determinations was made in the first year; their favourable results led to more determinations in 2008.

5.1.4 Global importance

The sampling site of this study was located in the southernmost part of the boreal zone, which has a substantially lower net primary production rate than the tropics (Field et al. 1998). The relationship between biomass production rate and the emission of chloromethane should be studied to adjust the global budget of HVOCs.

Halophytes on coastal wetlands and inland grasslands and shrublands at higher latitudes may have chloromethane production rates of global relevance. The estimation of the magnitude of these sources is hindered by the lack of field data and uncertainties in the estimations of the global coverage of these ecosystems. The sampling site of this study might be classified in a wider sense as a coastal salt marsh. The newest estimate for the source strength of coastal salt marshes is 4 +/- 2 % of the total atmospheric CH_3Cl input (Xiao et al. 2009). In light of the present results, the coastal regions play a minor role in the global CH_3Cl budget. However, changes in climate conditions might alter this picture in the future.

5.1.5 Temporal and spatial limitations

The total of 22 samples collected during the 2007 campaign might seem to be a small dataset; however, the VOC analysis has several aspects that set limitations for the amount of the samples. First, the measurement of one sample is very time consuming. In our system (described in 3.2), one analysis took more than an hour; in addition to the collected samples, standards and samples needed for quality assurance must also be measured, further increasing the sample load and time needed for measuring the field samples. The second restriction is the stability of the target compounds in the sample matrix. This can be tested before sampling, but the results of the stability tests should be interpreted with caution. The simulation of the precise sample matrix in laboratory conditions is very difficult, if not impossible. In the ideal case, an assumption might be made of the stability of the target compounds during a defined storage time. Therefore, for gaining the qualitatively best result, the

samples should be analysed as soon as possible after the sampling, which again limits the total amount of samples feasible for analysis. Considering the total sample load of this three-day sampling campaign, including the emission samples, control samples and the samples needed for quality assurance, the maximum sample amount was reached that was still considered to be analysed in an acceptable timeframe after the sample collection. The maximum storage time for chloromethane samples was three weeks, which was the time the compound remained stable on the adsorbent material in the storage experiment.

In the second sampling campaign in 2008, altogether we collected 76 samples plus the quality assurance samples. The higher sample amount was possibly due to changes in the storage procedure and the shorter analytical method (see 3.2), which helped to improve the stability of the samples and decreased the time needed for the sample analysis.

5.2 Other volatile organic compounds

Altogether, four different halogenated methanes were detected. Dichloromethane and chloroform are both widely used solvents, but also have natural sources (Laturnus et al. 2002, Cox et al. 2004). Chloroform emission is often recorded in areas where chloromethane is also emitted (Dimmer et al. 2001, Cox et al. 2004), but it shows a different kind of emission pattern. Hellén et al. (2006 a) found the boreal forest floor to emit chloroform at a rate of 100 - 800 ng m^{-2} h^{-1}, but they did not detect any chloromethane formation. These observations suggest that chloroform is derived from different processes than chloromethane, as in the marine environment (Laturnus 1998).

In the emission samples, acetone and hexanal were the predominant VOCs. Acetone is one of the most abundant non-methane hydrocarbons found in the atmosphere in remote areas and has multiple natural and anthropogenic sources (Singh et al. 1994). Shade and Goldstein (2006) detected a seasonal variation in acetone concentrations in Californian rural air, indicating that this substance is mostly of biogenic origin. Hexanal is derived from the decay of

fatty acids from biological material. For example, Heiden et al. (2003) found C_6-products, including hexanal, to be the main oxygenated volatile organic compounds from a variety of plant species. They suggested the oxidation of linoleic (18:2) and linolenic (18:3) acids by lipoxygenase to be the probable sources for these compounds.

5.3 Sulphur-containing gases

The emission of reduced sulphur gases (H_2S, DMS and CS_2) is linked to the soil redox potential, i.e., the amount of oxygen in soil. The flux of reduced sulphur gases is correlated with the soil redox potential. Devai and DeLaune (1995) noticed that the net emission of these gases in salt marsh soils increased when the redox potential decreased (became more negative). The anaerobic degradation of halomethanes begins with an initiative reaction step in which the halomethane reacts with a sulphide ion to form methanethiol (CH_3SH) and ends with the formation of DMS as the end product (Oremland et al. 1994). It is unknown to what extent terrestrially emitted DMS is related to halomethane degradation as this gas is primarily produced (at least in marine environments) as a degradation product of algae-derived DMSP (dimethylsulphoniopropionate) (Johnston et al. 2008). In freshwater systems, volatile organic sulphur compounds (VOSCs) are opposite to marine environment produced mainly by methylation of sulphide and to lesser extent by degradation of S-containing amino acids (Lomans et al. 2002). The coastal meadow of this study might be considered to be comparable with salt-marsh and estuarine environments in which the production of DMS (and methanethiol) originates from the degradation of DMSP, which is an osmolyte in many marine algae, dinoflagellates, coccolithophores and most interestingly in halophytic plant species (Lomans et al. 2002).

In light of the DMS production and high water content of site 3, this site had clearly anaerobic characteristics. The prevailing mechanism of halomethane degradation might be therefore also anaerobic. The emissions of sulphur-containing gases (CS_2 and DMS) were measured to find out if there was a correlation between these gases and CH_3Cl emissions, as both gases are often

detected in same environments. Further, DMS can be considered to be an end product in anaerobic halomethane degradation.

According to the data, the smallest CH_3Cl fluxes were recorded from site 3, which had high positive fluxes of both measured sulphur-containing gases. Site 4, which had the highest area-based CH_3Cl fluxes among all of the sites, had the smallest CS_2 fluxes and negative (uptake) fluxes for this gas in the daytime. Site 5 had an emission pattern for CS_2 that was hard to interpret, with relatively low positive fluxes in the night-time and midday, and the largest measured uptake rate considering all measurements and sites was made in a morning measurement. Site 5 was also very dry and had practically no organic material, which makes it highly unlikely that CS_2 would be produced in substantial amounts in its soil. A discrepancy can be seen between the parallel plots of this site (CS_2-flux from -284 - +750 ng m^{-2} h^{-1}) in the 10 - 11 h measurement. Of the three parallel measurements at this time point, one was clearly negative (uptake), one could not be quantified and one had a large positive flux. The positive fluxes in site 3 could be explained by the activity of sulphate-reducing bacteria and methanogenes, which degrade the phytogenic CH_3Cl to (CS_2) and DMS in the presence of sulphite. The negative fluxes during the daytime could be a result of various light-induced chemical or biological reactions in the soil-plant system, which transform CS_2 to another compound (e.g., oxidation to carbonyl sulphide (OCS) and the uptake of OCS by plants) (van Diest & Kesselmeier 2008).

Some studies (Kanda et al.1992, Fall et al.1988) have indicated that emissions of volatile organic sulphur compounds (VOSCs) are positively correlated with ambient air temperature and radiation. Emissions of CS_2 have also been detected from the roots of the plants belonging to a subfamily of *Mimosoideae* (Piluk et al. 1998). One major sink for CS_2 could be uptake by soil. Soils can function either as a sink or a source for this gas (Steinbacher et al. 2004) and this uptake may also be partly controlled by the porosity and water content of the soils, as for COS (van Diest & Kesselmeier 2008). It is evident that there are opposing processes in the soil-plant system: the production of CS_2 by plant roots and microbial reactions in the soil versus the oxidation to COS, uptake by

plants and soil, and the direct uptake of CS_2 by the soil. The uptake mechanism for CS_2 in soil might vary, and can happen via degradation by micro-organisms or by physical diffusion to soil pores. These mechanisms are likely controlled by different environmental factors.

The data from this study suggest soil moisture and the available pore space are the most important factors in regulating the net CS_2 emission, at least when the daytime processes are considered. Sites 4 and 5, which have substantially drier soils, functioned (with one exception) as sinks during the daytime, but the very wet site 3 liberated CS_2 during the whole investigated period. These results might be due to the high water content and consequent lack of free pore space in soil 3. This explanation is clearly not valid for the night-time positive fluxes, and it is not probable that there would be a dramatic change in the soil water content between night and day as there was no massive rain event during the measurement period. The day-night change must be connected to either radiation or temperature, which would imply a phenomenon induced by plant or soil bacteria.

The daytime uptake rates are either the result of lower production rates or enhanced degradation during the day in sites 4 and 5. The higher daytime production of CH_3Cl could be connected to the low production/enhanced degradation of CS_2. We hypothesised that low CS_2 production rates would be a sign of low rates of anaerobic degradation of CH_3Cl in the soils. Thus, high CH_3Cl fluxes would coincide with low or absent CS_2 fluxes if anaerobic degradation was the main soil sink. However, these explanations cannot account for the behaviour of the CS_2 fluxes at the investigated sites. No correlation between CS_2 and CH_3Cl fluxes was observed. The assessment of CH_3Cl/CS_2 dynamics is made even more difficult by the fact that so little is known about CH_3Cl formation or degradation mechanisms in terrestrial ecosystems.

5.4 Discussion - summary

Vegetation-derived CH_3Cl emissions correlated with temperature and had a clear diurnal cycle. The highest emission rates were recorded during the midday and afternoon. In some investigated areas, the gas flux turned from positive to negative during the night. Soil chemical and biological reactions played a minor role in controlling the CH_3Cl emissions flux. The background CH_3Cl concentration did not show a diurnal trend. The changes in the ambient air CH_3Cl concentration were controlled by the wind speed. No direct connection between the fluxes of sulphur-containing gases and CH_3Cl were found. However, some indications were found that suggested reduced soil conditions and high emissions of sulphur-containing gases are linked to lower CH_3Cl emission rates.

6. Conclusion: Terrestrial chloromethane emission

The vegetation of boreal coastal meadows is a source for atmospheric CH_3Cl. The emission rates are in the same range as for other coastal and inland areas. In 2007 and 2008, the daytime emission rate was approximately 701 ng m^{-2} h^{-1} and 790 ng m^{-2} h^{-1}, respectively, and no substantial differences were detected between different vegetation types. The night/evening emissions rates were clearly smaller or even negative, implying that the coastal ecosystem might also function as a sink for chloromethane in the absence of light. Although the different sites had substantial differences in their chemical and physical soil characteristics (i.e., moisture, OM content, texture, EC and metal content), none of the measured parameters seemed to have a direct influence on the CH_3Cl emission rates. The emissions did not correlate positively or negatively with the emitted sulphur compounds. Hence, it can be concluded that soil processes play a minor role in the CH_3Cl dynamics of a terrestrial ecosystem in this climatic zone. Under the experimental conditions, the major factors influencing the emission are those having a direct impact on the vegetation (i.e., air temperature and solar radiation).

7. Characterisation of the lipophylic compounds of three halophytic plant species

7.1. Introduction

Plant cells contain vast amounts of lipids. If a plant is observed from the outside to the inside, the first encounter with lipids is made immediately at the leaf (or stem) surface, which is coated with a wax layer. The compounds making up this layer are called epicuticular and cuticular waxes. The role of this layer is to protect the plant cells from dirt and to help control its water content. The surface waxes are mostly esters of fatty acids and fatty alcohols (alkanols), but also include long-chained alkanes and free alkanols (Vandenburg & Wilder 1970). Next to the surface lipids, plant cells include many membrane-enclosed structures, such as the cell membrane, nucleus membrane, vacuole and Golgi apparatus, and all of these are made of phospholipid layers. Many plants store energy in form of storage lipids, which are an important source of plant oils. In most plants, these storage lipids are triglycerides (Murphy 1994).

Halophytic (i.e., salt-loving) plants live in regions with elevated environmental salinity. Such areas are usually located at the sea coast or in inland areas with high soil salinity due to either salt-containing geological formations or human-induced salinity caused by irrigation in arid areas (Flowers et al. 1986). High environmental salinity causes many challenges for plant survival, because the ionic strength of the water and therefore the osmolytic pressure are often higher outside the plant cell than inside. Therefore the plants growing in a saline environment get excess chloride (and sodium) as chloride passively diffuses into the cell. Halophytic plants have many strategies to cope with this excess chloride. Many species form molecules, called osmolytes, which increase the osmotic pressure inside the cell preventing the intrusion of chloride-containing water into the cell. However, this procedure is mostly not efficient enough and thus plants have other methods to discard the unwanted chloride. Therefore, osmoregulation is also required inside the cell, and osmolytes must regulate the ion concentrations between different cell compartments (Flowers et al. 1986). The plant species belonging to *Chenopodiaceae* (the plant family of many salt

marsh halophytes) accumulate ions (Na^+ and Cl^-) inside the vacuole, and the osmolytes are organic molecules called organic solutes. These compounds are primarily organic acids, nitrogen-containing compounds and carbohydrates (Flowers 1986). Other common osmolytic compounds include proline, betaine and other amino acids and carbohydrates, such as sucrose. Lipophylic compounds do not act as osmolytes as they are not soluble in the watery matrix that fills the cell. There is very little available information about plant lipids in halophytes. Most studies have concentrated on the oil content of the halophytes and only very few have undertaken a complete inventory of their lipid content. The incorporation of the excess chloride into organic compounds does not seem to happen often in higher plants, and only a few chlorinated organic compounds are found in these plants (Gribble 1998). This study listed six chlorinated metabolites found in plants. All six contain an aromatic ring in the structure; one of the compounds functions as a plant growth hormone and the other compounds have insecticidal activity. Overall, the appearance of chlorinated compounds in halophytic plants has not been the object of many investigations. The discovery of CH_3Cl emission from salt marsh plants and also halophytic inland plant species (Rhew et al. 2000 and Rhew & Abel 2007) highlights the interesting role of the halogenation process in halophytes. In addition, the distribution of this reaction in the plants is unknown. Therefore the aim of this investigation was to determine if the plant lipid fraction in the three different halophytic plants would show signs of more widespread chlorination of plant organic compounds and show a connection to CH_3Cl synthesis.

7.2 Material and methods

The plant material was collected from a coastal salt marsh in the Wadden Sea National Park located at the German North Sea coast. The collection was made on August 8, 2007. Three different halophytic plant species were selected, namely: *Sueda maritima* (Sea Blite), *Halimione portulacoides* (Sea Purslane) and *Salicornia europaea* (Glasswort). All three plants are succulent halophytes belonging to the family of *Chenopodiaceae*. After collection, the plant material was stored in a cool and dark place for five days. Before the extraction of the lipids, the plants were rinsed with double distilled water and dried with tissue

paper; next, the yellow or brown parts of the plants were cut away and discarded.

7.2.1 Total lipid extract

Approximately 50 g of fresh plant material was collected for extraction and homogenised with an electronic mixer in small amounts of isopropanol. The extraction protocol proceeded with the following steps (Figure 7.1):

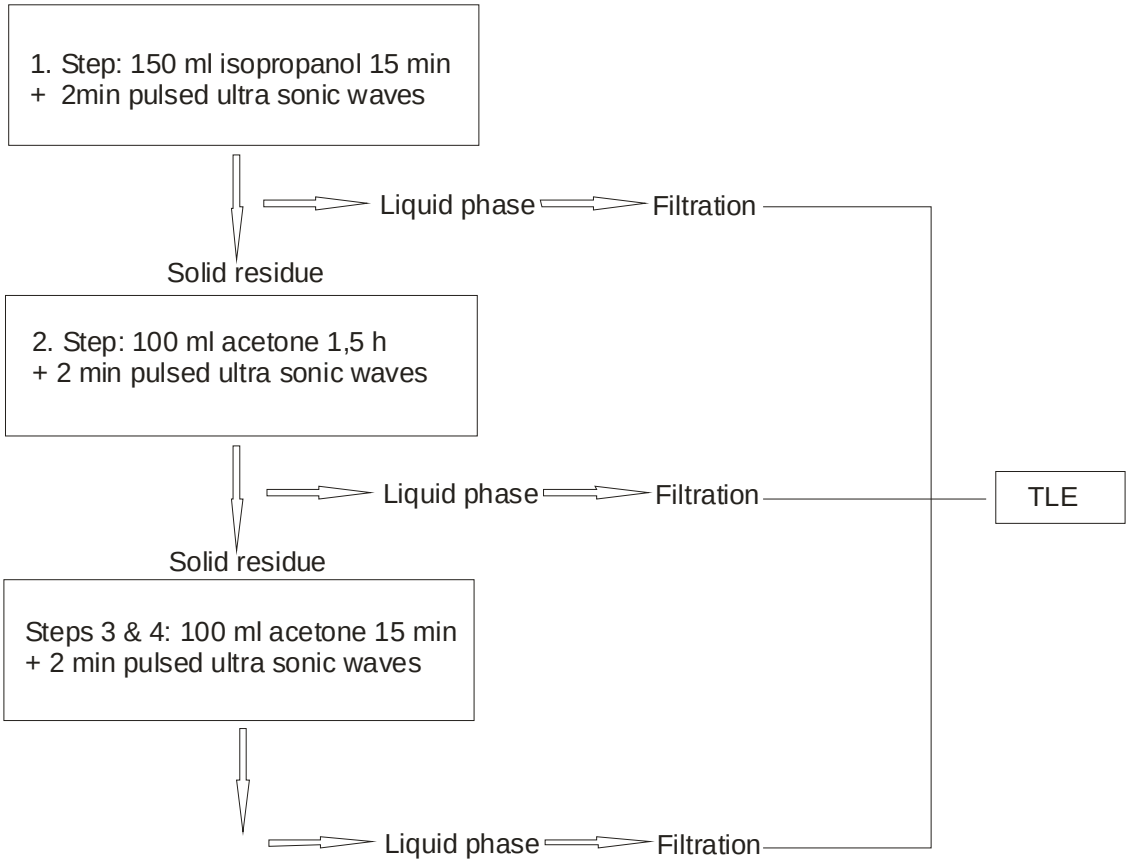

Figure 7.1 Extraction scheme of the total lipid extract

The plant material was extracted for its lipids in four steps starting with isopropanol, which was used to prevent the degradation of lipids by the activity of lipolytic enzymes (Nichols 1963). Next, ultra sonic waves were used (Bandelin soniplus HD 2070) to enhance the extraction of lipophylic material from the plant tissues. After each solvent extraction step, the liquid part was decanted and filtered through a glass-fibre filter using a vacuum. The filtered

aliquots were combined as the total lipid extract (TLE) and concentrated to a watery resin using a rotary evaporator. Liquid-liquid extraction was used to separate the water and hydrophilic substances from the TLE. The watery resin was shaken with ethyl ether at least five times in a separation funnel, and the ethyl ether soluble phase was collected for further treatment. The extracts were eluted through small amount of sodium sulphate (Na_2SO_4) to remove any remaining traces of water.

7.2.2. Fractionation

One half of each TLE was separated into three fractions with solid-phase column chromatography. A wet-packed (n-hexane) column of silica gel (Merck, Kieselgel 60) was used (h: 14 cm, ø: 1.5 cm) as the solid phase. Hydrocarbons were eluted using 52.2 ml of n-hexane; aldehydes and ketones were eluted with 75 ml of ethyl acetate (EE): n-hexane (1:9, V/V) mixture; and the polar substances were eluted with 150 ml of methanol (MeOH).

The third fraction (MeOH) was further treated by alkaline hydrolyses to release the bound polar lipids, especially the fatty acids. The solvent was evaporated from the samples and 10 ml of a 5% KOH/MeOH solution was added and let to react for 2 h in an 80℃ ultrasonic bath. After cooling the extract, the neutral lipids were extracted with hexane (1 x 10 ml and 4 x 5 ml), and the collected hexane fraction was concentrated to a small volume in a rotary evaporator. The remaining extract was acidified with a small amount of 1 M H_2SO_4, and the acidic lipids were extracted with ethyl ether (2 x 10 ml and 2 x 5 ml). The ethyl ether was thereafter evaporated in the rotary evaporator, and the resultant solid was dissolved in a small amount of hexane.

The ethyl ether extracted fraction consisting of the acidic lipids was further treated to separate the saturated and unsaturated fatty acids to different fractions and to remove some of the linolenic acid (18:3). The linolenic acid was present in such a large amount that it made it difficult to identify other fatty acids and not saturate the GC-MS. Silver nitrate $AgNO_3$ was used the remove the polyunsaturated fatty acid methyl esters (PUFAs) as described by Mu et al.

(1996 a). After silver nitrate treatment, the fatty acid methyl esters (FAMEs) were fractionated into three fractions using solid-phase extraction (SPE) cartridges according to a method described by Åkesson-Nilsson (2003) with modifications. The solvent mixture (n-hexane-diethyl ether-dichloromethane; 89:1:10, v/v) for the last fraction was replaced with an acetone-n-hexane (10:90, v/v) mixture. The first fraction in the method of Åkesson-Nilsson (2003) was divided into two fractions, with the first and second fractions containing 4 and 2 ml of hexane, respectively. These changes were made based on tests with standard material that showed that the saturated fatty acid methyl esters (FAMEs) were mostly eluted in the first two millilitres and the polyunsaturated FAMEs in the next four millilitres. The last fraction consisted of mostly hydroxyl FAMEs and the possibly present chlorinated FAMEs (Åkesson-Nilsson, 2003).

7.2.3 Derivatisation

All of the fractions were further treated to make the high molecular compounds more volatile and to simplify their gas-chromatographic analysis and identification. Fractions 2 and 3 from the CC (column chromatography) were derivatised with BSTFA (bis-N,O-trimethylsilyl trifluoroacetamide) to produce trimethyl silyl-derivates, which helped with the identification of long-chain alcohols. The derivatisation was conducted according to the following procedure: 1 ml of the fraction was dried under a stream of nitrogen; 400 µl of BSTFA was added, and the samples was left to react for one hour at +80℃; and finally 2 ml of n-hexane was added before further analysis.

The acidic fraction of the alkaline hydrolysis consisting of the fatty acids was derivatised to produce FAMEs. This was done by adding diazomethane dissolved in 200 µl of diethyl-ether into the nitrogen-dried extract and leaving it for 1 h at room temperature; then, the solvent was evaporated under a stream of nitrogen, and the FAMEs were dissolved in a small amount of n-hexane before further treatment or analysis.

7.2.4 Gas chromatography—mass spectrometry

The identification of all substances was made with the help of a Fisons Instruments 8060 gas chromatograph connected to a mass spectrometer (MD 800) from the same manufacturer. The mass spectrometer was operated at 70 eV with a mass range of m/z 50-650 (source T: 230℃; in terface T: 300℃). The instrument was equipped with a cool-on-column injector that followed the temperature of the column oven and with a DB-5 bonded phase capillary column (30 m; 320 µm i.d.; 0.25 µm film thickness). For the analyses of the hydrocarbon fraction, a DB-1 column (30 m; 320 i.d.; 0.25 µm film thickness) was also used. Helium was used as the carrier gas. The following temperature programme was used for all but the hydrocarbon fraction: 80℃ (3 min) to 310℃ (20 min) at a rate of 6℃ min^{-1}. The hydrocarbon fraction was chromatographed as follows: 60℃ (1 min) to 130℃ at a rate of 20℃ m in^{-1} , followed immediately by 4℃ min^{-1} to 310 (15 min). The identifications were made by comparing the resulting mass spectra with those in the NIST mass spectra library.

7.2.5 Gas chromatography—halogen sensitive detector (XSD)

Chlorinated straight-chain alkanes were quantified and their identification was confirmed using a HP 6890 gas chromatograph connected to an O.I Analytical model 5360A halogen sensitive detector (XSD). The GC was equipped with an on-column injector and a similar DB-5 capillary column as used in the GC-MS experiments. The GC was operated in constant flow mode with helium as the carrier gas and a flow velocity of 1.7 ml min^{-1}. The following temperature programme was used: 60℃ (1 min) to 270℃ (20 min) at a rate of 4℃ min^{-1}. The XSD was operated with a reactor temperature of 900℃. The compounds were quantified using 1-chlorooctane as the internal standard. The identification for 1-chloroalkanes was done by comparing the GC-XSD retention times to the retention times of standards (1-chlorodocosane, 1-chloroeicosane, 1-chlorooctadecane and 1-chlorotriacontane all from TCI Europe NV, Zwijndrecht, Belgium). Further confirmation of the compound structure was made with the help of the mass spectra, in which the typical low-intensity fractionation series

(next to the normal n-alkane series) of fragments with m/z of 91, 105, 119, and 133 for the 1-chloroalkanes was detected (Grossi et al. 2003).

7.2.6 Gas chromatography—flame ionisation detector (FID)

The halocarbon fraction (except the chlorinated compounds) was quantified using GC combined to a flame ionisation detector. This detector reacts based on the amount of carbon in the compound (i.e., the signal becomes more intense via a linear relationship to the amount of carbon in the analysed compound) (Riekkola and Hyötyläinen 2002) and is therefore well suited for the quantification of compounds consisting of only carbon and hydrogen, such as the alkanes analysed in this study. A Carlo Erba GC equipped with an on-column injector and a DB-5 capillary column with the same specifications (see 7.2.3) was employed. The oven was programmed with the following temperature programme: 80℃ (3 min) to 310℃ (20 mi n) at a 4℃ min^{-1} step. The compounds were quantified using n-tetratricontane (a 34-carbon alkane) as an internal standard.

7.2.7 Summary of the methods

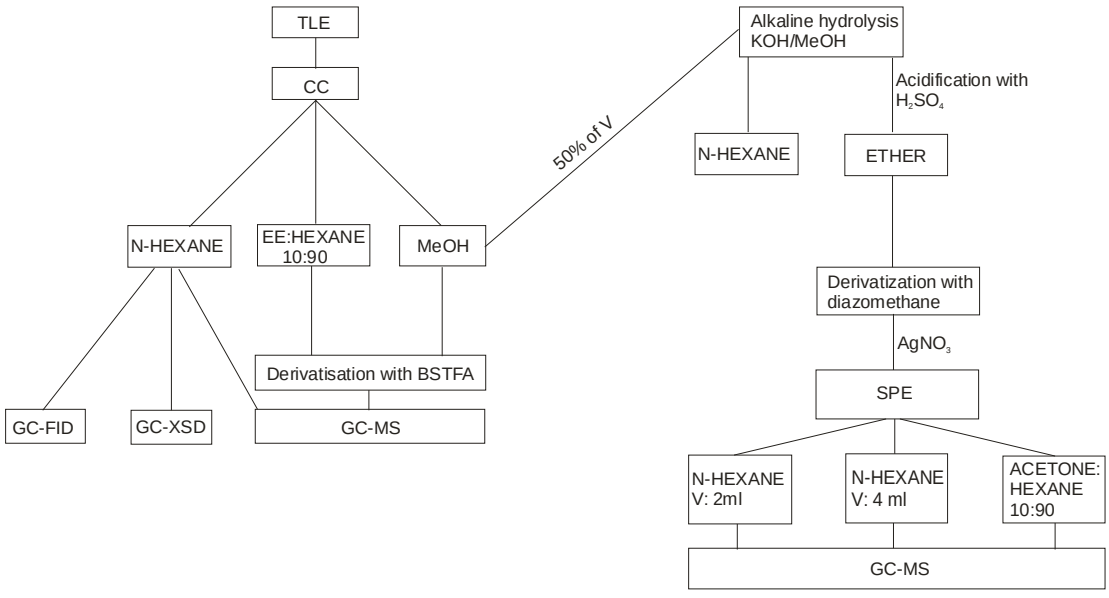

Figure 7.2 Schematic presentation of the analytical methods.

During all treatments of the plant extracts, the use of halogenated (especially chlorinated) solvents or other halogenated chemicals was avoided (Figure 7.2) to prevent the formation of halogenated products as artefacts during the separation process and analysis.

7.2 Results

7.2.1 Hydrocarbons

Fraction one, which was eluted with n-hexane, consisted mainly of straight-chained n-alkanes, iso-alkanes (2-methyl-) and anteiso-alkanes (3-methyl-) in all three plant extracts (Table 7.1). Although there were some common characteristics in the alkanes from the three species, such as dominance of odd-over-even chain-length alkanes, some major differences could be detected also. The most abundant alkanes in the *H. portulacoides* extract were n-pentacosane (C_{25}) and n-heptacosane (C_{27}) followed by nonacosane (C_{29}), which had a concentration of about half of the two most abundant compounds. In the *S. europaea* extract, the most abundant compound was tricosane (C_{23}), which was followed by pentacosane.

Surprisingly high amounts of anteiso-alkanes were detected in the *S. europaea* extract considering the abundance of the heptacosane and nonacosane isomers ai-C_{27} and ai-C_{29}. These results were different from the other two plant extracts, which both had low amounts of ante-isoalkanes relative to n-alkanes. In the *H. portulacoides* extract, the ante-iso and iso-alkanes were detected only as traces and could not be reliably quantified. Heptacosane was the most abundant compound of the *S. maritima* extract in the hydrocarbon fraction, followed by almost equal amounts of pentacosane and nonacosane. The concentrations of these compounds were roughly the of the heptacosane concentration. The *S. maritima* extract was distinct in having larger amounts of odd-chain-length iso-alkanes than the other two extracts.

Table 7.1 Concentration of hydrocarbons in the fresh weight (= f.w.) and total lipid extract (=TLE) of plant extracts.

	Halimione portulacoides		***Salicornia europaea***		***Sueda maritima***	
Compound	**µg g^{-1} f.w.**	**µg g^{-1} TLE**	**µg g^{-1}f.w.**	**µg g^{-1}TLE**	**µg g^{-1}f.w.**	**µg g^{-1}TLE**
C_{21}	0.29	46	0.63	204	-	-
C_{22}	0.38	60	0.25	81	-	-
i-C_{23}	-	-	0.18	57	-	-
C_{23}	2.06	322	3.11	1012	0.39	70
ai-C_{24}	-	-	0.16	53	-	-
C_{24}	1.78	279	0.24	77	0.21	38
i-C_{25}	-	-	-	-	0.18	32
ai-C_{25}	-	-	0.33	106	-	-
C_{25}	10.30	1608	1.71	557	3.20	571
ai-C_{26}	-	-	0.17	54	0.20	36
C_{26}	2.47	386	0.18	57	0.53	95
i-C_{27}	-	-	-	-	0.66	118
ai-C_{27}	-	-	1.13	367	-	-
C_{27}	9.41	1469	1.22	395	7.35	1312
ai-C_{28}	-	-	0.12	40	0.45	81
C_{28}	1.34	209	0.08	26	0.70	125
i-C_{29}	-	-	-	-	0.64	114
ai-C_{29}	-	-	0.49	161	-	-
C_{29}	4.13	645	0.87	283	3.54	631
ai-C_{30}	-	-	-	-	0.26	47
C_{30}	0.37	57	0.11	35	0.46	82
i-C_{31}	-	-	-	-	0.28	49
ai-C_{31}	-	-	0.19	62	-	-
C_{31}	0.47	73	0.56	183	0.45	80
∑ HC µg	**1623**		**607**		**1145**	
m TLE mg	**315**		**159**		**329**	
m plant g	**49.2**		**51.8**		**58.7**	

The total hydrocarbon content was highest in *H. portulacoides* (33 µg g^{-1} on a fresh weight basis), intermediate for *S. maritime* (20 µg g^{-1}) and lowest in *S. europaea* (12 µg g^{-1}).

7.2.2 1-Chloro-alkanes

A series of chlorinated straight chained alkanes ranging from C_{19}-C_{29} were detected in the hydrocarbon fractions of all three plant extracts. The distribution of the chain lengths of the chlorinated n-alkanes differed markedly from that of the non-chlorinated ones (Figure 7.3).

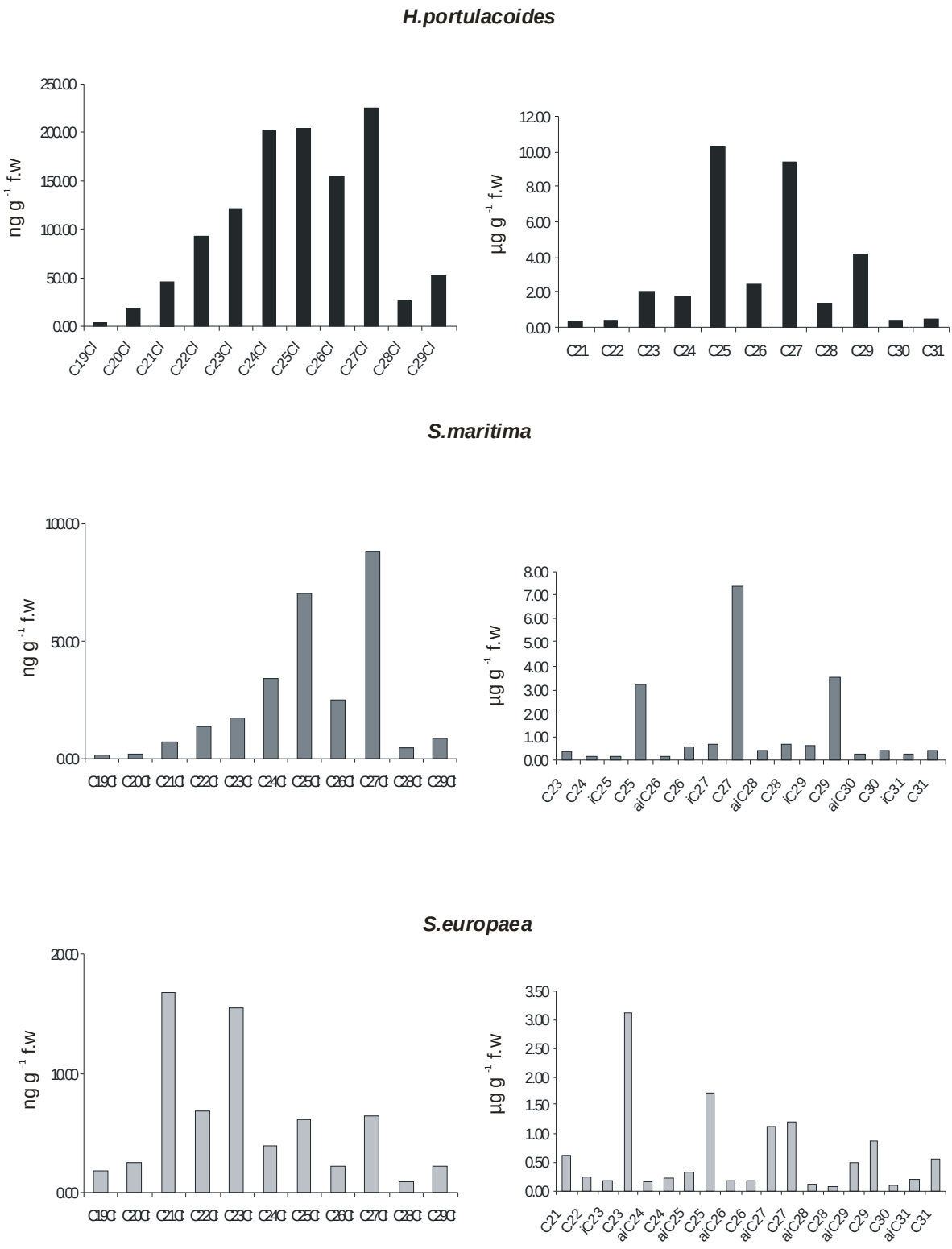

Figure 7.3 In the left column the concentrations of Cl-n-alkanes in the plant extracts relative to plant fresh weight (f.w.) and in the right side column the concentrations of non-halogenated alkanes relative to plant fresh weight of the corresponding plant extracts.

The chlorinated alkanes generally did not show the typical odd-over-even distribution, which the non-halogenated alkanes had shown. However, the *S. europaea* extract differed from the other extracts by having an odd-over-even domination, which was observed by chain lengths C_{21}, C_{23}, C_{25} and C_{27} being clearly more concentrated than the even-chain-length Cl-alkanes eluting next to and in between these compounds. The concentrations of the Cl-alkanes ranged from 5-220 ng g^{-1} (f.w.) in the *H. portulacoides* extract, from 1-90 ng g^{-1}(f.w.) in the *S. maritima* extract and from 1-17 ng g^{-1} (f.w.) in the *S. europaea* extract. When the concentrations were calculated relative to the mass of the total lipid extract (TLE dry weight), the relative abundances of the Cl-alkanes did not change between the three extracts. *H. portulacoides* still exhibited the highest concentrations of Cl-alkanes and *S. europaea* contained the lowest concentration (Table 7.2).

Table 7.2 Concentrations of individual Cl-alkanes of the investigated three halophytic plant species.

	Halimione portulacoides		***Sueda maritima***		***Salicornia europaea***	
Compound	**µg g^{-1} TLE**	**µg mg^{-1} HC***	**µg g^{-1} TLE**	**µg mg^{-1} HC**	**µg g^{-1} TLE**	**µg mg^{-1} HC**
Cl-C_{19}	0.80	0.15	tr	tr	0.01	0.08
Cl-C_{20}	3.05	0.59	0.01	0.17	0.02	0.11
Cl-C_{21}	7.05	1.37	0.02	0.65	0.11	0.76
Cl-C_{22}	14.40	2.79	0.04	1.27	0.04	0.31
Cl-C_{23}	18.88	3.66	0.05	1.66	0.10	0.70
Cl-C_{24}	31.45	6.10	0.10	3.30	0.02	0.18
Cl-C_{25}	31.83	6.17	0.21	6.82	0.04	0.28
Cl-C_{26}	24.17	4.69	0.07	2.38	0.01	0.10
Cl-C_{27}	35.12	6.81	0.27	8.50	0.04	0.29
Cl-C_{28}	4.12	0.80	0.01	0.42	0.01	0.04
Cl-C_{29}	8.07	1.57	0.03	0.83	0.01	0.10

* HC = sum of all quantified hydrocarbons

When the concentrations of the 1-chloroalkanes were calculated relative to the total hydrocarbon amount, *H. portulacoides* and *S. europaea* had the highest and lowest concentrations, respectively.

7.2.2 Aldehydes, ketones and alcohols

The second fraction from the column chromatography was analysed with GC-MS for identification of the substances and with GC-XSD to detect the presence of any halogenated compounds. The most abundant substances in this fraction

were even-chain-length alcohols or aldehydes as in the *H. portulacoides* extract (Table 7.3).

Table 7.3 Relative abundances of the identified compounds in fraction 2 of the plant extracts.

Halimione portulacoides		***Sueda maritima***		***Salicornia europaea***	
Compound	**Relative abundance***	**Compound**	**Relative abundance**	**Compound**	**Relative abundance**
Tetracosanal	< 5%	Tetracosanol	< 5%	Eicosanol[a]	30%
Pentacosanone	< 5%	Hexacosanal	10%	Docosanal	< 5%
Pentacosanal	< 5%	Hexacosanol	20%	Heneicosanol	< 5%
Hexacosanal	30%	Octacosanol	100%	Docosanol[b]	100%
Hexacosene	5%	Tricontanal	10%	Tetracosanal	< 5%
Heptacosanone	< 5%	Tricontanol	15%	Tricosanol	10%
Heptacosanal	5%			Tetracosanol	65%
Hexacosanol	10%			Hexacosanol	25%
Octacosanal	100%			Octacosanol	30%
α-Tocopherol	70%			Tricontanol	15%
Tricontanal	70%			Dotriacontanol	< 10%

* = relative to the peak height of the most abundant compound, i.e., the compound with a relative abundance of 100%
a = also called arachidyl alcohol
b = also called behenyl alcohol

The relative abundances were obtained from the chromatograms after derivatisation of the plant extracts with BSTFA, which reacted with the alkanols to yield the corresponding trimethyl-silyl-esters. This was done to improve the volatility of the alkanols, but might have also led to over-presentation of their abundance compared to aldehydes, which do not react with BSTFA due to the lack of an OH-group. However, the data in Table 7.3 give a good idea of the main compounds in this fraction of the plant extracts.

The most abundant compounds in fraction 2 of the *H. portulacoides* extracts were n-aldehydes with chain lengths of C_{26}, C_{28} and C_{30} (Table 7.3). Only one alkanol could be detected and had a chain length of C_{26}. Other alkanols are probably present in low concentrations. Surprisingly, a large amount of α-tocopherol was detected in this fraction; in addition, the other two plant extracts contained this compound in the corresponding fraction but its relative abundance was very low after derivatisation. When the fractions were analysed prior to treatment with BSTFA, α-tocopherol was relatively more abundant than after the derivatisation also in the two other extracts, but the difference was smaller than in the *H. portulacoides* extract.

S. maritima had a somewhat narrower range of substances in the second fraction than the other two plants, consisting mostly of even-chain-length alkanols (C_{26}, C_{28} and C_{30}). Octacosanol was largely predominant in this fraction. *S. europaea* extracts had the widest range of alkanols from C_{20} to C_{32} (even chain length), with the most abundant compounds being docosanol (C_{22}; 100%), tetracosanol (C_{24}; 65%), hexacosanol (C_{26}; 25%) and octacosanol (C_{28}; 30%). Also a few odd-chain-length alkanols heneicosanol (C_{21}) and tricosanol (C_{23}) were found. Aldehydes were present only in small amounts in both *S. maritima* and *S. europaea* extracts, with the former having only hexacosanal in a substantial amount and the latter having docosanal and tetracosanal in detectable amounts.

The GC-XSD analyses showed sporadic peaks, but there was no evidence in the GC-MS chromatograms that would have supported the presence of halogen atoms in the compounds that eluted during the same retention time. If present, these compounds would be in very low concentrations. Therefore, halogenated substances were not identified in this fraction.

7.2.3 Fatty acids and sterols

The third fraction was divided to two sub-fractions (Figure 7.2), namely acidic and neutral lipids. The neutral lipids consisted of different strerols and the acidic part of fatty acids. The fatty acids part was examined more intensively in this study because several investigations have reported naturally formed halogenated fatty acids in marine organisms (Mu et al. 1996b, Blumenberg and Michaelis 2007). The first injection of the fraction consisting of the fatty acids gave nearly identical results for all three plants. The GC-MS chromatogram had two very large peaks, which were identified as palmitic acid (16:0) and linolenic acid (18:3). To detect other fatty acids present in lower concentrations, this fraction was further treated as described in section 7.2.2, resulting in three more sub-fractions. In these three sub-fractions, a series of even-chain-length unsaturated fatty acids ranging from C14:0 to C26:0 and an odd-chain-length series ranging from C15:0 to C23:0 (in very low concentrations) were identified. In addition, a few saturated fatty acids were detected namely: linoleic acid 18:2,

palmitoleic acid 16:1 and a very low amount of behenic acid 22:2. The unsaturated fatty acids were found in the first sub-fraction, the saturated fatty acids were mostly present in the second sub-fraction, and phytol and some hydroxy-fatty acids were identified in the third sub-fraction. However, none of the substances showed sings of halogenation.

The neutral fraction consisted mostly of sterols, with the most abundant substances being phytol and β-sitosterol. No halogenated substances were found in this fraction.

7.3 Discussion

7.3.1 Hydrocarbon fraction

The odd-over-even carbon-chain length dominance of n-alkanes and their maximum amounts peaking from C_{21} to C_{29} observed in this study are classical examples of plant hydrocarbon distribution (Bianchi 1995). Small amounts of iso- and anteiso-alkanes also can be expected. All of these compounds are most commonly found in epicuticular (leaf surface) waxes of higher plants (Eglinton and Hamilton 1967 and Reddy et al. 2000). However, the relatively high concentration of some anteiso-alkanes (ai-C_{27} and ai-C_{29}) in the *S. europaea* extract was somewhat out of the ordinary. Anteiso-alkanes are found in high concentrations among the plant kingdom; in tobacco plants, they can make up to 68% of the total hydrocarbons (Grice et al. 2008). The total amount of anteiso-alkanes in the *S. europaea* leaves was considerably lower than in tobacco plants.

The presence of 1-chloro-n-alkanes was the most interesting finding in the plant leaf extracts of the three halophytes. Chlorinated alkanes did not have the same concentration distribution as the normal n-alkanes but followed a more random distribution pattern. Although no clear odd-over-even predomination was observed, the most abundant compound in all three plants had an odd carbon number. These findings are consistent with those by Grossi et al. (2003) for

three Mediterranean halophytes. Grossi et al. (2003) studied the following plant species: *Sueda vera* (close relative to *S. maritima*), *Sarcocornia fructiosa* (close relative to *S. europaea*) and *Haliomione portulacoides*. When comparing the 1-chloro-n-alkane distribution patterns of the close relatives with each other, *S. vera* and *S. maritima* exhibited almost identical concentration patterns concerning the chlorinated alkanes; the concentrations constantly increased from Cl-C_{21} to Cl-C_{25}, and then exhibited a drop at Cl-C_{26}, maximum at Cl-C_{27} and very low amounts at Cl-C_{28} and Cl-C_{29}. Surprisingly the two *H. portulacoides* individuals showed quite different distribution patterns. *H. portulacoides*, which was analysed by Grossi et al. (2003), had substantially lower concentrations of Cl-C_{24} and Cl-C_{26} than in this study. *S. fructicosa* and *S. europaea* showed a very different Cl-alkane distribution with the former having concentration maxima at Cl-C_{25} and Cl-C_{27} and the latter at Cl-C_{21} and Cl-C_{23}. The distribution of 1-Cl-alkanes does not seem to be connected exclusively to the plant species as the n-alkane distribution often is (for example Dove and Mayes 2005), but it might be more affected by the conditions at the growing site and/or the stage of the growing season. Because the Cl-alkanes are structurally similar to n-alkanes, we first assumed that their formation would result from chlorination of the corresponding n-alkanes. However, this would result presumably in the same distribution pattern, which was not observed herein. n-Alkanols or aldehydes are not a probable precursor for 1-Cl-alkanes as Grossi et al. (2003) demonstrated by comparing the concentration distributions. Chlorination of the leaf wax alkanes might occur randomly on the surface of the halophytic plants, which survive in very saline environments, and is induced by heat from the sunlight. High temperatures (pyrolysis) can produce 1-Cl-alkanes from geomacromolecules (Grossi et al. 2008), and temperatures during pyrolysis used in the former study were above 300°C, which is substantially higher than the ambient temperatures of coastal environments.

Very little is known about 1-Cl-alkanes and their formation in plants, making it hard to speculate about the connection between CH_3Cl production and Cl-alkane production. At the moment, only two studies have reported findings of Cl-alkanes in plants (this study and Grossi et al. 2003). Although the

mechanisms for formation of chlorinated alkanes in plants remain unknown, new substances other than CH_3Cl will be added to this group.

7.3.2 Alcohols, aldehydes, ketones, fatty acids and sterols

The other fractions of the plant extracts did not reveal the presence of halogenated substances. Overall, no surprising or out of the ordinary chemical constituents were found in these compound classes. The aldehyde and alcohol distribution had an even-over-odd distribution according to the chain lengths of these compounds, which is common in higher plants (Rommerskirchen et al. 2006, Stanley et al. 1987). Further separation and purification of the second fraction (aldehydes and alcohols) might have lead to more interesting findings. The main objective of this study was to screen for halogenated substances, so it was not considered purposeful to proceed in this direction as no positive result was gained from the XSD-analyses. The fatty acid fraction underwent an extensive separation protocol, which did not result in finding halogenated fatty acids. Therefore, if such compounds are present in the leaves of these three halophytic species, the concentration would be extremely low. The sterol fraction was less intensively studied as the other fractions due to the relatively small amounts of the substance in the fraction (purification resulted in a very pure sterol fraction) and because of the structural complexity of these compounds, thereby making simple halogenation hard to detect.

7.4 Characterisation of the lipophylic compounds of three halophytic plant species – summary

The analysed plants (*Sueda maritima* (Sea Blite), *Halimione portulacoides* (Sea Purslane) and *Salicornia europaea* (Glasswort)) were collected from a coastal salt marsh located on the German North Sea coast. Each plant was extracted for its lipid content and the yielded lipids were further separated to different fractions. The gained fractions were analysed with different gas chromatography techniques. The aim of the investigation was to identify halogenated compounds in the plant lipid matrix.

The major finding was the discovery and identification of a series of long-chain (C_{19} – C_{29}) 1-chloro-n-alkanes in the hydrocarbon fraction of each of the investigated plant species. The distribution pattern and concentrations of these compounds varied between the species. In light of this study, the mechanism leading to 1-Cl-alkane formation in plants remains unravelled and needs to be further investigated.

8. Summary

Volatile halogenated organic compounds (VHOCs) play an important in role in atmospheric chemistry. VHOCs with long atmospheric life times have especially harmful effects because they act as carriers for stratospheric halogens and enhance stratospheric ozone depletion. Chloromethane (CH_3Cl) is the largest natural gaseous source of stratospheric chlorine. This chemical compound is derived from various sources. The biggest identified sources for CH_3Cl are warm ocean waters and terrestrial living and senescent plants. The global CH_3Cl budget is bound with large uncertainties, considering the estimations for the strengths of each individual source and sink. Therefore, further elucidation of the environmental chemistry of CH_3Cl is needed to understand the biogeochemical processes controlling the global CH_3Cl cycle. In this study, a new geographic area was investigated according to its CH_3Cl cycling and relevant environmental parameters were recorded.

A boreal coastal meadow was found to be a source for CH_3Cl. The emission rates were comparable to those from other coastal sites. The measured emission rates in the investigated two years (2007 and 2008) were very similar. The calculated daily emission with its standard error was 10.36 (+/- 0.60) µg m^{-2} d^{-1} and 36.58 (+/- 2.54) ng g^{-1} d^{-1} normalised to area and biomass, respectively. Overall, three different vegetation types were investigated for their CH_3Cl fluxes, but no substantial differences were observed between them.

A variety of environmental parameters were measured in addition to CH_3Cl fluxes, with soil parameters, such as moisture, salinity, pH and organic matter content of particular interest. Next to soil parameters, fluxes of two sulphur-containing gases (dimethyl sulphide, DMS, and carbon disulphide, CS_2) were recorded parallel to CH_3Cl emission. DMS and CS_2 were measured as they are abundantly emitted from coastal and marine regions and are also end-products in anaerobic CH_3Cl degradation. Although there is theoretically a link between DMS and CS_2 production and CH_3Cl degradation, no connection between the fluxes of these gases and CH_3Cl could be recorded at the investigated site.

Overall, soil conditions and soil microbiological processes were found to be of minor importance in controlling the CH_3Cl emission. This seemed to be correlating only to the air temperature and the time of the day. At a few sites, negative (uptake) fluxes for CH_3Cl were measured at night. Uptake fluxes can be explained by CH_3Cl consumption in soil chemical and biological processes or to some extent based on physical uptake by diffusion to soil pore space. Therefore, soil processes are a controlling factor for CH_3Cl fluxes, but it is difficult to connect single soil parameters to the behaviour of the CH_3Cl flux due to the complexity of these processes.

Marine organisms like macro- and microalgae seaweed and fungus have been discovered to produce a variety of halogenated organic compounds. Also many terrestrial microbes produce especially chlorinated substances. So far, approximately 3500 naturally produced organic compounds have been identified. Inside the plant kingdom, the formation of halogenated compounds seems to be very rare. Until recently, only a handful of plant-derived compounds had been identified. The marine coastal environment with its high natural salinity and many halophytic, i.e., salt-loving plant species, was found to be an enticing environment to look for new halogenated plant-derived organic compounds.

Next to CH_3Cl coastal halophytes (*Sueda maritima* (Sea Blite), *Halimione portulacoides* (Sea Purslane) and *Salicornia europaea* (Glasswort)) were discovered to produce a series of chlorinated long-chain alkanes. The distribution pattern and concentration of these 1-chloro-n-alkanes differed markedly between the different plant species. The largest amount of Cl-alkanes was found in *H. portulacoides*, which also had the largest hydrocarbon content among the investigated species. The chlorination reaction does not seem to be acting in a wide range in halophytic plants as no other chlorinated organic compounds were found in the extracted plants. The amount of produced 1-chloroalkanes seemed to be connected to the overall hydrocarbon content in the plant. The mechanism behind Cl-alkane production needs to be further elucidated. On a highly speculative level it could be seen as an effect of a high chloride content of the plant growing environment.

References

Ahti T., Hämet-Ahti L. & Jalas J. 1968 Vegetation zones and their sections in the north western Europe. *Ann. Bot. Fenn*. 5: 169 - 11

Bianchi, G. 1995 Plant waxes In: Hamilton R. J. (Ed.) *Waxes: chemistry, molecular biology and functions*. The oily press, Dundee 175 - 222

Bill, M., Rhew, R., Weiss, R. & Goldstein, A. 2002 Carbon isotope ratios of methyl bromide and methyl chloride emitted from a coastal salt marsh. *Geophys. Res. Lett.* 29:(4) 1 - 4

Blumenberg, M., & Michaelis, W. 2007 High occurrences of brominated lipid fatty acids in boreal sponges of the order Halichondrida. *Mar. Biol*. 150:1153 - 1160

Braus-Stromeyer, S., Cook, A. & Leisinger, T. 1993 Biotransformation of chloromethane to methanethiol. *Environ. Sci. Technol*. 27: 1577 - 1579

Brown, J. & Shirey, B. A tool for selecting an adsorbent for thermal desorption applications. Supelco Technical Report, Supelco, Bellefonte, PA, USA pp. 36

Butler, J., Battle, M., Bender, M., Montzka, S., Clarke, A., Saltzman, E., Sucher, C., Severinghaus, J., & Elkins, J. 1999 A record of atmospheric halocarbons during the twentieth century from polar firn air. *Nature* 399: 749 - 755

Butler, J. 2000 Better budgets for methyl halides? *Nature* 403: 260 - 261

Christof, O., 2002 Leichtflüchtige halogenierte Kohlenwasserstoffe - Vorkommen, Verhalten und Bedeutung in Küstengebieten (in german), PhD-thesis, University of Hamburg, Hamburg, Germany

Cox M.L., Fraser P. J., Sturrock G. A., Siems S. T. & Porter L.W. 2004 Terrestrial sources and sinks of halomethanes near Cape Grim, Tasmania. *Atmos. Environ*. 38: 3839 - 3852.

Coulter, C., Hamilton, J. & Harper, D. 1993 Evidence for the existence of independent chloromethane and S-adenosylmethionine utilizing systems for methylation in *Phanerochaete chrysosporium*. *App. and Environ. Microbiol.* 59: 1461 - 1466.

Derwent, R., 1995 Sources, distribution and fates of VOCs in the atmosphere In: Hester, R. and Harrison R. (Eds.) *Volatile organic compounds in the atmosphere*, Royal Society of Chemistry, UK

Dettmer K., Knobloch T. & Engewald W. 2000 Stability of reactive low boiling hydrocarbons on carbon based adsorbents typically used adsorptive enrichment and thermal desorption. *Fresenius J. Anal. Chem. 366: 70 - 78*

Devai, I. & DeLaune, R 1995 Formation of volatile sulfur compounds in salt marsh sediment as influenced by soil redox condition. *Org. Geochem*. 23: (4) 283 - 287

Dimmer C.H., Simmonds P.G., Nickless G. & Bassford M. R. 2001 Biogenic fluxes of halomethanes from Irish peatland ecosystems. *Atmos. Environ*. 35: 321 – 330

Dove, H. & Mayes, R. 2005 Feed quality: Natural plant markers – Alkanes In. Pond, W. & Bell, A. (Eds.) *Encyclopedia of animal science*, Marcel Dekker, New York, USA

Eglinton, G., & Hamilton, R.1967. Leaf epicuticular waxes. *Science* 156, 1322 - 1335

Fall, R., Albritton, D., Fehsenfeld, F., Kuster, W. & Goldan, P. 1988 Laboratory studies of some environmental variables controlling sulfur emissions from plants. *J. Atmos. Chem.* 6: (4) 341 - 462

Field C. B., Behrenfeld M.J., Randerson J.T. & Falkowski P.1998 Primary production of the biosphere: Integrating terrestrial and oceanic components. *Science* 281: 237 - 240

Flowers, T., Hajibagheri, M.& Clipson, N. 1986. Halophytes. *Quart. Rev. Biol*. 61: 313 – 337.

Gribble, G., 1998 Naturally occurring organohalogen compounds. *Acc. Chem. Res*. 31: (3) 141 – 152

Gribble, G., 2003 The diversity of naturally produced organohalogens. *Handbook of environmental chemistry* 3 part P 1 - 15, Springer Berlin/Heidelberg, Germany

Gribble G., 2004 Natural organohalogens: A new frontier for medicinal agents? *J. Chem. Educ.* 8:1(10) 1441

Grice, K., Lu, H., Zhou, Y., Stuart-Williams, H. & Farquhar, G. 2008 Biosynthetic and environmental effects on the stable carbon isotopic compositions of anteiso- (3-methyl) and iso- (2-methyl) alkanes in tobacco leaves. *Phytochemistry* 69: 2807 - 2814

Grossi, V. & Raphel, D. 2003 Long-chain (C_{19}-C_{29}) 1-chloro-n-alkanes in leaf waxes of the halophytes of the Chenopodiaceae. *Phytochemistry* 63: 693 - 698

Grossi, V., de Mesmay, R., Galtayries, A., Raphel, D. & Derenne, S. 2008 Artificial formation of medium and long-chain 1-haloalkanes during pyrolysis of polar geomacromolecules. *Org. Geochem*. 39: 342 - 352

Hamilton J., McRoberts W., Keppler F., Kalin R. & Harper D. 2003 Chloride methylation by plant pectin: An efficient environmentally significant process. *Science* 301: 206 - 209

Heiden A., Kobel K., Langebartels C., Schuh-Thomas G. & Wildt J. 2003 Emissions of oxygenated volatile organic compounds from plants part I: Emissions from lipoxygenase activity. *J. Atmos. Chem.* 45: 143 - 172

Heldt H.-W., 2004. *Plant Biochemistry*. Academic Press, San Diego

Hellén H., Hakola H., Pystynen K.-H., Rinne J. & Haapanala S. 2006 a C_2-C_{10} hydrocarbon emissions from a boreal wetland and forest floor. *Biogeosciences* 3: 167 - 174

Hellén H., Hakola H., Pirjola L. Laurila T. & Pystynen K.-H. 2006 b Ambient air concentrations, source profiles, and source apportionment of 71 different C_2-C_{10} volatile organic compounds in urban and residental areas of Finland. *Environ. Sci. Technol.* 40: 103 - 108

Janssen, D., Pries, F & van der Ploeg, J., 1994 Genetics and biochemistry of dehalogenating enzymes *Annu. Rev. Microbiol. 48: 163 - 191*

Jeffers M., McRoberts W. & Harper D. 1997 Identification of a phenolic 3-O-methyltransferase in the lignin-degrading fungus *Phanerochaete chrysosporium*. *Microbiology* 143: 1975 - 1981

Johnston, A., Todd, J., Sun, L., Nikolaidou-Katsaridou, M., Curson, V. & Rogers, R. 2008 Molecular diversity of bacterial production of the climate changing gas, dimethyl sulphide, a molecule that impinges on local and global symbioses. *J. Experimen. Bot*. 59: (5) 1059 - 1067

Kanda, K. & Minami, K. 1992 Measurement of dimethyl sulfide emissions from lysimeter paddy fields. *Ecol. Bull*. 42: 195 - 198

Kelly, D. & Smith, N. 1990 Organic sulphur compounds in the environment – Biochemistry, microbiology and ecological aspects. In Marshall, K. (Ed.) *Advances in microbial ecology* 11: 345-385, Plenum Press, New York, USA

Keppler F., Eiden R., Niedan V., Pracht J. & Schöler H. F. 2000 Halocarbons produced by natural oxidation processes during degradation of organic matter. *Nature* 403: 298 - 301

Keppler, F., Kalin, R., Harper, D., McRoberts, W. & Hamilton, J. 2004 Carbon isotope anomaly in the major plant C_1 pool and its global biogeochemical implications. *Biogeosciences* 1: 123 - 131

Kesselmeier J., & Staudt M. 1999 Biogenic volatile organic compounds (VOC): An overview on emission, physiology and ecology. *J. Atmos. Chem.* 33: 23 - 88

Laturnus, F., Adams, F. & Wiencke, C. 1998 Methyl halides from Anarctic macroalgae. *Geophys. Res. Lett.* 25: (6) 773 - 776

Laturnus, F., Mehrtens, G. & Grøn, C. 1995 Haloperoxidase-like activity in spruce forest soil – a source of volatile halogenated organic compounds? *Chemosphere* 31: 3709 - 3719

Laturnus F., Haselmann K. F., Borch T. & Grøn C. 2002 Terrestrial natural sources of trichloromethane (chloroform, $CHCl_3$) - An overview. *Biogeochemistry* 60: 121 - 139

Lomans, B., van der Drift, C., Pol, A. & Op den Camp, H. 2002 Microbial cycling of volatile organic sulfur compounds. *Cell. Mol. Life Sci*. 59: 575 - 588

Lovelock, J. (1975) Natural halocarbons in the air and in the sea. *Nature* 256: 193 - 194.

Manley S., Wang N., Walser M. & Cicerone R. 2007 Coastal salt marshes as global methyl halide sources from determinations of intrinsic production by marsh plants. *Global Biogeochem. Cyc.* 20: GB3015, doi: 10.1029/2005GB002578, 2006

Manley S. L. 2002 Phytogenesis of halomethanes: A product of selection or a metabolic accident ? *Biogeochemistry* 60: 163 - 180

McAnnulla, G., Woodall, C., McDonald, I., Studer, A., Vuilleumier, S., Leisinger, T., & Murrell, J. 2001 Chloromethane utilization gene cluster from *Hyphomicrobium chloromethanicum* strain CM2 and development of functional gene probes to detect halomethane-degrading bacteria. *App. Environ. Microbiol*. 67: (1) 307 - 316

McDonald I. R.,Warner K., McAnulla C., Woodall C., Oremland R. & Murrell J. 2002 A review of bacterial methyl halide degradation: biochemistry, genetics and molecular ecology. *Environ. Microbiol.*4: 193 - 203

Mead, M., Khan, A., Nickless, G., Greally, B., Tainton, D., Pitman, T. & Shallcross, D. 2008 Leaf cutter ants: a possible missing source of biogenic halocarbons. *Environ. Chem.* 5: 5 – 10

Miller, L., Kalin, R., McCauley, S., Hamilton, J., Harper, D., Millet, D., Oremland, R. & Goldstein, A. 2001 Large carbon isotope fractionation associated with oxidation of methyl halides by methylotrophic bacteria. *PNAS* 98: 5833 -5837

Moore, R., Groszko, W., & Niven, S. 1996 Ocean-atmosphere exchange of methyl chloride: Results from NW Atlantic and Pacific Ocean studies. *J. Geophys. Res.* 101: (C12) 28529 – 28538

Montreal Protocol on Substances that Deplete the Ocean Layer (1987) United Nations Environment Programme, Final Act.

Mu, H., Wesén, C., Novák, T., Sundin, P., Skramstad, J. & Göran Odham 1996 a Enrichment of chlorinated fatty acids in fish lipids prior to analysis by capillary gas chromatography with electrolytic conductivity detection and mass spectrometry. *J. Chrom. A* 731: 225 - 236

Mu H., Wesén, C., Sundin, P. & Nilsson, E. 1996 b Gas chromatographic and mass spectrometric identification of tetrachloroalkanoic anddicbloroalkenoic acids in eel lipids. *J. Mass Spec*. 31: 517 - 526

Murphy, D.1994 Biogenesis, function and biotechnology of plant storage lipids. *Prog. Lipid Res.* 33: 71 - 85

Nichols, B. 1963 Separation of the lipids of photosynthetic tissues: improvements in analysis by thin-layer chromatography. *Biochim. et Biophys. Acta* 70: 417 - 422

Niskanen R. 1989 Extractable aluminium, iron and manganese in mineral soils I. Dependence of extractability on the pH of oxalate, pyrophosphate and EDTA extractants. *J. Agr.Sci. Fin.* 61: 79 - 87

Norseth K. 1987 Climate and hydrology of norden. In: Varjo E. & Tietze W. (eds.), *Climate and hydrology of Norden,* Bornträger, Berlin pp. 120 - 128

OECD-SIDS, Unep publications 2005, SIDS initial assessment report for SIAM 15, Boston, USA

Oremland, R., Miller, L. & Strohmaier, F. 1994 Degradation of methyl bromide in anaerobic sediments. *Environ. Sci. Technol*. 28: 514 – 520

Piluk, J., Hartel, P. & Haines, B. 1998 Production of carbon disulfide (CS_2) from L-djenkolic acid in the roots of *Mimosa pudica* L. *Plant and Soil* 200: 27 - 32

Redeker K., Treseder K. & Allen M. 2004 Ectomycorrhizal fungi: A new source of atmospheric methyl halides? *Global Change Biol.*10: 1009 - 1016

Reddy, C., Eglinton, T., Palic, R., Benitez-Nelson, B., Stojanovic, G., Palic, I., Djordjevic, S. & Eglinton, G. 2000 Even carbon number predominance of plant wax n-alkanes: a correction. *Org. Geochem*. 31: 331 - 336

Rhew R., Miller B. R. & Weiss R.F. 2000 Natural methyl bromide and methyl chloride emissions from coastal salt marshes. *Nature* 403: 292 - 295

Rhew R., Miller B. R., Vollmer M. K. & Weiss R. F. 2001 Schrubland fluxes of methyl bromide and methyl chloride. *J. Geophys. Res.* 106: 20 875 - 20 882

Rhew R., Miller B. R., Bill M., Goldstein A. H. & Weiss R. F. 2002 Environmental and biological controls on methyl halide emissions from southern California coastal salt marshes. *Biogeochemistry* 60: 141 - 161

Rhew, R., Østergaard, L., Saltzman, E. & Yanofsky, M. 2003 Genetic control of methyl halide production in *Arabidopsis*. *Current Biology*, 13: 1809 – 1813,

Rhew R., Teh Y. A. & Abel T. 2007 Methyl halide and methane fluxes in the northern Alaskan coastal tundra. *J. Geophys. Res.* 112: G02009, doi:10.1029/2006JG000314,2007

Rhew R.& Abel T. 2007 Measuring simultanious production and consumption fluxes of methyl chloride and methyl bromide in annual temperate grasslands. *Environ. Sci Technol.* 41: 7837 - 7843

Riekkola & Hyötyläinen 2002 Kolonnikromatografia ja kapillaarielektromigraatiotekniikat (2. ed.) Analyyttisen kemian laboratorio, Helsingin yliopisto, Yliopistopaino, Helsinki, Finland

Rommerskirchen, F., Plader, A., Eglinton, G., Chikaraishi, Y. & Rullkötter, J. 2006 Chemotaxonomic significance of distribution and stable carbon isotopic composition of long-chain alkanes and alkan-1-ols in C_4 grass waxes. *Org. Geochem*. 37: (10) 1303 - 1332

Saito T. & Yokouchi Y. 2006 Diurnal variation in methyl halide emission rates from tropical ferns. *Atmos. Environ.* 40: 2806 - 2811

Saini, H., Attieh, M. & Hanson, A. 1995 Biosynthesis of halomethanes and methanethiol by higher plants via a novel methyltransferase reaction. *Plant, Cell and Environ.* 18: 1027 - 1033

Saxena, D., Aouad, S., Attieh, J. & Saini, H. 1998 Biochemical characterization of chloromethane emission from the wood-rotting fungus *Phellinus pomaceus*. *App. Environ. Microbiol.* 64: (8) 2831 - 2835

Scheffer and Schachtschabel 2002 Lehrbuch der Bodenkunde (15. ed.), Spektrum Akademischer Verlag Heidelberg/Berling, Germany, pp. 593

Schäfer H., Miller G. L., Oremland R. S. & Murrell J. C. 2007 Bacterial cycling of methyl halides. *Adv. Appl. Microbiol.* 61: 307 - 346

Shade G. W. & Goldstein A. H. 2006 Seasonal measurements of acetone and methanol: Abundances and implications for atmospheric budgets. *Global Biogeochem. Cyc.* 20: GB1011, doi:10.1029/2005GB002566, 2006

Sharkey T. D.& Yeh S. 2001 Isoprene emission from plants. *Annu. Rev. Plant Physiol. Plant Mol. Biol.* 52: 407 - 436

Siira J. 1984 On the vegetation and ecology of the primary saline soils of the Bothnian Bay. *Aquilo Ser. Bot.* 20: 1 - 13

Siira J. 1985 Saline soils and their vegetation on the coast of the Gulf of Bothnia, Finland. *Ann.Bot.Fenn.* 22: 63 - 90

Simmonds, P., Derwent, R., Manning, A., Fraser, P., Krummel, P., O'Doherty, S., Prinn, R., Cunnold, D., Miller, B., Wang, H., Ryall, D., Porter, L., Weiss, R. & Salameh, P. 2004 AGAGE Observations of methyl bromide and methyl chloride at Mace Head, Ireland and Cape Grim, Tasmania, 1998–2001. *J. Atmos. Chem*. 47: 243 – 269

Singh H. B., O'Hara D., Herlth D., Sachsse W., Blake D. R., Bradshaw J. D., Kanakidou M., & Crutzen P. J. 1994 Acetone in the atmosphere: Distribution, sources, and sinks. *J. Geophys. Res.*, 99:1805 - 1819

Stanley, L. & Simoneit, B. 1987 Characterization of extractable plant wax, resin, and thermally matured components in smoke particles from prescribed burns. *Environ. Sci. Technol.* 21: 163 - 169

Steinbacher, M., Bingemer, H. & Schmidt, U. 2004 Measurements of the exchange of carbonyl sulfide (OCS) and carbon disulfide (CS_2) between soil and atmosphere in a spruce forest in central Germany. *Atmos. Environ*. 38: 6043–6052

Studer A. 2001 Aerobic microbial degradation of chloromethane. Ph.D-thesis, Swiss federal institute of technology Zürich, Switzerland, pp. 170

Teh Y. A., Rhew R., Atwood A. & Abel T. 2008 Water, temperature, and vegetation regulation of methyl chloride and methyl bromide fluxes from a shortgrasss steppe ecosystem. *Global Change Biol.* 14: 77 - 91

Traunecker , J., Preuß, A. & Diekert, G. 1991 Isolation and characterization of a methyl chloride utilizing, strictly anaerobic bacterium. *Arch. Microbiol*. 156: 416 - 421

Vandenburg, L. & Wilder, E. 1970 The structural constituents of carnauba wax. *J. Am. Oil Chem. Soc*. 47: (12) 514 - 518

van Diest, H. & Kesselmeier, J. 2008 Soil atmosphere exchange of carbonyl sulfide (COS) regulated by diffusivity depending on water-filled pore space. *Biogeosciences* 5: 475 – 483

vanLoon and Duffy 2000 Enviromental chemistry. Oxford university press, Oxford, UK, pp. 492

van Pee, K-H. & Unversucht, S. 2003 Biological dehalogenation and halogenation reactions. *Chemosphere* 52: 299 - 312

Varner R., Crill P. & Talbot R. 1999 Wetlands: a potentially significant source of atmospheric methyl bromide and methyl chloride. *Geophys. Res. Lett.* 26: 2433 - 2436

Watling R. & Harper D.1998 Chloromethane production by wood-rotting fungi and an estimate of the global flux to the atmosphere. *Mycol. Res.* 102: 769 - 787

WMO 2007 Scientific assesment of ozone depletion 2006. Global ozone reseach and monitoring project report no. 50, World meteorological organization, Geneva, Switzerland

Wohlfarth, G., and Diekert, G. 1997 Anaerobic dehalogenases.
Curr. Opin. Microbiol. 8: 290 - 295.

Wuosmaa, A. & Hager, L. 1990 Methyl chloride transferase: A carbocation route for biosynthesis of halometabolites. *Science* 249: 160 – 162

Xiao, X., Prinn, R., Fraser, P., Simmounds, P., Weiss, R., O'Doherty, S., Miller, B., Salameh, P., Harth, C., Krummel, P., Porter, L., Mühle, J., Greally, B., Cunnold, D., Wang, R., Montzka, S., Elkins, J., Dutton, G., Thompson, T., Butler, J., Hall, B., Reimann, S., Vollmer, M., Stordal, F., Lunder, C., Maione, M., Arduini, J. & Yokouchi, Y. 2009 Optimal estimation of the surface fluxes of methyl chloride using 3-D global chemical transport model. *Atmos. Chem. Phys. Discuss*. 9: 27693 - 27744

Yokouchi Y., Noijiri Y., Barrie L.A, Toom-Saundry D., Machida T., Inuzuka Y., Akimoto H., Li H.-J., Fujinuma Y. & Aoki S. 2000 A strong source of methyl chloride to the atmosphere from tropical coastal land. *Nature* 403: 295 - 298

Yokouchi Y., Ikeda M., Inuzuka Y. & Yukawa T. 2002 Strong emission of methyl chloride from tropical plants. *Nature* 416: 163 - 165

Yokouchi Y., Saito T., Ishigaki C. & Aramoto M. 2007 Identification of methyl chloride-emitting plants and atmospheric measurements on a subtropical island. *Chemosphere* 69: 549 – 553

Åkesson-Nilsson, G. 2003 Isolation of chlorinated fatty acid methyl esters derived from cellculture medium and from fish lipids by using an aminopropyl solid-phase extraction column*. J. Chrom. A* 996: 173 - 18

APPENDIX

A. Calculation of the emission fluxes

The design of our closed chamber system (Fig. 2) was somewhat different from that of a traditional closed chamber. The constant sampling causes a steady flow through the chamber. Furthermore, the back flow of chloromethane-free air dilutes the concentration of the target compound inside the chamber. After the enclosure of a plant in the chamber, the time-dependent mass density of chloromethane $t \rightarrow \rho(t)$ in the chamber depends on the emission flux of chloromethane from plant Q and the air flux through chamber J. We assume instantaneous mixing, a constant source flux Q, and a constant air flux J during the measurement period. We denote the volume of the chamber by V and define $q = Q/V$ and $j = J/V$. The change in ρ is then described by an inhomogeneous first-order linear differential equation

$$\rho'(t) = q - \rho\, j \quad (A.1)$$

with the initial condition $\rho(0) = \rho_0$.

The solution of this differential equation is

$$\rho(t) = \rho_0\, e^{-jt} + q/j\,(1-e^{-jt}) \quad (A.2),$$

where q/j is the steady-state mass density of chloromethane in the chamber, which is reached after a sufficiently long waiting time.

The air at the entrance of the trap contains chloromethane with a density ρ(t) provided that the volume of air contained in the tube connection between the chamber and the trap is small compared to the volume of air sampled during the measurement. In this case, the mass of chloromethane absorbed in the trap per unit time is $m(t) = \rho(t)\, J$. The mass of chloromethane M_T collected on the absorbent during the sampling time T is then obtained by

$$M_T = \int_0^T m(t)\, dt = J \int_0^T [\rho_0 e^{-jt} + q/j\,(1-e^{-jt})]\, dt.$$

The calculation of the integral yields

$$M_T = V\,[qT + (\rho_0 - q/j)\,(1-e^{-jT})]$$

In a reference sample with q = 0, we collect the mass

$$M_T^{(q=0)} = \rho_0 V\,(1- e^{-jT}).$$

From the difference $M_T - M_T^{(q=0)}$, which is measured in the field experiment, we directly obtain the emission flux Q:

$$Q = (M_T - M_T^{(q=0)}) / [T - 1/j\,(1 - e^{-jT})] \quad (A.3).$$

B. Publication (directly connected to this work)

Article reproduced here with the permission of Boreal Environment Research.

BOREAL ENVIRONMENT RESEARCH 14: 915–931
ISSN 1239-6095 (print) ISSN 1797-2469 (online)

Helsinki 18 December 2009

Emissions of volatile halogenated compounds from a meadow in a coastal area of the Baltic Sea

Arja Valtanen[1)2)], Stephan Solloch[1)], Helinä Hartikainen[2)] and Walter Michaelis[1)]

[1)] *Institute of Biogeochemistry and Marine Chemistry, University of Hamburg, Bundesstraße 55, D-20146 Hamburg, Germany*
[2)] *Department of Applied Chemistry and Microbiology, P.O. Box 27, FI-00014 University of Helsinki, Finland*

Received 7 Oct. 2008, accepted 2 Feb. 2009 (Editor in charge of this article: Veli-Matti Kerminen)

Valtanen, A., Solloch, S., Hartikainen H. & Michaelis, W. 2009: Emissions of volatile halogenated compounds from a meadow in a coastal area of the Baltic Sea. *Boreal Env. Res.* 14: 915–931.

Chlorine radicals are well-known catalysts in the ozone depletion reactions. This study was undertaken to monitor emissions of chloromethane (CH_3Cl), an important source of chlorine to the troposphere and stratosphere, from a boreal coastal meadow on the shoreline of brackish-water sea. We sampled volatile organic compounds in the atmosphere above two halophytic vegetation types on three days in July 2007, overall 22 measurements were conducted. Two experimental sites were dominated by *Salicornia europaea* and two sites were covered by mixed vegetation. A variety of substances of anthropogenic and natural origin were identified, the biogenic organic compounds predominating. The vegetation types did not differ markedly in their CH_3Cl flux rates, the daily flux from *S. europaea* being 10.97 μg m^{-2} d^{-1} and that from the mixed vegetation 9.92 μg m^{-2} d^{-1}. The recorded fluxes agree well with those reported from other coastal ecosystems. Emissions from boreal coastal areas might therefore be a relevant CH_3Cl source on the local and global scales.

Introduction

Biogenic volatile organic compounds (BVOCs) are atmospheric trace gases released from biogenic sources (e.g. algae, bacteria and higher plants). BVOCs comprise compounds of varying chemical composition from simple saturated and unsaturated hydrocarbons to organic acids and esters. Therefore, these compounds are often divided into subgroups such as nonmethane hydrocarbons (NMHCs) and oxygenated volatile organic compounds (OVOCs) according to their chemical structure and reactivity. Isoprene and monoterpenes followed by alcohols and carbonyl-group containing compounds are the quantitatively predominant compounds or compound groups (Kesselmeier and Staudt 1999). BVOCs usually have atmospheric lifetimes of a few minutes to hours (Kesselmeier and Staudt 1999) and hence participate mainly in the tropospheric processes influencing ozone concentration and the formation of secondary particles.

Since the end of the last decade, halogenated volatile organic compounds (HVOCs) and especially halomethanes (chloro-, bromo-, and iodomethane) have gained increasing attention. In this group of BVOCs, CH_3Cl and CH_3Br have relatively long atmospheric lifetimes (1.0

and 0.7 years, respectively, WMO 2007), which enable them to be transported into the stratosphere where they and their degradation products participate significantly in ozone depletion reactions. The global budgets for these compounds were severely imbalanced, with the known sinks outweighing the known sources (WMO 2007), until the discovery of large terrestrial plant sources (Rhew *et al.* 2000, Yokouchi *et al.* 2000, 2002) brought these estimations more into balance. Today, tropical and subtropical vegetation seems to be the major source for chloromethane (Saito and Yokouchi 2006, Yokouchi *et al.* 2007) due to the large coverage of tropical rainforests and their high primary production. Next to the tropics, substantial fluxes have been recorded from coastal wetlands (Rhew *et al.* 2000, 2002, Dimmer *et al.* 2001, Cox *et al.* 2004, Manley *et al.* 2007) and various dryland ecosystems (Rhew *et al.* 2001, Rhew and Abel 2007, Teh *et al.* 2008). According to these studies the extent of the net flux depends strongly on the plant species, the ambient temperature and the amount of photosynthetically active radiation.

Soils are one of the largest known sinks for halomethanes (WMO 2007) and soil reactions have an influence on the net emission flux of HVOCs. On the other hand, the soil and its inhabitants may function as a source for halomethanes. Keppler *et al.* (2000) suggested the abiotic halomethane formation in soils to be a potential source, and the degradation of dead plant material has been shown to produce large amounts of halomethanes under laboratory conditions (Hamilton *et al.* 2003). Moreover, microorganisms living in soils participate in halomethane cycling. Some fungi produce halomethanes (Watling and Harper 1998, Redeker *et al.* 2004) and many bacteria are known to degrade them (McDonald *et al.* 2002, Schäfer *et al.* 2007). The current information indicates that the terrestrial halomethane budget is extremely complex, with multiple formation and degradation processes going on simultaneously in soil.

Being a net result of opposing formation and degradation reactions, the picture of halomethane emissions from terrestrial ecosystems is complex. Therefore, more experimental and monitoring data from different kinds of soil ecosystems are needed. The estimates being extrapolated to global scale so far are based on measurements representing relatively narrow geographical areas and ecosystem types (Table 1). The variables controlling the emissions from land sources still need to be clarified, as they vary considerably between different locations. In this study, we provide information on chloromethane emissions from a boreal ecosystem on the shoreline of the brackish Baltic Sea. Our main objective was to estimate the chloromethane flux from this ecosystem. The characteristics of the soil samples collected under two vegetation types were determined to obtain information on the abiotic and edaphic parameters most probably affecting hydromorphological features and chloromethane production in boreal coastal areas.

Material and methods

Location

Samples were collected from a coastal meadow located on the island Jungfruskär (60°08´23.94´´N, 21°04´39.80´´E) in the Finnish archipelago national park in the Baltic Sea (salinity in this part of the Baltic Sea 6‰–7.5‰) (Fig. 1). The islands in the archipelago are rocky and the covering soil layer is mostly less than 1-meter thick. These characteristics are a result of the retreating ice mass that peeled off the loose soil material and exposed the bedrock at the end of the last ice age (10 000 B.P.). The sampling location is biogeographically situated in the northernmost part of the temperate to boreal transition zone, also called the hemiboreal zone (Ahti *et al.* 1968). In this region, the duration of the growing season is approximately 180 days per year (Nordseth 1987).

The meadow is located on the eastern side of the island and it surrounds a lagoon-like small bay, and has an area of approximately 1 ha. For our investigations, we chose four sampling sites representing two different kinds of vegetation. In type 1 vegetation, *Salicornia europaea* was almost the only higher plant species present. Type 2 vegetation was a mixture of different plant species and consisted mostly of *Glaux maritima*, *Juncus gerardii*, *Agrostis stolonifera* and *Carex nigra*. Type 2 vegetation covered

Table 1. Reported terrestrial net CH_3Cl emission rates. Fluxes were calculated per hour by dividing the data from the original source given as daily or yearly average fluxes by 24 or 24 × 365 if they were not already given in the units used. The fluxes given in molar units were also transformed into mass unit fluxes.

CH_3Cl flux area ($ng^{-1}\ m^{-2}\ h^{-1}$)	CH_3Cl flux dry biomass ($ng\ g^{-1}\ h^{-1}$)	Location	Predominant vegetation	Reference
924 ± 122	0.74 ± 0.05	NE Colorado U.S. 40°N, 104°W, short grass steppe	*Atriplex canescens*	Teh *et al.* (2008)
72–88 × 10^3	1367–1494	California U.S 38°N, 121°W,	*Frankenia salina, Cressa truxillensis*	Rhew and Abel (2007)
5 × 10^3	23	grassland	*Lepidium latifolium*	
24 × 10^3	140	Iriomote Island, Japan 24°N, 123°E, subtropical forest	33 different subtropical and tropical species	Yokouchi *et al.* (2007)[a]
1370	7.99	California U.S. 33°N, 117°W,	*Spartina foliosa*	Manley *et al.* (2007)[a]
1370	1.83	coastal salt marsh	*Salicornia virginica*	
297 × 10^3	582		*Frankenia grandifolia*	
160 × 10^3	297		*Batis maritima*	
–	2400 ± 600	Glasshouse	*Cyatheaceae podophylla*	Saito and Yokouchi (2006)[a]
–	490 ± 170		*Cyatheaceae lepifera*	
300	–	Tasmania 41°S, 145°E, coastal wetland	*Pachycornia arbuscula*	Cox *et al.* (2004)
380	–	Ireland 53°N, 9°W coastal marsh	*Ranunculus flammula, Apium inundatum*	Dimmer *et al.* (2001)
3850	–	conifer forest floor (median)	*Pinus sylve, Picea sitchensis, Abies alba*	
605	–	peatland (median)	grasses, mosses	
2314	–	California U.S. 32–33°N, 116-117°W,	*Brassica juncea*	Rhew *et al.* (2001)[b]
1178		three shrubland biomes	*Carbobrotus edulis*	
3702	–		*Artemisia californica*	
168	–		*Larrea tridentata*	
158 × 10^3	–	California U.S. 32°N, 117°W,	*Batis maritima/ Salicornia bigelovii*	Rhew *et al.* (2000)
274 × 10^3	–	coastal salt marsh	*Salicornia bigelovii*	
1010 × 10^3	–		*Batis maritima*	
1103	–	New Hampshire U.S 43°N, 71°W,	*Sphagnum* spp., *Carex* spp., shrubs (poor fen)	Varner *et al.* (1999)
386	–	wetland	*Sphagnum* spp. (rich fen)	

[a] emissions only from vegetation, soil emissions deducted.
[b] daily maximum values.

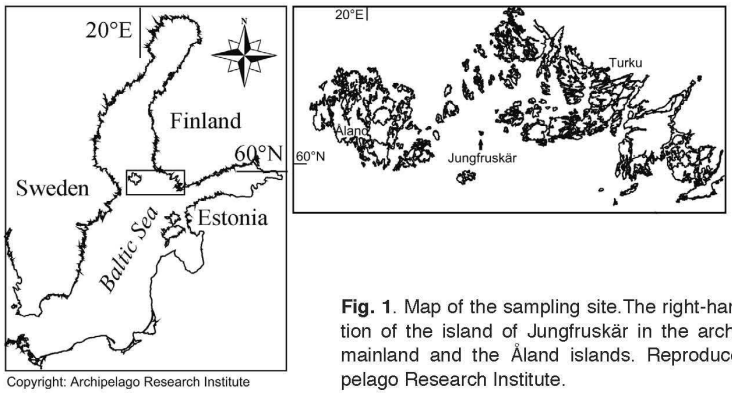

Fig. 1. Map of the sampling site.The right-hand-side panel shows the location of the island of Jungfruskär in the archipelago between the Finnish mainland and the Åland islands. Reproduced with permission of Archipelago Research Institute.

about 70%–80% of the meadow area, while *S. europaea* grew mostly in a few smaller patches where the vegetation was burned off or in areas that were totally or partly flooded by brackish sea water. Below, sampling sites are denoted as *S. europaea* 1 and 2 (vegetation type 1), and mixed vegetation 1 and 2 (vegetation type 2). Other species growing in the meadow were: *Phragmites australis*, *Eleocharis palustris*, *Odontites littoralis* and *Carex panicea*. During the sampling campaign, 10–12 July 2007, the sea water level was unusually high and parts of the meadow vegetation were flooded.

Gas collection

Gas fluxes were recorded using a dynamic closed chamber method. Our chambers consisted of a transparent acryl glass cylinder (diameter 14.4 cm, wall thickness 0.3 cm, height 20 or 30 cm) with a lid of the same material mounted on an aluminium-plastic base. The base was constructed from an aluminium tube (diameter 11.0 cm) which was surrounded by a plastic ring. The junction was made gastight with silicon gum. The plastic ring had a 2–3-cm-wide channel in which the acryl glass cylinder was placed. When the cylinder was in place, the channel was filled with saturated sodium chloride solution to assure a gas-tight seal. Acryl glass was chosen for the chamber material as it has almost the same inertness and density as mineral glass but is lighter and less fragile. It also shows smaller absorbance of sunlight by letting through UV wavelengths which do not penetrate mineral glass. Hence the light conditions during the enclosure were kept as natural as possible. Emission cycles (24-hour) were measured for the two vegetation types. The emissions were recorded at five and six different timepoints for *S. europaea* sites and mixed sites, respectively, and on five occasions during the day for control (no vegetation) enclosures. We tried to perform the vegetation and control incubations as evenly spaced as possible throughout days and nights. In every sampling timepoint parallel samples were taken i.e. two plots of the same vegetation type were sampled simultaneously.

The aluminium base was inserted into the soil to a depth of 2–5 cm, and the cylinder was placed on the base channel and sealed as described above. The emission samples were collected on a mixed adsorbent bed (*see* below) by pumping the air from the chamber through the adsorbent tube continuously for two hours. The pump was turned on immediately after the placement of the chamber on its base. The sampling flow was kept at 50–60 ml min^{-1} during the pumping. When the collection time was completed, the adsorbent tube was closed with 1/4´´ Swagelok® fittings with Teflon® ferrules and stored in a cool box until analysis in the laboratory. After the completion of the sampling time the chamber was removed from the base allowing the air surrounding the plant to mix with the ambient air. After the sampling period was completed for a given site, the plant material inside the enclosure was harvested for the determination of the biomass.

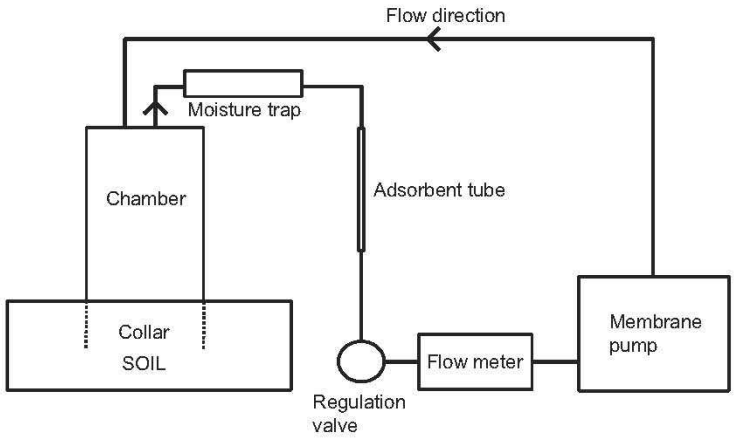

Fig. 2. A schematic presentation of the used closed chamber system

Five to six samples in 24 hours resulting in total of 22 samples might seem a small dataset, but it must be kept in mind that VOC analysis has several aspects, which set limitations for the amount of the samples. First of all, the measurement of one sample is very time consuming. In our system described later, one analysis took more than an hour and next to collected samples also standards and samples needed for the quality assurance must be measured, which further increases the sample load and the time needed for measuring the field samples. The second restriction is the stability of the target compounds in the sample matrix. This can be tested before sampling, but the results of stability tests should be interpreted with precaution. The simulation of the precise sample matrix — in laboratory conditions for example — is very difficult, if not impossible. In the best case, an assumption might be made of the stability of the target compounds during a defined storage time. Therefore, for gaining the qualitatively best result, the samples should be analysed as soon as possible after the sampling, which again limits the total amount of samples. Considering the total sample load of this three-day sampling campaign, including the emission samples, control samples and the samples needed for quality assurance, the maximum sample amount was reached, which still was considered to be analysed in acceptable timeframe after the sample collection. The maximum storage time for chloromethane samples was three weeks, which was the time the compound stayed stable on the adsorbent material in the storage experiment.

Sampling system

The sampling system (Fig. 2) consisted of a moisture trap: a plastic tube (229 mm × 38 mm) with aluminium ends filled with $Mg(ClO_4)_2$ granules, a stainless steel adsorbent tube (178 mm, OD 1/4´´, Gerstel), a regulation valve (Swagelok®), a thermal flow meter with totalisator (Profimess GmbH, Bremerhaven, Germany) and a membrane pump (KNF Neuberger GmbH, Freiburg, Germany). Different parts of the system were connected with Silcosteel® coated stainless steel tubing (1/8´´) and gas-tight Swagelok®-fittings or Tygon®-tubing in places where more flexibility was needed. The tightness of the fittings was tested in the laboratory before sampling. The adsorbent bed was made of a combination of three adsorbents: Tenax TA and two types of Carboxen (all from Supelco, Bellefonte, PA, USA).

Analytical methods

The samples were analysed using thermal desorption-gas chromatography-mass spectrometry (TD-GC-MS). Our analytical setup consisted of a thermal desorption system 1 (TDS 3) and a cold injection system (CIS) (both Ger-

stel GmbH & Co. KG, Müllheim an der Ruhr, Germany) combined with a GC (Agilent series 6890N) and a mass selective detector (Agilent series 5975B). The GC was equipped with a GasPro PLOT column (30 m × 0.32 mm, J&W Scientific) and programmed with the following temperature programme: 40 °C held 5 min, heated to 220 °C (rate 6 °C min^{-1}) held 10 min, and finally heated to 240 °C (rate: 25 °C min^{-1}) and held 10 min. The GC was operated in the constant flow mode with a carrier gas flow of 2.7 ml min^{-1}. The compounds were identified according to their retention times and mass spectra. For quantification of the halomethanes, one-point calibration with single compound calibration standards (CH_3Cl, CH_3Br or CH_3I, Linde Gas, Germany) was used. The calibration standards were measured daily at least 3 times, and the measurements showed a relative standard deviation of less than 5%.

Calculation of chloromethane fluxes

The fluxes were calculated with the following equation:

$$\text{Flux} = \left[\frac{M_T - M_T^0}{VT\left(1 - e^{-JT/V}\right)V^2/J} V/A \right] 60\,\text{min},$$

where M_T (ng) is the mass of chloromethane collected from the plant enclosure in the sampling time T (min), M_T^0 (ng) is the mass of chloromethane collected from the enclosure without vegetation in the sampling time T, V (dm^3) is the volume of the chamber, J (dm^3 min^{-1}) is the sampling flow and A is the area of the chamber base.

When the emissions were normalised to biomass, the term V/A was replaced with V/m, where m represents the dry biomass harvested from the enclosure.

This equation is valid if the following circumstances should apply inside the chamber:

1. chloromethane flux stays constant during the enclosure time,
2. emitted chloromethane is immediately distributed equally into the whole chamber volume after its liberation,
3. there is a constant laminar air flow sweeping through the chamber.

The enclosures without vegetation were located in the area without vegetation nearest to the corresponding vegetated enclosure site. In all cases, the distance between these enclosures was less than three meters. A total of five incubations without vegetation at different times of day were conducted in the course of the threes days. For calculation of the fluxes we used the average of these five values. The used equation and its induction is presented in detail in the Appendix.

Soil analyses

Two soil samples (0–20 cm) were collected under each vegetation type and soil properties were determined to obtain information on abiotic parameters most likely to affect the chloromethane production in and hydromorphological features of the soil. For the collection a steel corer was used (length: 50 cm, diameter: 8 cm). All the analyses except for TOC were conducted on the fresh surface layers of the soils, which we considered to be the most relevant horizon with regard to possible chloromethane production. Total organic carbon was analyzed from air dried surface layers. The visual characteristics of the soil cores (laminas and their colour) were recorded. The determination of soil texture was based on sensory analysis in the field, no textural analysis was conducted in the laboratory. For the laboratory analyses, the organic soil horizon was separated from the mineral soil and plant roots and small stones were removed from it. The organic soil material was then homogenized. The soil under vegetation type 1 (*S. europaea*) is here to fore referred to as soil 1 and soil under vegetation type 2 (mixed hay and grass species) as soil 2.

For pH measurements, 1 g of fresh soil was suspended in 2.5 ml of 0.01 M $CaCl_2$, shaken by hand for several minutes and allowed to stabilize for approximately 15 min before dipping the glass electrode into the solution. For electrical conductivity (EC), a soil suspension of 1:5 (w/v) (fresh soil) in milliQ-purified water was shaken by hand and allowed to stabilize for 15 minutes prior to the measurement with a conductivity meter (CDM210, MeterLab Radiometer, Copenhagen). Both pH and electrical conductivity were analysed in triplicates.

The chloride concentration in the suspension used for the EC measurement was measured by pipetting 0.5 ml of the suspension into the analyser vial, and the analysis was conducted with an MK II Chloride Analyzer 926 (Sherwood). Manganese and iron were extracted according to Niskanen (1989). Soil samples of 2.5 g were shaken in 50 ml of ammonium oxalate (0.029 M $(NH_4)_2C_2O_4$ + 0.021M $H_2C_2O_4$, pH 3.3) for two hours (150 rpm) in a vertical table shaker, centrifuged, and the supernatants were filtered through filter paper (S & S, Blauband) prior to analysis. Iron and manganese concentrations in the extracts were measured with an ICP-MS (Perkin-Elmer, Elan 6000). Total organic carbon (TOC) in the air-dried sample was determined with an automatic TOC-analyzer (Shimadzu TOC-Vcph + TNM-1). For total organic carbon, iron, manganese and chloride analyses, five parallel determinations were conducted.

Results

Soil samples

Soil 1 (*S. europaea*) had an approximately 3.5-cm-thick surface layer with the uppermost 1 cm enriched with organic material (OM) as compared with lower parts of the layer, where the amount of sand started to increase. The layer was dark grey. The layer (3.5–7 cm) beneath the surface layer was pale yellow-brown and quite coarse in texture, and included several small stones. Right below the sandy layer, a grey clay layer began. Only the surface soil to about 20 cm depth was sampled and, therefore, the thickness of the clay layer could not be determined as it went deeper than the sampling depth. In the organic layer, the plant root growth was mostly shallow and near the soil surface. There were very few roots in the sandy horizon and no visible roots in the clay layer.

Soil 2 (mixed vegetation) had a thicker surface layer (about 7.5 cm) rich in OM. It contained plenty of roots. The second visually distinct layer was a pale grey mixed sand/clay layer that also contained roots and appeared to have a higher water content and lower density than the clay layer in soil 1. This layer also extended beyond our sampling depth of 20 cm. The organic layer in soil 1 was thinner than in soil 2 because the recent burning of the surface vegetation had destroyed most of the decomposed organic material.

Both soils had near-neutral pH (Table 2) and can be classified as neutral chloride soils according to Siira (1984, 1985). The largest difference between the soil samples was in TOC, it being three times higher in soil 2 than in soil 1. Furthermore, in soil 2 the concentrations of chloride and iron, as well as the value of EC, were also somewhat higher than in soil 1, whereas pH was lower.

Identified VOCs

The mean temperature within the chambers on the sampling days (10–12 July 2007) was 20.6 °C and mean relative humidity was 72%. No temperature rise or humidity accumulation was observed in the majority of the incubations. The major components in the emission samples were acetone and hexanal, followed by methyl acetate, pentanal, ethyl acetate, benzene and toluene (Fig. 3). These compounds were identified by comparing their recorded mass spectra with those in the spectral library (NIST). The most abundant VOCs in our samples were isobutane, 2-methyl-propene, butene and pentane (Fig. 4). Isobutane, butane, and butene and its structural

Table 2. Soil parameters from the soil surface layers under the two vegetation types.

	pH	$EC_{1:5}$ (mS cm^{-1})	TOC (%)	Mn/Fe ($\mu g\ g^{-1}$)	Cl^{-1} (mg g^{-1})
Soil 1 (*S. europaea*)	6.7	1.9	3.2	1.2/11.4	2.4
Soil 2 (mixed vegetation)	5.9	3.1	11.0	0.9/16.6	3.4

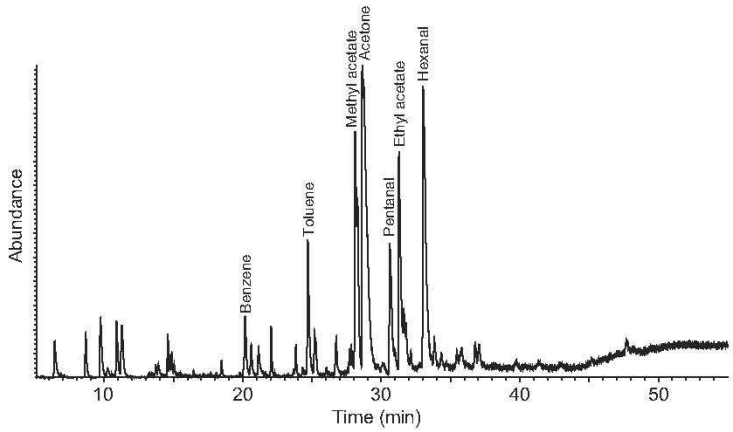

Fig. 3. Typical chromatogram of a plant (*S. europaea*) emission sample (5–55 min). Abundance (*y*-axis) is a relative variable, therefore, no unit is given.

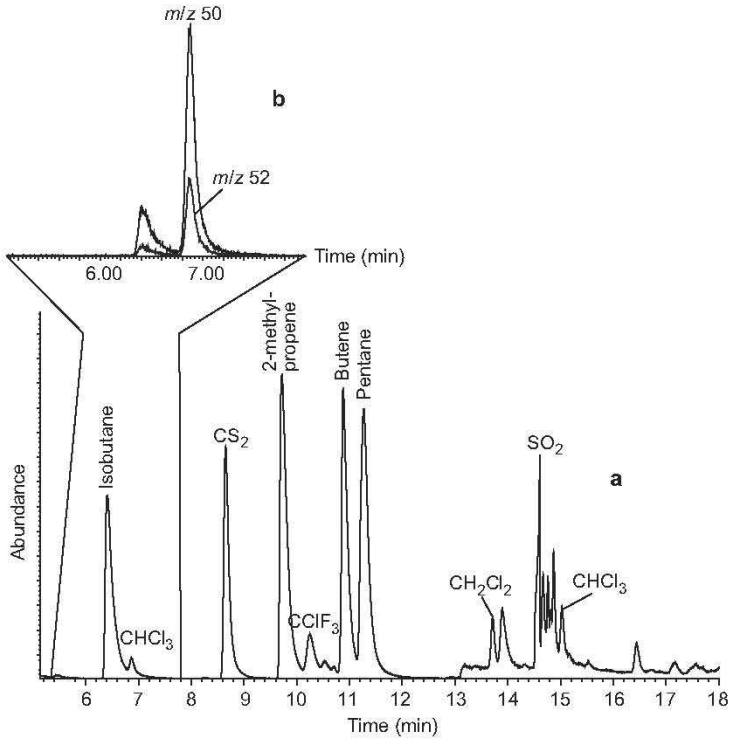

Fig. 4. (**a**) Magnification of the retention times from 5 to 18 min (same chromatogram as in Fig. 3), (**b**) extracted ion chromatogram displaying the main ion fragments (*m/z* 50 and 52) of chloromethane. Abundance (*y*-axis) is a relative variable, therefore, no unit is given.

isomer 2-methyl-propene (isobutene) were identified by comparing their retention times with the retention times of the gas standards containing butane, butene and their iso-forms (C_1–C_4 alkane and C_2–C_4 alkene minican standards, Linde Gas, Germany). Isobutane normally eluted right before chloromethane. However, in a few samples where isobutane was present in a high concentration relative to chloromethane, partial co-elution was observed (Fig. 4a). On such occasions, quantitation was conducted with the help of the extracted ion chromatograms (Fig. 4b). We also observed some sulphur-containing compounds in the emission samples. Carbon disulphide (CS_2) and sulphur dioxide (SO_2) were present large amounts, but dimethyl sulphide and

methanethiol were also often detected. SO_2 is an artefact generated by the adsorbent materials during the desorption step. It was also detected in the blank runs, where only the conditioned adsorbent tubes were analyzed. Several halogenated C_1 and C_2 compounds could be detected in the collected gas samples, $CHCl_3$, CH_2Cl_2, CCl_3F (CFC-11) and CH_3Cl being the most abundant.

Chloromethane emission

The flux measurements had a relatively large gap in the *S. europaea* sites between 08:00 and 14:00 local time (Table 3). The highest flux value for *S. europaea*, 841 ng CH_3Cl m^{-2} h^{-1} was observed between 14:00 and 16:00. From the mixed vegetation the highest flux value, 562 ng CH_3Cl m^{-2} h^{-1}, was recorded in late afternoon between 16:00 and 18:00. The lowest chloromethane fluxes occurred between evening and early morning and followed a similar trend in both vegetation types (Table 3 and Fig. 5).

The net fluxes showed relatively large differences in magnitude and diurnal distribution between the different sites of the same vegetation type (Table 3 and Fig. 5a–b). In *S. europaea* site 1, the net emission fluxes varied from 63 to 865 ng CH_3Cl m^{-2} h^{-1} and in *S. europaea* site 2 from 480 to 817 ng CH_3Cl m^{-2} h^{-1}. In the mixed vegetation site, the net emissions were between 0–365 and 292–759 ng CH_3Cl m^{-2} h^{-1} for sites 1 and 2, respectively. These discrepancies between the sites became smaller when fluxes were normalized to dry biomass for *S. europaea* (Fig. 5a), but remained relatively wide for the mixed vegetation type (Fig. 5b).

Salicornia europaea had a higher tissue water content (Table 4) than the mixed vegetation species, which diminished the emission values when the fluxes were related to the fresh biomass. On the other hand, *S. europaea* sites possessed a higher above-ground biomass (Table 4), which explains why they had higher area-normalised fluxes than the mixed vegetation sites. The mean flux values normalised to dry biomass showed almost no differences between the two vegetation types (Fig. 5c). Our mean flux values were based on the averages taken from the two different sites of each vegetation type. The number of observations is too small to give statistically valid results, which is a common problem in chamber-based emission measurements.

As there was no apparent difference between the two vegetation types concerning their emission rates, the both types were taken as a one group (all species) in calculating the daily flux from the study area. All observation (n = 21) were divided into two groups: (1) background emission fluxes recorded 00:00–04:00 and 18:00–24:00 (n = 17) local time and (2) maximum emission fluxes recorded 14:00–18:00

Table 3. Net chloromethane fluxes (ng m^{-2} h^{-1}) from plant incubations.

Date	Time	*S. europaea* 1	*S. europaea* 2	*S. europaea* average
11 July	03:00–05:00	337	502	419
11 July	07:00–09:00	63	596	329
10 July	14:00–16:00	865	817	841
10 July	18:00–20:00	138	644	391
10 July	22:00–24:00	117	480	299
		Mixed 1	Mixed 2	Mixed average
12 July	00:00–02:00		593	
12 July	04:00–06:00	0*	292	144
12 July	08:00–10:00	220	606	413
11 July	12:00–14:00	252	705	478
11 July	16:00–18:00	365	759	562
11 July	20:00–22:00	166	718	442

* Calculated flux was slighly negative. As only positive fluxes were considered possible (no mechanism is known for degradation of chloromethane in plants), the positive flux is given as 0 for this measurement.

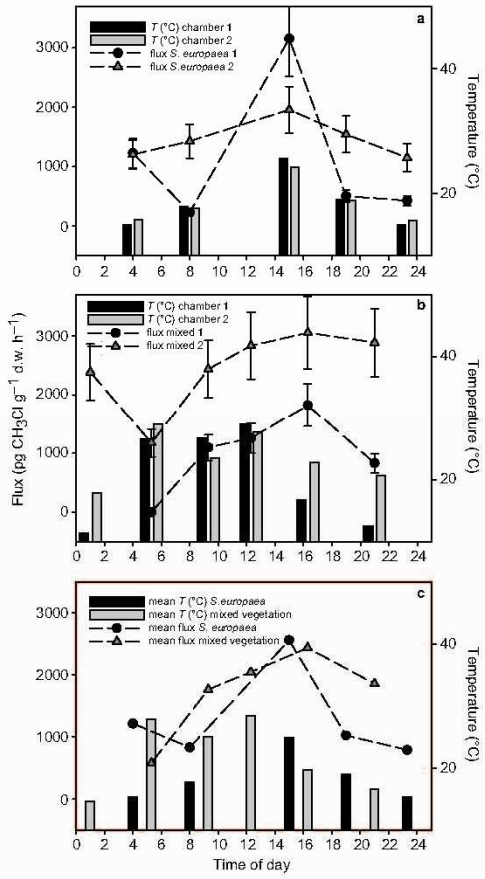

Fig. 5. Dry biomass-normalised chloromethane fluxes and corresponding average temperatures in the chambers during the incubations. (**a**) *S. europaea* sites, (**b**) mixed vegetation sites, (**c**) mean emission from each vegetation type. In plots a and b the error bars represent the analytical uncertainty of ±20% of the GC-MS-system used for analysing the samples. Note the different scales.

(n = 4). The mean fluxes (± standard deviation) were 378 (± 241) ng m^{-2} h^{-1}, 1330 (± 863) pg g^{-1} (d.w.) h^{-1} and 701 (± 228) ng m^{-2} h^{-1}, 2496 (± 704) pg g^{-1} (d.w.) h^{-1} background and maximum group, respectively. It was assumed that the background mean flux represented the mean flux in 20 hours of the day and maximum fluxes the mean flux in four hours of a day. The daily flux was calculated as a sum of the background flux and the maximum flux times their appearance time in hours, by dividing this with 24 hours we gained the weighted means. The weighted means (± standard errors) for all species were 432 (± 25) ng m^{-2} h^{-1} and 1524 (± 105) pg g^{-1} (d.w.) h^{-1}, resulting in the daily fluxes of 10.36 (± 0.60) μg m^{-2} d^{-1} and 36.58 (± 2.54) ng g^{-1} (d.w.) d^{-1}.

Discussion

Soil

In the soil samples the clay layer starting at a depth of 7–8 cm had a uniform pale grey colour and showed no visual signs of oxic conditions, e.g. any red-brown colour from oxidised iron. It is therefore probable that the subsoils stay anoxic because of the high water level due to the nearness of the shoreline and poor penetration of oxygen-containing water through the compact clay layer.

According to Keppler *et al.* (2000), the main properties of soils influencing abiotic chloromethane production are (i) soil chloride concentration, (ii) organic carbon content, and (iii) reducible iron (Fe III) concentration. Also, the

Table 4. Biomass water content and mean above-ground biomass.

	Fresh biomass (g)	Dry biomass (g)	Water content (%)	Mean biomass (above ground) (kg m^{-2})	
				Fresh weight	Dry weight
S. europaea 1	27.2	2.6	90.4		
S. europaea 2	40.4	4.0	90.2		
Mean	33.8	3.3	90.3	3.6	0.4
Mixed 1	5.8	1.9	67.0		
Mixed 2	10.0	2.4	76.7		
Mean	7.9	2.1	72.8	0.8	0.2

ambient environmental conditions like temperature, soil moisture and pH, and the chemical composition of the soil OM play major roles. In the present study, the soils differed to some extent in pH, EC and Cl concentration. pH was lower in soil 2 owing to its high content of OM known to contain humic and fulvic acids. It is likely that the higher EC in soil 2 was attributable primarily to the higher Cl^- concentration caused by flooding of brackish water, although the dissolved organic acids may also have had some effect. In the absence of particle size data (bulk density) it is difficult to estimate which one of the soils was actually more saline.

In our opinion, the major factor determining the vegetation type in the experimental location was burning that cleared the patches (soil 1) of other vegetation and gave an advantage to the pioneer species *S. europaea*, rather than any chemical or physical differences between the soils. Soils possess a variety of biological components that either produce or degrade chloromethane. Chloromethane production has been reported for ectomycorrhizal fungi (Redeker *et al.* 2004) and wood-rotting fungi (Watling and Harper 1998). On the other hand, several bacterial strains have been found to be capable of using chloromethane as a sole carbon source (reviewed in McDonald *et al.* 2002 and Schäfer *et al.* 2007). Thus, soil can function as a sink or a source for chloromethane and hence forms a highly complex biological system, which renders it challenging to assess the possible abiotic generation of volatile compounds. However, soil biological processes were beyond the scope of this study.

In the light of the measured soil parameters, abiotic halomethane formation would be more likely in soil 2, because of the higher content of OM, chloride and redox-sensitive elements (iron). Abiotic chloromethane production might therefore be a factor affecting the flux data for mixed vegetation sites, especially as all the soil controls were measured on soil 1, because no unvegetated patch were available at the sampling site 2. Thus, the chloromethane fluxes for the mixed vegetation sites might be overestimated due to underestimation of the contribution from soil.

Volatile non-halogenated organic compounds

The mixed adsorbent bed used was designed to trap a wide range of VOCs (C_1–C_4), but our special interest was focused on halogenated organic species. Four different halogenated methanes were detected. Dichloromethane and chloroform are both widely-used solvents, but have also natural sources (Laturnus *et al.* 2002, Cox *et al.* 2004). Chloroform emission is often recorded from areas where chloromethane is also emitted (Dimmer *et al.* 2001, Cox *et al.* 2004), but it shows a different kind of emission pattern. Hellén *et al.* (2006a) found boreal forest floor to emit chloroform at a rate of 100–800 ng m^{-2} h^{-1}, but they did not detect any chloromethane formation. These observations suggest that chloroform is derived from different processes than chloromethane.

In our samples, acetone and hexanal were the predominant VOCs. Acetone is one of the most abundant non-methane hydrocarbons found in the atmosphere in remote areas and has multiple natural and anthropogenic sources (Singh *et al.* 1994). Shade and Goldstein (2006) detected a seasonal variation in acetone concentrations in Californian rural air, indicating that this substance is mostly of biogenic origin. Hexanal is derived from decay of fatty acids from biological material. For example, Heiden *et al.* (2003) found C_6-products, including hexanal, to be the main oxygenated volatile organic compounds from a variety of plant species. They suggest the oxidation of linoleic (18:2) and linolenic (18:3) acids by lipoxygenase to be the probable source for these compounds.

Isoprene (2-methyl-1,3-butadiene) and monoterpenes are the most common biogenic VOCs emitted by vegetation, especially trees. We could not detect isoprene in our samples. This is probably due to the unsuitability of our adsorbent system. Isoprene has been observed to break down rapidly after sampling in Carboxen-type adsorbents (Dettmer *et al.* 2000). It is also possible that the meadow vegetation does not emit isoprene, because not all plant species have the gene encoding isoprene synthesis (Sharkey and Yeh 2001).

Chloromethane fluxes

Plant material

In our study, relatively large discrepancies remained between the chloromethane emission levels among the different sites of the mixed species after normalising to dry biomass. For *S. europaea*, the differences between the two sites became clearly smaller when normalised to biomass. The differences in the fluxes from the mixed vegetation sites are partly due to variation in the relative coverage of different plant species between the two sites. Halomethane flux rates have been found to strongly depend on the species (Manley *et al.* 2007, Yokouchi *et al.* 2007). There might also be true differences between the emissions rates from plant individuals of the same species. In fact, high intra-species variations have been detected in tropical plants (Yokouchi *et al.* 2007) and salt marsh vegetation (Rhew *et al.* 2002). The amount of biomass of a given species is therefore not solely responsible for variations in the extent of the emissions, but the developmental stage and overall health of the individual plant might also contribute to differences in emissions. The correlation between the flowering of plants and halomethane (not necessarily chloromethane) emissions found by Manley *et al.* (2007) suggests that the plant age and developmental status are key factors in regulation of the amount of liberated gas.

In our study, the *S. europaea* sites showed slightly higher rates than the mixed sites when the CH_3Cl fluxes were based on the area, but slightly lower rates when based on biomass. Overall, the differences in CH_3Cl emission rates between the two vegetation types were not substantial, in comparison with over 100-fold differences between Californian saltmarsh species (Table 1) found by Manley *et al.* (2007). The mean area-based net flux (= daily mean divided by 24) recorded in our study was 432 ng m^{-2} h^{-1}. It is in the same range as the fluxes obtained by Cox *et al.* (2004) and Dimmer *et al.* (2001) and those reported by Rhew *et al.* (2001) for a *Larrea tridentata*-dominated site and by Varner *et al.* (1999) for a rich fen. The fluxes reported for *Atriplex canescens* (Teh *et al.* 2008), *Spartina* and *Salicornia* (Manley *et al.* 2007) as well as for a poor fen (Varner *et al.* 1999) were approximately two times higher than our daily maximum value. The daily average values obtained by Manley *et al.* (2007) were all recorded between 09:00 and 14:00, which partly overlaps the window of time wherein we found the maximum emissions. Hence, the comparison of the maximum values appears to be appropriate.

Only three studies listed in Table 1 report emission values from which the influence of soil emissions is deducted, all other studies give total emission values that include soil emission. Moreover, only a few studies (Dimmer *et al.* 2001, Rhew *et al.* 2001, 2000) took daily variations into account. These facts complicate comparisons between the emission values of different studies.

The subtropical biomass-based emissions rates (Table 1) are three orders of magnitude larger than our mean biomass-normalized rate of 1.52 ± 0.11 ng g^{-1} (d.w.) h^{-1} for all species. This discrepancy derives from the differences in the vegetation composition and environmental parameters e.g. temperature, salinity and insolation. Chloromethane formation is a characteristic feature probably regulated at the genus level in plants (Yokouchi *et al* 2007). Perhaps the magnitude of emission is also controlled at the genus level. The two *Salicornia* (*europaea* and *virginica*) species have emission rates of the same magnitude, despite the differences in their geographic settings. There is a 3-fold difference in the dry biomass-normalised fluxes of *Salicornia* between our study and that of Manley *et al.* (2007). Also, different *Frankenia* species have shown about 2-fold differences in their dry biomass-normalised emission rates (*F. salina*: 1367–1494 ng g^{-1} h^{-1} (Rhew and Abel 2007) and *F. grandifolia*: 582 ng g^{-1} h^{-1} (Manley *et al.* 2007). This might be caused partly by methodological differences in the calculation of the daily mean fluxes and partly by differences between the sites. As already mentioned, it is difficult to compare the emission rates of *S. bigelovii* (Rhew *et al.* 2000) with other data, because the study neither differentiated between soil- and vegetation-derived emissions nor presented biomass-normalized rates. Compared with our data, the most similar biomass-normalised emis-

sion rates have been reported for the short grass steppe species *A. canescens* (Teh *et al.* 2008) and coastal salt marsh species *S. virginica* (Manley *et al.* 2007).

Environmental parameters

Halomethane production by plants has been shown to be an enzymatic process (Wuosmaa & Hager 1990, Manley 2002). However, in addition to plant species and physiological characteristics, environmental factors also regulate emission rates. Halomethane emissions have been found to correlate with air temperature and the amount of photosynthetically active radiation (Dimmer *et al.* 2001, Rhew *et al.* 2002, Saito and Yokouchi 2007). Manley *et al.* (2007) point out the difficulty in field studies in differentiating between effects caused by changes in the light intensity and those caused by temperature, as these two factors normally correlate strongly. During the sample and control incubations, we monitored temperature and the relative humidity in the chambers, because they are the major factors affecting enzyme activity in plant cells (Heldt 2004). In most cases, temperature in the chamber correlated quite well with the amount chloromethane emitted [linear regression: r^2 = 0.63–0.98 (n = 5 or 6)]; only the mixed vegetation site 2 had a poor correlation (r^2 = 0.45, n = 6) between these two parameters.

Salinity has been thought to be an important factor in halomethane production (WMO 2007), but it seems not to directly correlate with emission rates (Yokouchi *et al.* 2002, Manley *et al.* 2007). Still, soil salinity is an important environmental parameter as it has a strong influence on the type of vegetation that grows in a given ecosystem. Investigations made in different kinds of shrubland (Rhew *et al.* 2001) and grassland (Rhew and Abel 2007, Teh *et al.* 2008) ecosystems reveal a close relationship between the net chloromethane production and the halophytic plant species present. The highest chloromethane net emission rates measured from dry grassland have been obtained from a hypersaline site (Rhew and Abel 2007).

Interestingly, in dryland ecosystems the water content in the soil seems to be an important factor controlling the chloromethane net emission and uptake. In the studies of Rhew *et al.* (2001), Rhew and Abel (2007) and Teh *et al.* (2008), chloromethane net emissions occurred only during dry seasons (soil water content ≤ 10%). Water content is of crucial importance in controlling the biological activity in the soil. Soil bacteria can degrade chloromethane either under oxic or anoxic conditions, but in general aerobic degradation processes are considered to be more efficient and faster than anaerobic processes. Further studies are needed to determine if there is a moisture regime optimal to microbial oxidation.

There might be also a certain temperature and salinity "threshold" in the northern ecosystems for chloromethane production. For example, Dimmer *et al.* (2001) could detect relatively high halomethane emission rates from Irish peatlands and forest floors, but Hellén *et al.* (2006a) could not detect any emissions from the Finnish inland peatland or the coniferous-forest floor. This suggests that the salinity in inland sites in Finland was probable not high enough to initiate halomethane formation. In this study, performed on a coastal area of the Baltic Sea, we could detect at least chloromethane emissions. Thus, the halogenated hydrocarbons measured by Hellén *et al.* (2006b) in the air of urban and residential areas in southern Finland may originate in areas affected by brackish water. Hellén *et al.* (2006b) modelled the measured halogenated hydrocarbons as having their origin in a distant source, but the type of this source could not be identified. A temperature threshold might have been the reason why Rhew *et al.* (2007) could record almost no halomethane emission from a tundra coastal site in Alaska, where the salinity is most probably at least the same or higher than on the Baltic Sea coast in Finland.

Geographic location

When considering the CH_3Cl emissions from vegetation, the (bio)geographic location of the sampling site is of a paramount importance. It is this factor which mainly determines the vegetation type by dictating the length of the growing season, the temperature and the diurnal light

conditions. Halophytes on coastal wetlands and inland grass- and shrublands at higher latitudes may have chloromethane production rates of global relevance. Estimating the magnitude of these sources is hindered by the lack of field data and uncertainties in the estimations of the global coverage of these ecosystems. Our sampling site was located in the southernmost part of the boreal zone, which has a substantially lower net primary production rate than the tropics (Field *et al.* 1998). The relationship between biomass production rate and the emission of chloromethane, not investigated so far, should be studied in order to adjust the global budget of HVOCs.

Representativeness of the collected data

Four vegetated plots were sampled using chambers with basal area of 0.0095 m^2 during three days in the first half of July 2007. The collected dataset is relatively limited in space and time.

The sampling days were situated in the middle of the thermal growing season in this climatic zone, which is the time of the year having the highest mean temperature. The mean temperature of July in the years 1971–2000 was 16.9 °C (*see* www.fmi.fi/saa/tilastot.html) in this region. Our sampling days where somewhat warmer, than the long-term average, but not exceptional so for July. Currently, there exists controversial information about the seasonal emission patterns of monohalomethanes. The study of Manley *et al.* (2006) recorded monohalomethane emissions from a Californian saltmarsh region for 1.5 years, but could not find a distinct seasonal emission pattern in the region. Cox *et al.* (2004) however found the largest chloromethane net emissions during the spring and summer time. These studies were performed in regions with very different climatic conditions as the investigated area in our study. It would be logical to expect seasonality in the vegetation derived emissions of the boreal coastal meadows due to the deciduous nature of their plant species and the harsh (snow coverage, low temperatures) weather conditions of the non-growing season in this area.

As mentioned before, Manley *et al.* (2006) noticed that flowering was coinciding with maximal emissions of chloromethane in some plant species. In the time of our measurements also some of the sampled species (e.g. *Glaux maritima* and some of the *Carex* species) were flowering. This fact together with the relatively high temperatures in the sampling days leads to the conclusion that our results are probably in the higher end of the scale for chloromethane emissions during the growing season of 2007. The vegetation of the study area showed species, which are typical at the brackish water affected coastal region of this part of the Baltic Sea (Siira 1985).

A better picture of the emissions would be gained, when more enclosures could be used and several sampling campaigns in different years and times of year could be undertaken. As our sampling location was very remote lacking the advantages of a continuously occupied research station or an institute (storage possibilities, energy, personnel, etc.), the sampling campaign was bound with a considerable logistic effort and costs. Considering this we had to settle for one campaign during the growing season. Despite of the limitation of our dataset, it still provides new and valuable information from an area, which has not been investigated in this context before.

Next to limitation in space and time our results might also be biased because of the missing information about the chloromethane emissions and degradation of the different soil types, so that only indirect estimations of the contribution of the investigated soils could be made.

Conclusion

The observed chloromethane fluxes from a boreal coastal meadow were 10.36 ± 0.60 $\mu g\ m^{-2}\ d^{-1}$, and 36.58 ± 2.54 $ng\ g^{-1}$ (d.w.) d^{-1} for the boreal coastal meadow vegetation. These emissions rates were similar to those obtained from other coastal ecosystems. No significant differences were detected between the emission rates of the vegetation types. The emission rates from both vegetation types varied strongly among different times of day (2–14-fold differences between the maximum and minimum rates). These variations were mostly well-correlated with changes in air temperature.

Chloromethane emission data from boreal coastal vegetation are scarce and, to our knowl-

edge, the current study is the first to report such data. Its results suggest that boreal coastal areas might be a considerable source of chloromethane, contributing substantially to the atmospheric concentration on the local and perhaps also on the global level. Further investigations should be made to discover the actual extent of this source and the mechanisms controlling the emissions. More information on the influence of soil parameters and especially of soil biology on chloromethane formation and degradation is needed. Also the seasonal behaviour of the emissions needs to be elucidated.

Acknowledgements: We thank Leif Lindgren from Metsähallitus for his guidance and help in plant species identification on Jungfruskär. Sabine Beckmann is warmly acknowledged for assistance in the field work and Miia Collander for her help in the soil analyses. Richard Seifert is thanked for scientific discussions and help in preparing the manuscript. Sebastian Rast is greatly acknowledged for the clarification of the flux calculation principle. We thank also the three anonymous reviewers for their help in improving the quality of this paper. Arja Valtanen thanks the Maj and Tor Nessling foundation, and the German Research Foundation DFG (MI157/18) for financial support.

References

Ahti T., Hämet-Ahti L. & Jalas J. 1968. Vegetation zones and their sections in the north western Europe. *Ann. Bot. Fennici* 5: 169–211

Cox M.L., Fraser P.J., Sturrock G.A., Siems S.T. & Porter L.W. 2004. Terrestrial sources and sinks of halomethanes near Cape Grim, Tasmania. *Atmos. Environ.* 38: 3839–3852.

Dettmer K., Knobloch T. & Engewald W. 2000. Stability of reactive low boiling hydrocarbons on carbon based adsorbents typically used adsorptive enrichment and thermal desorption. *Fresenius J. Anal. Chem.* 366: 70–78.

Dimmer C.H., Simmonds P.G., Nickless G. & Bassford M.R. 2001. Biogenic fluxes of halomethanes from Irish peatland ecosystems. *Atmos. Environ.* 35: 321–330.

Field C.B., Behrenfeld M.J., Randerson J.T. & Falkowski P. 1998. Primary production of the biosphere: integrating terrestrial and oceanic components. *Science* 281: 237–240.

Hamilton J.T.G., McRoberts W.C., Keppler F., Kalin R.M. & Harper D.B. 2003. Chloride methylation by plant pectin: An efficient environmentally significant process. *Science* 301: 206–209.

Heiden A.C., Kobel K., Langebartels C., Schuh-Thomas G. & Wildt J. 2003. Emissions of oxygenated volatile organic compounds from plants. Part I: emissions from lipoxygenase activity. *J. Atmos. Chem.* 45: 143–172.

Heldt H.-W. 2004. *Plant biochemistry*. Academic Press, San Diego.

Hellén H., Hakola H., Pystynen K.-H., Rinne J. & Haapanala S. 2006a. C_2–C_{10} hydrocarbon emissions from a boreal wetland and forest floor. *Biogeosciences* 3: 167–174.

Hellén H., Hakola H., Pirjola L., Laurila T. & Pystynen K.-H. 2006b. Ambient air concentrations, source profiles, and source apportionment of 71 different C_2–C_{10} volatile organic compounds in urban and residental areas of Finland. *Environ. Sci. Technol.* 40: 103–108.

Keppler F., Eiden R., Niedan V., Pracht J. & Schöler H.F. 2000. Halocarbons produced by natural oxidation processes during degradation of organic matter. *Nature* 403: 298–301.

Kesselmeier J. & Staudt M. 1999. Biogenic volatile organic compounds (VOC): an overview on emission, physiology and ecology. *J. Atmos. Chem.* 33: 23–88.

Laturnus F., Haselmann K.F., Borch T. & Grøn C. 2002. Terrestrial natural sources of trichloromethane (chloroform, $CHCl_3$) — an overview. *Biogeochemistry* 60: 121–139.

Manley S.L., Wang N.Y., Walser M.L. & Cicerone R.J. 2007. Coastal salt marshes as global methyl halide sources from determinations of intrinsic production by marsh plants. *Global Biogeochem. Cyc.* 20, GB3015, doi: 10.1029/2005GB002578.

Manley S.L. 2002. Phytogenesis of halomethanes: a product of selection or a metabolic accident? *Biogeochemistry* 60: 163–180.

McDonald I.R.,Warner K.L., McAnulla C., Woodall C.A., Oremland R.S. & Murrell J.C. 2002. A review of bacterial methyl halide degradation: biochemistry, genetics and molecular ecology. *Environ. Microbiol.* 4: 193–203.

Niskanen R. 1989. Extractable aluminium, iron and manganese in mineral soils. I. Dependence of extractability on the pH of oxalate, pyrophosphate and EDTA extractants. *J. Agr. Sci. Fin.* 61: 79–87.

Norseth K. 1987. Climate and hydrology of norden. In: Varjo E. & Tietze W. (eds.), *Climate and hydrology of Norden*, Bornträger, Berlin, pp. 120–128.

Redeker K.R., Treseder K.K. & Allen M.F. 2004. Ectomycorrhizal fungi: a new source of atmospheric methyl halides? *Global Change Biol.* 10: 1009–1016.

Rhew R., Miller B.R. & Weiss R.F. 2000. Natural methyl bromide and methyl chloride emissions from coastal salt marshes. *Nature* 403: 292–295.

Rhew R., Miller B.R., Vollmer M.K. & Weiss R.F. 2001. Schrubland fluxes of methyl bromide and methyl chloride. *J. Geophys. Res.* 106: 20875–20882.

Rhew R., Miller B.R., Bill M., Goldstein A.H. & Weiss R.F. 2002. Environmental and biological controls on methyl halide emissions from southern California coastal salt marshes. *Biogeochemistry* 60: 141–161.

Rhew R., Teh Y.A. & Abel T. 2007. Methyl halide and methane fluxes in the northern Alaskan coastal tundra. *J. Geophys. Res.* 112, G02009, doi:10.1029/2006JG000314.

Rhew R. & Abel T. 2007. Measuring simultaneous production and consumption fluxes of methyl chloride and methyl bromide in annual temperate grasslands. *Environ. Sci Technol.* 41: 7837–7843.

Saito T. & Yokouchi Y. 2006. Diurnal variation in methyl halide emission rates from tropical ferns. *Atmos. Environ.* 40: 2806–2811.

Schäfer H., Miller G.L., Oremland R.S. & Murrell J.C. 2007. Bacterial cycling of methyl halides. *Adv. Appl. Microbiol.* 61: 307–346.

Shade G.W. & Goldstein A.H. 2006. Seasonal measurements of acetone and methanol: abundances and implications for atmospheric budgets. *Global Biogeochem. Cyc.* 20, GB1011, doi:10.1029/2005GB002566.

Sharkey T.D. & Yeh S. 2001. Isoprene emission from plants. *Annu. Rev. Plant Physiol. Plant Mol. Biol.* 52: 407–436.

Siira J. 1984. On the vegetation and ecology of the primary saline soils of the Bothnian Bay. *Aquilo Ser. Bot.* 20: 1–13.

Siira J. 1985. Saline soils and their vegetation on the coast of the Gulf of Bothnia, Finland. *Ann. Bot. Fennici* 22: 63–90.

Singh H.B., O'Hara D., Herlth D., Sachsse W., Blake D.R., Bradshaw J.D., Kanakidou M. & Crutzen P.J. 1994. Acetone in the atmosphere: distribution, sources, and sinks. *J. Geophys. Res.* 99: 1805–1819.

Teh Y.A., Rhew R., Atwood A. & Abel T. 2008. Water, temperature, and vegetation regulation of methyl chloride and methyl bromide fluxes from a shortgrasss steppe ecosystem. *Global Change Biol.* 14: 77–91.

Varner R.K., Crill P.M. & Talbot R.W. 1999. Wetlands: a potentially significant source of atmospheric methyl bromide and methyl chloride. *Geophys. Res. Lett.* 26: 2433–2436.

Watling R. & Harper D.B. 1998. Chloromethane production by wood-rotting fungi and an estimate of the global flux to the atmosphere. *Mycol. Res.* 102: 769–787.

WMO 2007. *Scientific assesment of ozone depletion 2006.* Global Ozone Research and Monitoring Project Report no. 50, World Meteorological Organization, Geneva.

Yokouchi Y., Noijiri Y., Barrie L.A., Toom-Saundry D., Machida T., Inuzuka Y., Akimoto H., Li H.-J., Fujinuma Y. & Aoki S. 2000. A strong source of methyl chloride to the atmosphere from tropical coastal land. *Nature* 403: 295–298.

Yokouchi Y., Ikeda M., Inuzuka Y. & Yukawa T. 2002. Strong emission of methyl chloride from tropical plants. *Nature* 416: 163–165.

Yokouchi Y., Saito T., Ishigaki C. & Aramoto M. 2007. Identification of methyl chloride-emitting plants and atmospheric measurements on a subtropical island. *Chemosphere* 69: 549–553.

Appendix: Calculation of the emission fluxes

The design of our closed chamber system (Fig. 2) was somewhat different from the design of a traditional closed chamber. The constant sampling causes a steady flow through the chamber. Furthermore, the back flow of chloromethane free air dilutes the concentration of the target compound inside the chamber. After the enclosure of a plant in the chamber, the time-dependent mass density of chloromethane $t \to \rho(t)$ in the chamber depends on the emission flux of chloromethane from the plant Q and the air flux through the chamber J. We assume instantaneous mixing, a constant source flux Q, and a constant air flux J during the measurement period. We denote the volume of the chamber by V and define $q = Q/V$ and $j = J/V$. The change in ρ is then described by an inhomogeneous first order linear differential equation

$$\rho'(t) = q - \rho j \tag{A1}$$

with the initial condition $\rho(0) = \rho_0$.

The solution of this differential equation is

$$\rho(t) = \rho_0 e^{-jt} + \frac{q}{j(1-e^{jt})} \tag{A2}$$

where q/j is the steady state mass density of chloromethane in the chamber which is reached after a sufficiently long waiting time.

The air at the entrance of the trap contains chloromethane with a density $\rho(t)$ provided that the volume of air contained in the tube connection between the chamber and the trap is small as compared with the volume of air sampled during the measurement. In this case, the mass of chloromethane absorbed in the trap per unit time is $m(t) = \rho(t)J$. The mass of chloromethane M_T collected on the absorbent during the sampling time T is then obtained by

$$M_T = \int_0^T m(t)\,dt = J\int_0^T \left[\rho_0 e^{-jt} + \frac{q}{j\left(1-e^{-jt}\right)}\right] dt$$

The calculation of the integral yields

$$M_T = V\left[qT + \left(\rho_0 - \frac{q}{j}\right)\left(1-e^{-jT}\right)\right]$$

In a reference sample with $q = 0$, we collect the mass

$$M_T^{(q=0)} = \rho_0 V\left(1-e^{-jT}\right)$$

From the difference $M_T - M_T^{(q=0)}$ that is measured in the field experiment, we directly obtain the emission flux Q:

$$Q = \frac{\left(M_T - M_T^{(q=0)}\right)}{T - \frac{1}{j\left(1-e^{-jT}\right)}} \qquad \text{(A3)}$$